**University of Cape Town**

**Department of Mechanical Engineering**


# Development of a Biomass Gasification Pre-treatment System



**Author:** Warren Randall

**Supervisor: P**rof. Andrew Yates

Dissertation submitted in partial fulfilment of the requirements for the degree of Master of Science in Mechanical Engineering.

December 2013

# DECLARATION

I understand the meaning of plagiarism and declare that all of the work contained in this thesis, save for that which is properly acknowledged, is my own.

Warren Randall

December 2013

# ACKNOWLEDGEMENTS

The Author wishes to express his sincere gratitude to the following people:

- Prof. Andrew Yates, for his time, advice and guidance throughout this thesis.
- The workshop staff of the University of Cape Town, particularly Mr Glen Newins and Mr Hubert Tomlinson for their constant help and expertise in the manufacturing of various components.
- Mr John Laing from J&A Engineering Services for his help in the manufacture of the screw feeding system.
- My colleagues at SAFL for their guidance and help throughout my thesis, in particular Mr Dylan Smit for his help with the feeding system and Mr Gary McFarlane for his assistance with LabVIEW.
- My parents and brother, whose unfailing belief was a constant source of encouragement throughout my degree.
- My best friend for her love, support and encouragement.

This project was supported and sponsored by Sasol Advanced Fuels Research Group.

# SYNOPSIS

## *Background*

Over the past few decades, the ability to reliably extract energy through biomass gasification has proven to be fairly elusive. Environmental issues, sustainable development, and an increase in oil prices have kindled a renewed interest in biomass gasification technology. Biomass gasification is the incomplete combustion of biomass resulting in the formation of combustible gases consisting of carbon monoxide (CO), hydrogen ($H_2$) and traces of methane ($CH_4$). The use of biofuels for energy is a promising solution for alternate fuel sources due to the fact that the emissions can be low and the fuel is easily obtainable. Biomass is a renewable source of energy and will still be available when fossil fuels are exhausted. As in any plant; all subsystems need to work reliably in order for the facility to be a success. One such subsystem is the pre-treatment process for gasification. A biomass handling system needs to provide continuous flow of feedstock to the gasifier for reliable gas production. The development of a dependable fuel handling system is dictated by the shape and particle size of the feedstock. This is due to the varying composition and physical properties of biomass fuels. These fuels tend to have poor flow properties due to their fibrous nature and the fact that the particles can interlock and support their own weight. Another issue associated with the use of biomass for gasification is the moisture content of the fuel which ranges between 30% and 65% when freshly cut. Drying the biomass before it is fed into the gasifier, improves the reaction stability and can increase the gasification conversion efficiency leading to higher quality gas. This gas is either called syngas or producer gas, and if wood is the feedstock it is referred to as wood gas. Some gasifiers require a moisture content of less than 20% for reliable operation. There exists the option of open air drying although this method takes time and is labour intensive. Commercially available driers do exist but there is also the option of using the "waste" heat generated from the gasifier or other "waste" heat sources in the system for drying, such as the exhaust heat from an associated engine (if applicable). Designing a gasification plant with a drier allows the "waste" heat to be recovered thereby increasing the system efficiency.

## *Objectives*

This project was focussed on drying and feeding timber-yard waste for a gasifier and the assessment of the feedstock drying on the gasifier performance. This required a thermodynamic model to be developed in order to assess the effect of drying as was highlighted in the literature survey. A heat exchanger model was also developed which formed the basis for the design of the drier. The project aim was to develop a reliable feed process for a lab-scale gasifier that was able to dry the proposed feedstock to below 10%. The plant was to be as far as possible, automated, with minimal maintenance requirements.

## *Test Facility Design*

A modular design approach was adopted for this project where the biomass pre-treatment process was designed as three sub-systems and then merged together to form a complete unit. The sections included the fuel handling section (hopper), feeding section, and the drying section (with heat exchanger). The hopper was specified as one cubic meter in size and would feed material to the gasifier at a feed rate determined by the gasifier fuel consumption. The feeder pipe was 3m in length with a nominal diameter of 130mm and inclined at 20˚ to allow the feedstock to enter the top of the gasifier which stood at 1.8m. A 3m long auger, mounted inside the feeder pipe, was used to convey to feedstock from the hopper to the gasifier. The screw had an outside diameter of 60mm, a pitch of 60mm and a blade thickness of 2mm and was driven by a 0.25kW SEW Eurodrive motor with a variable speed controller. Agitators were mounted inside the hopper to aid in the feeding by preventing the feedstock from compacting, bridging or forming rat holes. The agitators were coupled to a 10B chain drive and driven by a modified automotive windscreen wiper motor.

The heat exchanger model revealed that 16 tubes, 2.2m long, with an inside diameter of 10mm and a wall thickness of 1mm would be adequate to dry the feedstock, with an initial moisture content of 50%,  to below 10%. A shell and tube counter flow heat exchanger design was selected with a single pass for the exhaust gas and also for the air. The air would flow inside the tubes and the exhaust gas in the shell around the tubes. The exhaust gas was supplied by the engine from a 5kW gen-set unit. A 1.2 kW modified vacuum cleaner fan, with a rotor diameter of 120mm running at 2500rpm, was chosen to drive the air through the system. Three 1.3 kW electric heaters were purchased to load the generator unit so that the temperature of the exhaust gas reached the desired level of 500°C. The feeder pipe, heat

exchanger and the plumbing (connecting pipes) were all insulated with fiberglass blanket to ensure minimal heat loss to the surrounding environment.

The system was controlled by means of a LabVIEW programme that was designed by the author for a NI Compact-Daq control chassis. Temperature readings for the heat exchanger were measured using K-type thermocouples.

The moisture content of the feedstock was determined by measuring the weight of a sample before and after it was placed in an oven and dried in air at 105°C to a constant weight.

## *Results*

In terms of the current project, it was desired to design a drier for a 20kW downdraft gasifier that was intended for the use with a 5kW gen-set. The gasifier fuel consumption rate was calculated at 1.36g/s based on an assumed gasifier conversion efficiency of 75%. The feedstock was green timber-yard waste having an inlet moisture content of around 50%. The thermodynamic model revealed that drying the biomass completely before gasification would result in a theoretical increase in gasifier conversion efficiency from 54% to 81% assuming that the gen-set engine exhaust used to dry the feedstock was treated as "waste" heat which was not factored into the energy audit to determine conversion efficiency.

The ideal operating conditions were found through experimentation and were achieved when the gate valve was 50% open and with a feed rate of 4.3g/s. Under these conditions the system was able to completely dry the feed stock with an initial moisture content of 53% thus leading to a significant increase in gasifier conversion efficiency.

## *Findings*

A reliable, semi-automated feeding system was designed and built and allowed the feedstock to be successfully fed from a hopper to the top of a gasifier. The feeder occasionally would "jam" but this issue was rectified by programming. Paddles were welded on the auger in an effort to increase the feeding efficiency. These paddles only aided the feeding when placed in specific locations and did prevent rat holes from forming. The agitators that were mounted in the hopper worked adequately to prevent the biomass from bridging.

A gasifier model was developed and based on a downdraft gasifier with ponderosa pine as the feedstock. At a gasification bed exit temperature of 800°C, the associated equivalence ratio was calculated at 3.13 which was within the typical theoretical range for gasification equivalence ratio. The model suitably quantified the effect of moisture content on the lower heating value of the produced gas and gasifier efficiency as well as the gas products.

The average moisture content of the timber-yard waste samples were 53.7% with a standard deviation of 1.6%. The heat exchanger proved to be extremely successful, drying feed stock with a moisture content of over 50%, to a target below 10%. Therefore, the system effectively increased the caloric value of the wood gas from 3.7MJ/kg to 5.5MJ/kg and the gasifier conversion efficiency from 54% to 81%.

## *Future Work*

The future of this project lies in the modification of the feeding system to allow for more reliable feeding. The process could be improved by using a more powerful feeder motor and incorporating modifications that allow the entire system to be fully automated.

Unfortunately the pre-treatment system was never run in conjunction with the gasifier and therefore this is an interesting endeavour for future research. The range of different fuels that the system can handle was not investigated and this is a topic for future testing.

# TABLE OF CONTENTS

# LIST OF FIGURES

# LIST OF TABLES

# GLOSSARY

Agglomerates: to form or collect into a rounded mass

Ash: the mineral content in the fuel that remains in oxidized form after complete combustion

Biomass: a natural substance which stores energy from the sun by photosynthesis.

Bridging: feedstock with low bulk density forms a bridge which obstructs continuous flow

Bulk density: the weight per unit volume of loosely packed biomass

Carbonaceous material: substance rich in carbon.

Channelling: the flame aided by air/oxygen burns holes into the feedstock, often called rat holes.

Char: a charred substance, combustible residue remaining after the destructive distillation of coal.

Cracking: a process where long-chain hydrocarbons or complex kerogens are broken down into simpler molecules by breaking of the carbon bonds

Homogenous: same composition, size throughout

Hygroscopic: readily taking up and retaining moisture

Slag: glass-like substance that becomes sticky when hot

Slurry: a watery mixture of insoluble matter

Stratified gasification: open top/core gasification

Tar: a product of highly irreversible process taking place in the pyrolysis zone. It is rich in polyaromatic hydrocarbons and ranges in appearance from brown and watery to black and viscous.

Equivalence ratio: Fuel/air ratio ($\phi$>1 = rich)

Net air emissions: are any gas additions to air (air pollution)

Throatless gasifier: open core gasifier

# NOMENCLATURE & ACRONYMS

OD – Outside diameter

A – Area

d – Diameter

FBD – Free body diagram

F – Force

Gr – Grashof number

h – Differential height

*h* – Convection coefficient

HCl - Hydrogen chloride

ID – Inside diameter

F – Frequency

k – Conduction coefficient

KCl – Potassium chloride

KOH – Potassium Hydroxide

L –Length

η - Efficiency

μ - Dynamic viscosity

*v* - Viscosity

I – Current

$U_m$ – Mean velocity

ppm – Parts per million

ppe – personal protective equipment

ΔP – Differential pressure

Nu – Nusselt number

Q – Flow rate

q – Heat transfer

r – Radius

Re – Reynolds number

RPM – Revolutions per minute

ρ – Density

S.I. – Spark ignition

S.Steel –stainless steel

σ– Stress

τ - Shear stress

T – Temperature

v – Velocity

λ – Helix angle

K – Pipe/fitting loss coefficient

Δt – Change in time

Pr – Prandtl number

V - Voltage

# 1. INTRODUCTION

## 1.1 Background

Gasification of biomass feedstock into a useful gaseous fuel enhances its potential as a renewable energy resource. Extensive research and funding has been dedicated to the improvement of gasification systems. The reliable performance of the biomass pre-treatment system is integral to the success of this research. The pre-treatment process includes the feeding and drying of the biomass feedstock and it needs to perform optimally in order to obtain wood gas of the highest quality. Solids do not flow freely like liquids and biomass in particular is infamous for its poor flow characteristics. Biomass fuels also contain moisture and depending on the type of biomass and its treatment, the moisture content can vary considerably. If possible, biomass fuels with low moisture content are preferred for gasification to minimise the energy loss due to evaporation. Typically green biomass fuels have a moisture content of between 30% and 60% but can be as high as 90%. Without pre-treatment, unrecoverable energy is used to evaporate this moisture from the feedstock inside the gasifier. This loss poses both operational and efficiency losses particularly for energy applications.

## 1.2 Aim and scope of project

The thesis aimed to investigate the pre-treatment of timber-yard waste (generally wood shavings) for gasification and in particular, the effect of moisture content contained in biomass feedstock on gasifier performance and the quality of the gas. The project adopted a modular approach with the first step being the assessment of the issues of bridging/arching, compacting and channelling associated with this particular feedstock. A prototype hopper and feeder was built and different configurations and methods of feeding were experimented with. The experimentation and literature review highlighted the need for agitation of the feedstock and also concluded that a screw feeder would be the most viable option for this project. The screw feeder posed no significant maintenance or cost issues and allowed drying to take place in the tube from which the biomass was fed. The system was automated and controlled by computer allowing for further automated processes to be incorporated. The next step was to design and build a prototype drier that would suitably dry the feedstock before it was fed into the gasifier. The system design was based on a 20kW downdraft gasifier coupled

to a 5kW gen-set available at the Sasol Advanced Fuel Laboratory (SAFL) at the University of Cape Town (UCT). There existed the option of using the "waste" heat from the engine exhaust gas for drying, see Figure 1.1. The scope of the project included a semi-automated feeding system and a drier. The feed process comprised a screw feeder that was able to convey biomass at 7.1g/s which was more than adequate for the gasifier fuel consumption rate of 1.36g/s. The drier was able to dry the timber-yard waste from an average moisture content of 50% to below 10% resulting in a theoretical increase of gasifier conversion efficiency from 54% to 81%. This project provided hands-on experience relating to the issues associated with biomass handling and pre-treatment system and included a safety analysis of each of the systems. The desired outcome was to dry the given feedstock to below 10% and to design a system that would run continuously, with minimal supervision.

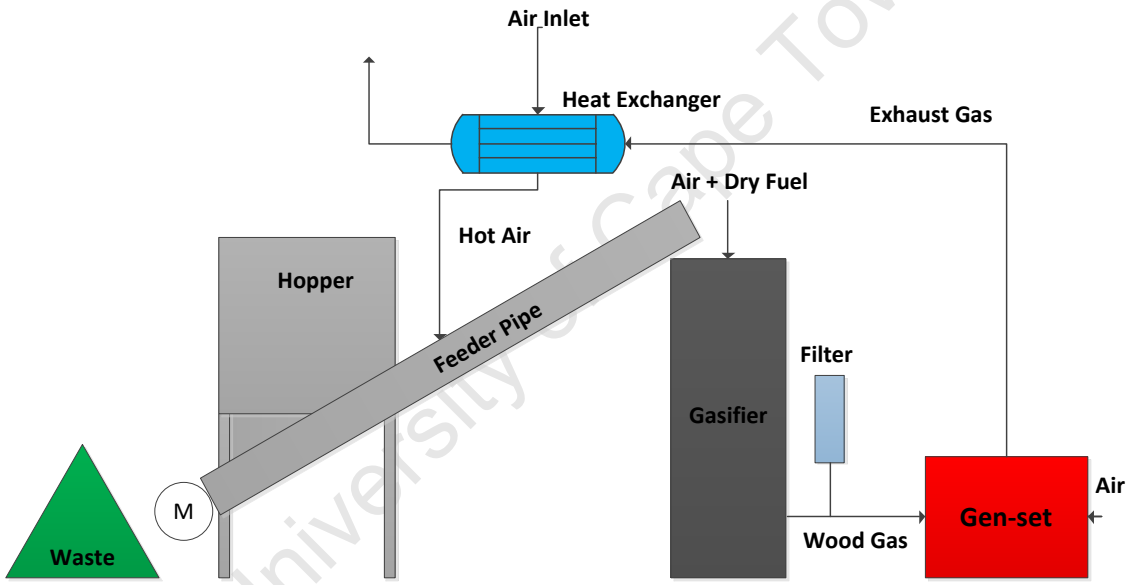


Figure 1.1: Schematic of the complete system

## *1.3 Project plan*

The project commenced in November 2011 and finished in December 2012.

The outline of the project is as follows:

A literature review was undertaken to provide basic understanding of the gasifier system and the issues of moisture content and feeding associated with the proposed feedstock. Thereafter a computational thermodynamic model of a downdraft gasifier operating on ponderosa pine

was developed. This model was used to calculate the ideal operating conditions for the gasifier using timber-yard waste. The model also validated the benefit of drying the feedstock before gasification. A heat exchange model was developed for the design of the drier system. Experimental work was done to assess the handling of the biomass feedstock. This experimental work included the development of prototypes for feeding the feedstock which formed the basis for the final feeding system design. A detailed design was undertaken and reviewed before being sent for manufacture. After preliminary investigation into the functionality of the system, testing was performed that allowed for the establishment of the complete system capabilities. The data was analysed and interpreted to enable conclusions to be drawn and recommendations to be identified for further research.

# 2. LITERATURE REVIEW

## 2.1 Gasification Overview

Gasification is an attractive means for converting biomass into useful energy. Biomass generally refers to all the products of photosynthesis. However, in gasification the term is used only for the portion of plant matter from which thermal energy is derived [1]. Biomass fuels, such as wood or grass, are carbon based renewable energy resources that are much less prone to environment pollution than fossil fuels and therefore have an excellent potential to replace fossil fuels in some applications [2]. Considerable research and effort has been devoted to improving the design of gasifiers. However, just as important to the success of the biomass energy system is the performance of the ancillary equipment, in particular the pre-treatment system [2]. Unfortunately, relatively little interest has been devoted to these systems. The pre-treatment system encompasses the feeding and drying systems of the feedstock. The pre-treatment system is vital in order to obtain wood gas of the highest quality from a given biomass and is a crucial hurdle to overcome in order to begin the transition towards renewable energy from biomass [2].

## 2.2 Gasification Theory

Thermal conversion and combustion, of biomass is an ancient means of extracting energy from a biological material and was traditionally very inefficient. Compared to solid or liquid fossil fuels, traditionally used biomass has only 0.33-0.50 of their gravimetric energy densities, as expressed by the calorific value [3]. Gasification is a process that converts carbon based materials or carbonaceous material such as coal, petroleum, or biomass into a useful gaseous fuel that can be burned to release energy. This is achieved by partially oxidizing or partially combusting the raw material, at high temperatures, with a controlled amount of oxygen and/or steam [4]. Combustion and gasification are closely related thermo-chemical processes, but there are key differences between them. Gasification transforms energy into chemical bonds in the product gas whereas combustion breaks those bonds to release energy [5]. Hydrogen and carbon are reformulated from the feedstock in gasification to produce combustible gases CO and $H_2$ with higher hydrogen/carbon ratio, while combustion oxidizes the hydrogen and carbon monoxide into water and carbon dioxide, respectively [5].

The gas produced from gasification is called syngas or producer gas. If wood is the feedstock, the product is called wood gas. The partial combustion takes place in an oxygen-lean environment of temperatures greater than 700°C in which the gasifier is the reactor [4]. It is only at temperatures above 1100°C that the thermal conversion steps are efficient and CO is a significant waste product of incomplete combustion [3]. The products from complete combustion of carbon based fuels generally contain nitrogen, water vapour, carbon dioxide and possibly excess oxygen [3, 4]. However, because of the excess fuel used in gasification process, the additional gases produced are hydrogen and carbon monoxide as well as traces of methane and products such as tar; see Figure 2.1[4].

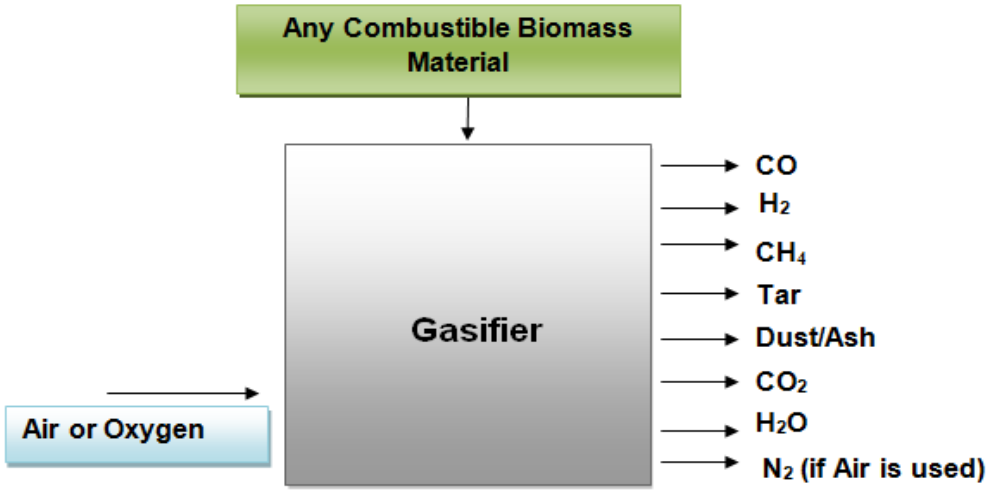


Figure 2.1: Products of gasification [4]

Gasification can be used to produce different products depending on the conditions used:

- When oxygen is used as the gasification medium, the producer gas has a high CO content.
- The use of air reduces the heating value of the producer gas due to the dilution with nitrogen.
- If water is present in the feedstock and high temperatures are reached, hydrogen may also be formed although excess water will result in the formation of higher concentrations of $CO_2$ which reduces the heating value [3].

The typical processes involved in gasification are:

1. Drying
2. Pyrolysis
3. Partial combustion
4. Gasification of decomposition products –Reduction

Drying in the gasifier takes place when the feedstock receives heat from the hot zone downstream in the gasifier. The feed is dried and irreversibly releases water that is loosely bound in the biomass at a temperature above 100°C [5]. Freshly cut biomass can have moisture content as high as 60% and most gasifiers operate optimally with moisture in the range of 10% to 20% [2]. This is due to the unrecoverable energy required to drive off the excess moisture. High moisture content feedstock also lowers the heating value of the wood gas [2, 3].

Pyrolysis is the thermal decomposition of a substance. The partial removal of carbon by heating occurs spontaneously at high temperatures and does not involve reactions with oxygen [5]. An example is in the case of wood when it comes into contact with molten lava i.e. heat. Extreme pyrolysis is called carbonization and leaves mostly carbon residue. The products that form (volatile products and char) depend upon pressure, temperature and residence time. In general, up to 200°C mostly water is released. From 200°C to 280°C $CO_2$, acetic acid and water are given off [4]. The real pyrolysis takes place between 280°C and 500°C; here large quantities of tar and gases containing $CO_2$ are produced. Methyl alcohol is also formed along with light tars. Between 500°C and 700°C the gas production is small and contains hydrogen [4].

Third is the partial combustion process. The combustible matter in a fuel (volatile products and char) is usually composed of carbon, hydrogen and oxygen. In complete combustion $CO_2$ is obtained from the carbon in the fuel and $H_2O$, in the form of steam, from the hydrogen. The combustion process is an exothermic oxidation reaction and yields a theoretical oxidation temperature of up to 1450°C. The molar air to fuel ratio required for complete combustion of biomass, defined as stoichiometric combustion, is 6:1 to 6.5:1. In gasification however the process occurs at conditions with air to fuel ratio being 1.5:1 to 1.8:1, which is 20-40% of the stoichiometric air needed for combustion [4]. This is assuming that the biomass has a typical average composition of $CH_{0.2}(0.6H_2O)$[6].

The reactions are as follows:

$$C + O_2 \Leftrightarrow CO_2 \quad (2.1)$$

$$2H_2 + O_2 \Leftrightarrow 2H_2O_{(g)} \quad (2.2)$$

Lastly, the products of partial combustion such as, $H_2O$, $CO_2$ and un-combusted partially cracked pyrolysis products pass through a red-hot charcoal bed in which the following reactions take place:

$$C + CO_2 \Leftrightarrow 2CO \quad (2.3)$$

$$C + H_2O \Leftrightarrow CO + H_2 \quad (2.4)$$

$$CO + H_2O \Leftrightarrow CO_2 + H_2 \quad (2.5)$$

$$C + 2H_2 \Leftrightarrow CH_4 \quad (2.6)$$

Where:

C – Carbon containing organic compound

O – Oxygen

$CO_2$ – Carbon dioxide

CO – Carbon monoxide

$H_2$ – Hydrogen

$H_2O$ – Water (steam)

$CH_4$ – Methane

Reactions 2.3 and 2.4 are endothermic, reduction reactions and can reduce the gas temperature. The temperature in the reduction zone ranges from 800°C to 1000°C. A lower reduction zone temperature will yield lower calorific value syngas. Reaction 2.5 is known as the water-gas shift reaction [4]. The summary of the reactions are shown in Figure 2.2 with the reduction reactions illustrated in Figure 2.3.

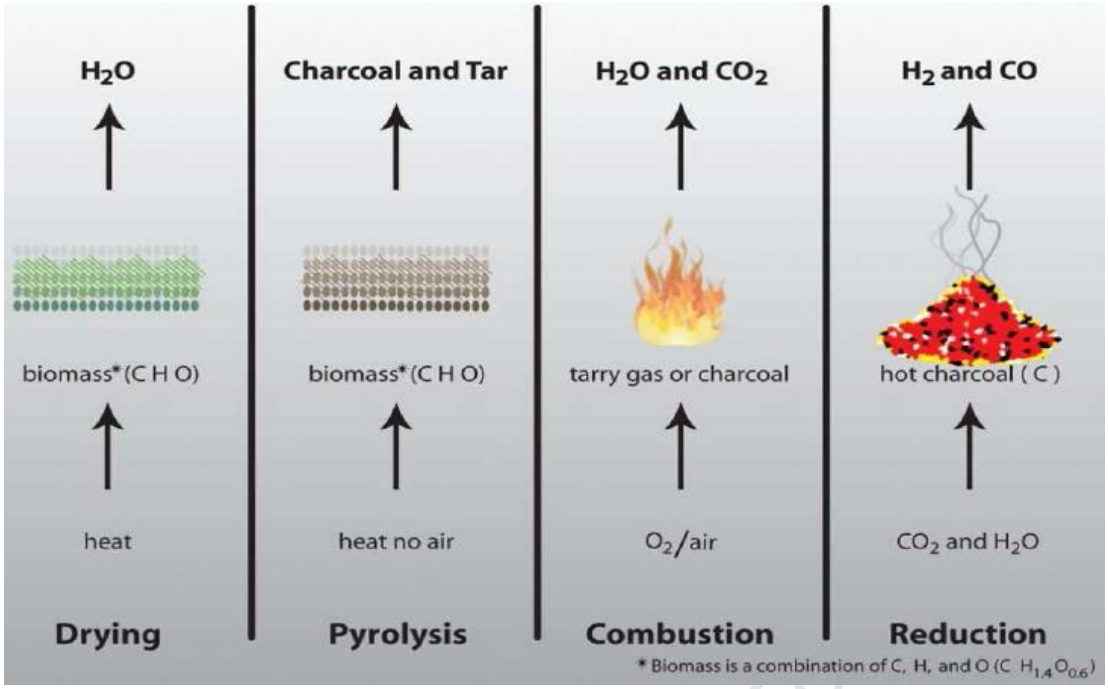


Figure 2.2: Summary of Gasification Reactions [7]

The high temperature process refines out corrosive elements such as potassium, which form salts like KCl, KOH etc. and chlorine, liberated as HCl, allowing clean gas production [8].

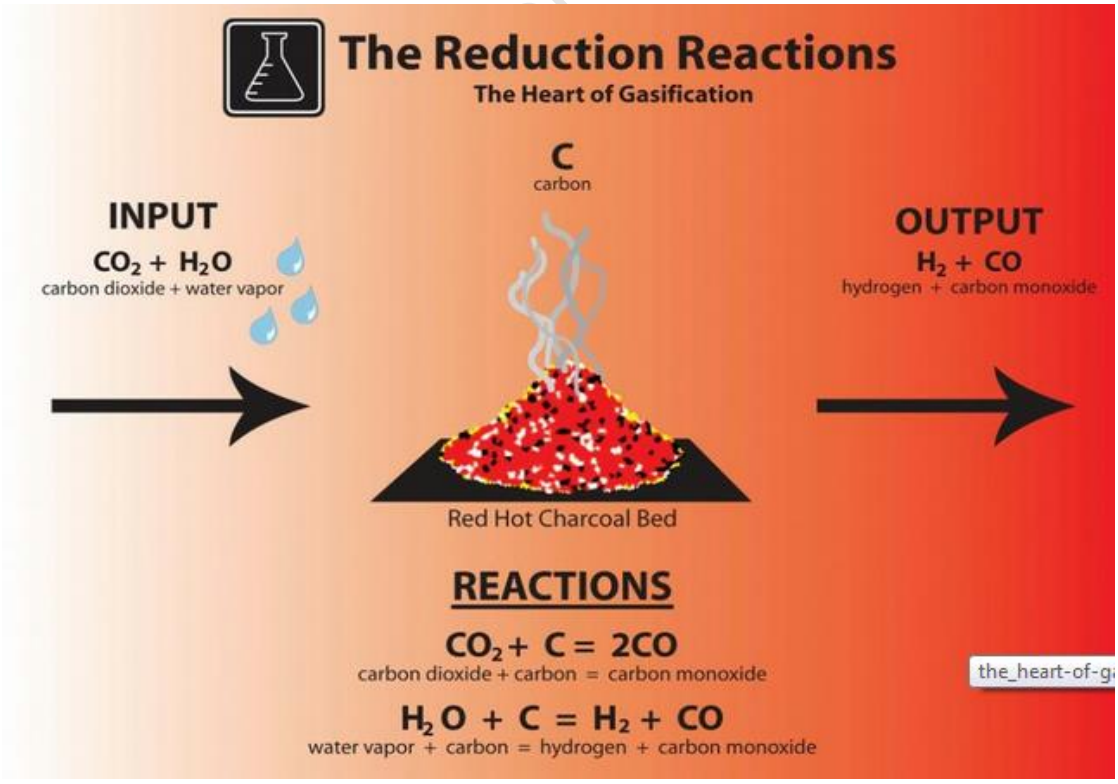


Figure 2.3: Illustration of Reduction reactions [7]

## 2.3 Chemistry of Biomass and Syngas

Biomass can be considered to consist of charcoal ($CH_{0.2}$) and water using the generic formula [6]:

$$CH_{1.4}O_{0.6} = CH_{0.2}(0.6H_2O) \quad (2.7)$$

The generic formula for syngas is thus:

$$CH_{1.4}O_{0.6} + 0.4O_2 \rightarrow 0.7CO + 0.3CO_2 + 0.6H_2 + 0.1H_2O \quad (2.8)$$

Typically a few percent of methane is formed as well [4]. Syngas is a mixture of combustible and non-combustible gases as shown in the above equation. The composition varies depending on the moisture content and type of feedstock and the temperature of the gas leaving the reduction zone (to be shown in Chapter 5). When atmospheric air is used as the gasifying medium, the product gas includes approximately 50% nitrogen [1]. The general composition of the producer gas obtained by wood gasification is given in Table 2.1, on a volumetric (molar) basis.

Table 2.1: Typical Properties of wood gas

| | Wood gas (%vol) | | | |
|---|---|---|---|---|
| References | [9, 10] | [11] | [4] | [1] |
| Component | | | | |
| Moisture | Unknown | 19-25 | 12-20 | Unknown |
| Nitrogen | 50-54 | 45-66.5 | 55-60 | 45-55 |
| Carbon monoxide | 17-22 | 10-18 | 17-20 | 18-22 |
| Carbon dioxide | 9-15 | 12-15 | 10-15 | 9-12 |
| Hydrogen | 12-20 | 7-9.5 | 16-20 | 13-19 |
| Methane | 2-3 | 2.4-4.5 | 2-3 | 1-5 |
| Heating value ($MJ/m^3$) | 5-5.9 | 3.7-6.3 | 5-5.86 | 4.5-6 |

Note: Table 2.1 refers to wood as a feedstock and not a specific species.

Carbon monoxide is produced from the reduction of carbon dioxide, Figure 2.3, and its quantity ranges from 17% to 22% on a volume basis. Carbon monoxide has a high octane number of 106, which makes it suitable for use in a spark ignition engine, but it has a low burning velocity. Hydrogen is also produced by the reduction reaction in the gasifier, Figure 2.3, and possesses an octane number of between 60 and 66. It increases the burning velocity

of the wood gas and together with methane is primarily responsible for the higher heating value of the gas. Nitrogen and carbon dioxide are non-combustible gases in the wood gas and they effectively reduce the specific energy of the wood gas and hence the power output of an engine operating on the gas. A high percentage of carbon dioxide indicates incomplete reduction while the presence of moisture in the gas composition is associated with the moisture content of the feedstock or the humidity in the air used for gasification [1]. Producer gas is usually used for heat production or the generation of mechanical power. The gas mixes homogeneously with air when compared to solid fuels, resulting in cleaner and more efficient combustion. Compression ignition engines can operate in dual fuel mode using 70% - 80% producer gas under normal load conditions whereas spark ignition engines can run on 100% producer gas [12]. The gas can also be used to produce methanol and hydrogen or converted via the Fischer-tropsch process into synthetic fuel [4]. The gas resulting from gasification generally has a low heating value of between 4 MJ/L and 10MJ/L [3].

## *2.4 Types of Gasifiers*

There are four mainstream types of gasifiers available at present: counter-current fixed bed (updraft), co-current fixed bed (downdraft), fluidized bed and entrained flow gasifiers.

Downdraft gasifiers are different to the updraft gasifier in that the gasification agent flows in a co-current configuration with the fuel downwards and gas is removed from the bottom; see Figure 2.4 [13]. The reaction zones in a downdraft gasifier are similar to those in an updraft gasifiers, except the locations of the reduction and oxidation zones are interchanged [14]. The downdraft gasifier has a flexible adaption of gas production to load and a low tar content (< 1%) in the gas as all the tar must pass through the hot bed of char and is reduced to primarily CO and $H_2$ [13]. It operates at higher exit temperatures, around 700 °C, has more entrained particulate matter in the exit gas and lower overall efficiency, due to the high temperature of the producer gas, than an updraft gasifier [13]. The downdraft gasifier with a throat is known to produce good quality wood gas, requires less cleaning and is therefore well suited for engine applications because of the low tar content [14, 15]. The disadvantage is that the design tends to be tall and it is not feasible for fuels of small particle sizes. The gas is also hot at the exit and therefore it has a low thermal efficiency, unless it is recovered by pre-heating the feedstock or inlet air [13].

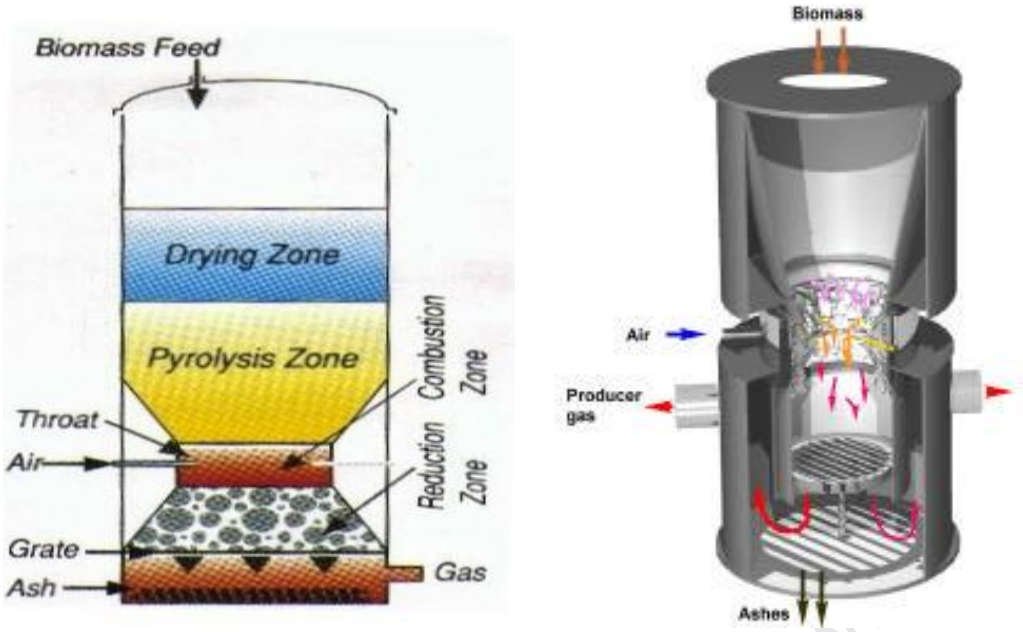


Figure 2.4: Gasification process for downdraft gasifier (left [14])(right [9])

## 2.5 Feedstock

In the past, wood was the primary global energy source whereas today the world is reliant on fossil fuels. The energy requirements of the world are expected to double within the next 50 years. In comparison to fossil fuels, biomass contains relatively less carbon but more oxygen and has a lower heating value, in the region of 12-16 MJ/kg [13]. A sustainable share of biomass of about 20% in a future global energy mix seems to be achievable according to Henrich, 2007 [8]. A significant amount of about 25% of the biomass is expected to come from agricultural waste, namely cereal straw such as wheat, maize rice or barley. Nearly half of the straw that is harvested is not needed, and is available for energy production. These by-products are automatically harvested with the crops at only a small additional cost. Biomass energy obtained from special plantations will be almost double the cost [8].

In industrialized countries, residual wood from forestry or agriculture biomass are usually more expensive than coal. At present the biomass costs are similar to crude oil when based on heating values, but biomass is cheaper when compared to the price of oil plus its tax. Biomass waste is available at almost zero cost. In many countries with low wages, biomass fuels are cheaper than fossil fuels. Because of the dispersed nature of biomass, such facilities are smaller and less automated compared to fossil powered stations. For this reason investment costs are higher; a plant that is ten times smaller may be double the price per unit energy. This can be overcome by using both biofuels and fossil fuels inside the plant. Wood would

pose no problem for this idea but herbaceous biomass like straw, poses a problem due to its high ash content [8].

Residual biomass has distinct characteristic which influence the operation of a gasifier system. These include: shape, size, voidage, bulk density, apparent particle density etc.. The chemical characteristics of such residual biomass are moisture content, ash content, ash fusion temperature, ash deformation temperature etc. [1]. All of these parameters affect the design and operation of the gasifier system. Wood and straw are the most abundant biomass, with cellulose fibres as the major component. Besides the different shapes and densities of the biomass fuels they are also classified according to their ash content. Wood, without bark, can produce a relatively clean gasifier fuel, usually containing less than 1% ash whereas straw has a higher ash, potassium and chlorine content. The ash associated with straw and other such materials become sticky or melts during thermal conversion. A sticky ash can cause gasifier slagging and agglomerates to form inside the gasifier [8]. These inorganic elements are needed for faster metabolism. The same rule applies to aquatic biomass species which grow even faster. The use of fast growing biomass is not suited for bioenergy production due to the expensive fertilizers required. The combustible organic content in solid municipal wastes originates mainly from biomass such as paper, cardboard or garden refuse [8].

# 3. BIOMASS HANDLING

Biomass preparation and handling is vital in order to obtain the highest quality wood gas from gasification. The fuel can rarely be fed directly into the gasifier. The feedstock must be properly prepared and handled; this involves drying, sizing and feeding [2]. The following section outlines these processes and describes some of the possible equipment that is used.

## *3.1 Fuel Handling*

Liquids or gases are somewhat easy to handle as they constantly deform under shear stress. They also take the shape of the vessel they occupy and flow easily under gravity, provided they are heavier than air. Therefore liquids and gases display no major problems during storage, handling and feeding. Solids on the other hand can support their own shear stress and do not flow freely. They can form a bridge over the area they are expected to flow through because they do not deform. Biomass is particularly infamous for this because of its fibrous nature and non-uniform shape [5]. It has peculiar properties which relate to its grain structure, which must be considered when designing the feed and handling systems [16]. The poor flow characteristics of biomass pose endless headaches for operators and designers of biomass systems [5]. Biomass feed systems must provide continuous flow into the gasifier while simultaneously accounting for the pressure changes from atmospheric pressure to the gasifier operating pressure. The throat of the downdraft gasifier is an especially problematic zone for poor flow of low-density biomass causing bridging or channelling and therefore leading to increased tar production [13]. Gasification systems are made up of various components that are used to complete the gasification process. In any complex system the reliability of the process can be reduced to the weakest link in the component chain. The first, and probably the most crucial, component in a gasification system is the feeding mechanism used to feed the biomass into the gasifier. The varied mix of biomass fuels each present their own unique problems [17].

## *3.2 Storage*

The main purpose of storage is to maintain the biomass in an acceptable condition, and location, for easy transfer to the next stage of operation. The stored biomass should be protected from any moisture i.e. rain or snow. Open air storage is however the most common practice due to the large volumes of biomass available. Indoor storage requires sufficient

ventilation and drainage for safety and environmental protection and is therefore more expensive than open air storage. A major biomass concern is that it is hydroscopic, readily absorbs moisture, especially if it is stored indoors. Long term storage can cause physical and chemical changes to the biomass that can adversely affect the flow and gasification properties. For this reason it is necessary to periodically turn over the stored biomass. Generally the retrieving of biomass from storage works on the first-in first out principle where the fuel at the bottom is used first [5].

The properties of the biomass determine the ease with which it is retrieved and handled. If the fuel bin is not filled uniformly, bridging can occur and cause unreliable discharging [5]. However, due to varying size and shape of certain biomass fuels, timber yard waste for example, uniform filling is not always possible due to varying particle shapes and sizes.

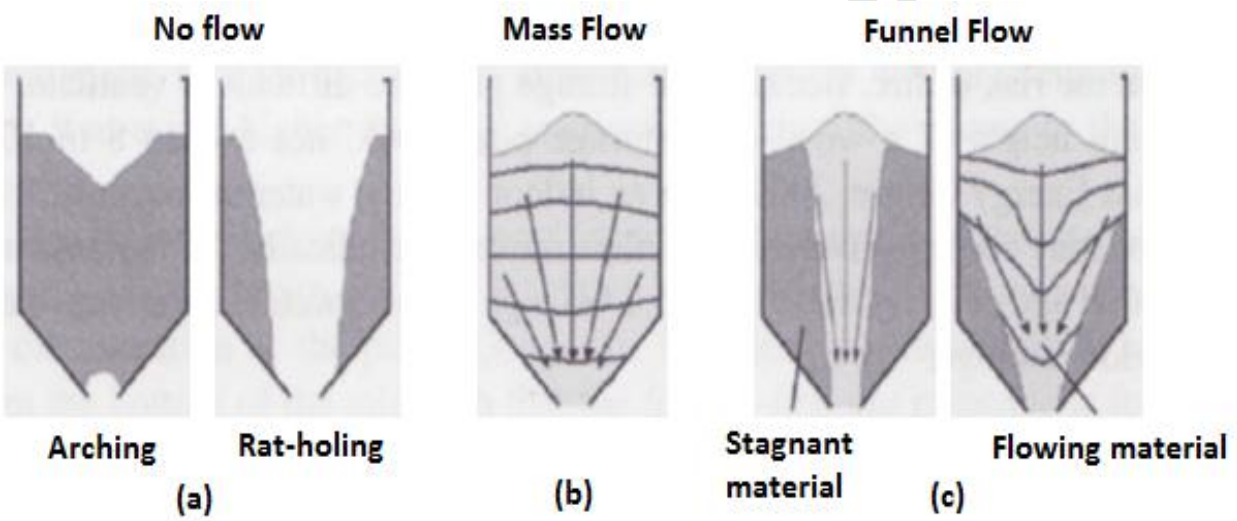


Figure 3.1: Schematic of types of flow through a hopper: (a) no flow, (b) mass flow, and (c) funnel flow

Hoppers assist the removal of biomass from temporary storage. Key aspects in their design include modes of solid flow, slope angle of discharge, and the size of discharge end. Figure 3.1 illustrates various flow problems that can arise with hopper operation. Funnel flow is characterised by an annular zone of stationary solids and a moving core of solids at the centre. The solids flow primarily through the core while solids in the boundary either move very slowly or not at all, see Figure 3.1(c). Smaller particles tend to move through the core while the larger particles stay in the annulus. If a stationary annulus is formed and the discharge stops, a rat hole is formed through the hopper that becomes void and stops flow as arching forms, see Figure 3.1(a) [5].

Mass flow is the ideal mode of flow because the solids flow across the entire hopper cross-section, see Figure 3.1(b). There are some differences in velocity but this allows an uninterrupted and consistent flow with very little radial size separation, which allows the hopper to follow the first in-first out principle. The steeper the cone angle of the hopper, the higher the probability of the mass flow of solids through it [5].

Rat holing often occurs when in the flow of biomass with particles that are cohesive and rough. To aid solid flow, the rat hole needs to be collapsed by aeration in the hopper or by agitation. Arching arises when cohesive particles form a barricade over the hopper exit, usually in the shape of an arch or bridge. The arch can be interlocking, with the particles mechanically locking to form the obstruction. Course particles can also form an arch while competing for an exit, see Figure 3.1(a). Inconsistent flow from a poorly designed hopper will often result in both rat holes and arching. Collapsing a rat hole can result in the falling material compacting over the exit and thus causing bridging/arching.

In order to achieve consistent mass flow, the following conditions need to be met:

- The hopper needs to be adequately smooth
- The hopper sides should be sufficiently steep to force particles to flow at the walls
- The exit must be large enough to prevent arching
- The exit should be large enough achieve the maximum desired discharge rate

The smoothness and slope angle of the sides depend on the friction of the particles and the hopper surface. The factors that affect wall friction for a given fuel are:

- Hopper material
- Roughness of the wall
- Moisture content and size variations of the biomass particles
- The time the particles remain stationary
- Corrosion of wall material due to reaction with solids
- Effect of abrasive materials on the wall

Hopper smoothness can be enhanced by coating it with a smooth lining. This coating can also aid in protecting the walls from corrosion or abrasion.

Mass flow can also be affected by the size of the hopper exit. If the exit is too small arching can occur.

The probability of this occurring increases when:

- Particles are large compared to the outlet size
- The solids are high in moisture
- Particles are of a high shape factor (length to thickness ratio)
- Particles are cohesive and have a rough surface

Wedge shaped hoppers require a smaller width to prevent bridging compared to conical hoppers. Poor feeder design is a very common cause of flow problems, which can undermine the customer acceptance of a biomass gasifier installation [5].

## *3.3 Feeding*

Different types of feeders are used depending on the type of biomass and other process parameters. Feeders can be divided into two groups, namely those for harvested biomass and those for non-harvested biomass. Harvested biomass fuels are associated with plants like straw and grass, which have substantial moisture content. Non harvested fuels include wood chips, rice husks, barks and shells. These fuels generally have a smaller aspect ratio compared to harvested fuels and some are granular.

Harvested fuels are usually baled in fields and sometimes these bales are left in the field to dry. Baling facilities and bale handling systems already exist. Whole bales are typically fed into a shredder and a rotary cutter to reduce the size for feeding into a gasifier or combustor. Wood and by-products from food-processing are usually granular in shape. Bark and wood chips are generally not the right size when they are delivered, so they need to be shredded. Feeders for non-harvested fuels are similar to those used for conventional fuels like coal [5].

### *3.3.1 Feeder types*

There are six main feeder types: gravity chute, screw conveyor, pneumatic injection, rotary spreader, moving-hole feeder, and belt feeder. These can be broadly classified into traction, non-traction, and others. The traction type uses linear motion of a surface which carries the fuel for example a belt feeder. In the non-traction type, rotary motion is used as in a screw feeder. Other feeders use gravity or pressure to move the fuel [5].

Whichever feeder is used it should provide the following:

- Reliable uninterrupted flow of material
- Desired control of the flow rate over the required range
- Uniform withdrawal of material through the outlet of the supply hopper – particularly important for mass flow
- Loads acting on feeder should be minimal which implies minimal power requirement, particle wear and tear, and abrasive wear of feeder components [18]

Gravity Chute Feeder

The gravity chute is simple in that fuel particles drop into the bed with the help of gravity. The pressure in the gasifier needs to be at least slightly lower than atmospheric else hot toxic gas will flow back into the hopper, creating health and operational hazards. Because of the chute being open to the atmosphere and the associated entry of air into the gasifier, this arrangement is only really suitable for a throatless, stratified downdraft gasifier design. The fuel is not well dispersed from the gravity chute feeder and therefore much of the volatile matter is released below the feeder outlet, which creates a localized reduction environment. This can be resolved by extending the chute into the gasifier. This extension needs to be insulated to prevent premature devolatilization of the fuel passing through it. Also, a pressure surge can blow fine particles back up the feeder and the reducing conditions could encourage corrosion. A gravity feeder is not a metering device; it cannot control or measure the flow rate of the fuel [5].

Screw Feeder

A screw feeder is a positive-displacement device. Not only can it move fuel from a low pressure to a high pressure zone but it can also control the amount of fuel that is fed by changing the speed of the feeder drive [5]. It is excellent for dusty materials and has fewer moving parts and therefore less maintenance when compared to a belt feeder [18]. A common problem with screw feeders is plugging or jamming. Solids in the screw flights tend to be compressed as they move downstream, often compacting the fuel to an extent where no fuel falls off the screw [5].

The problems can be avoided by:

- using a variable pitch screw feeder [5, 18]
- using a variable diameter to avoid compression of the fuel towards the outlet of the feeder [5, 18]
- using a helical wire screw
- or using multiple screws [5, 18]

A helical wire screw is well suited for highly fibrous biomass. It is an open coil helical spring with no centre shaft. Due to less metal contact with the feed material there is a lower chance of build-up. Multiple screws are very well suited to operate with large-biomass fuels. Some feed systems utilise three or even four screw feeders. A major and very common problem with screw feeders occurs when feeding biomass with high moisture content. The torque needed for driving the screw is proportional to the vertical force exerted on the hopper outlet by the bulk of the fuel in the hopper; it is also strongly dependant on the screw diameter. The choke section, the part of the screw that extends past the hopper outlet, accounts for more than half of the total torque that is required, especially with compressible material [5].

Rotary Spreader

A spreader wheel is used to disperse the fuel over a wide area in the gasifier. It is typically made up of a pair of blades rotating at high speed; a slight radial offset in the blade orientation helps to throw the biomass over a lateral area. It is not a metering device and it simply encourages segregation of particles over the bed [5].

Pneumatic Injection

A pneumatic transport system helps to feed fuel that has already been metered. It is especially effective for fine solids and works well for counter gravity feeding. It transports dry fuel particles at high velocities and is better suited for less reactive fuels, fuels that requires a high residence time in the gasifier. The fuel is usually fed from underneath a bubbling fluidized bed. However, because of the high velocity and thus momentum of the fuel particles, erosion is a common problem with this specific feeder. One method of overcoming this problem is by using pulsed air [5].

Moving-hole Feeder

A moving-hole feeder is well suited to fluffy biomass or fuels that contain flakes which do not flow freely. These types of solids cause excessive compacting in a hopper or screw feeder. This feeder is different from the others in that it does not draw fuel from only one section. It basically consists of slots that move back and forth with no friction between the stored fuel and the feeder deck. At a determined rate, a moving hole slides under the hopper, and the solids drop into the trough that carry the fuel at the desired rate. The solids do not compact as they do with a screw feeder. Rat holes in the hopper are also avoided by using vertical instead of angled walls [5].

Belt Feeder

A belt feeder is ideally suited for biomass fuel that does not flow freely, fuel that is cohesive, fibrous, friable, course, elastic, sticky or bulky [5, 18]. They are not however recommended for fine or granular biomass fuels. The belt is usually located under the outlet of the hopper. It is supported on rollers that can be mounted on a load cell to directly measure the feed mass rate. The speed and width of the belt depend on the density and size of the fuel that is transported. Permissible weight, speed and belt width is provided by most manufacturers. Such data is used for design of the belt feeder [5].

Rotary Feeder

An example that was not included in the six main feeders is the rotary feeder, see Figure 3.2. These feeders are limited to hoppers having circular or square outlets and are thus not as well suited for handling cohesive bulk solids as screw or belt feeders. Elongated rotary feeders or star feeders can however be used to feed across the narrow dimension of a slotted outlet. A rotary feeder is useful for handling fine powders (larger particles will jam on the rotor) and can be used as an air lock when feeding into a higher or lower pressure environment [18].

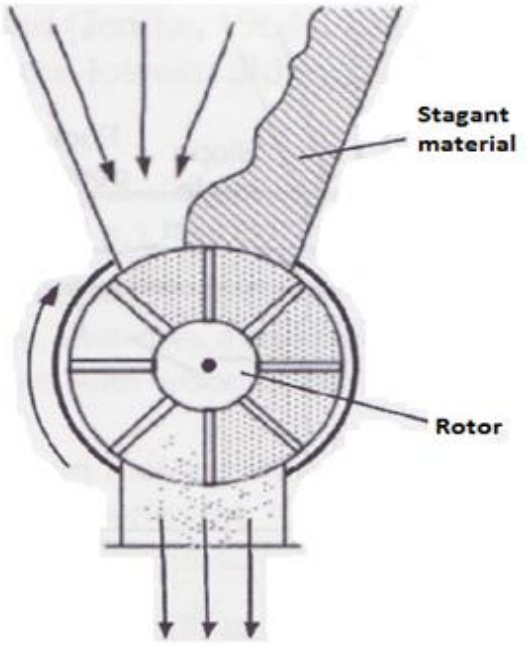


Figure 3.2: Schematic of rotary feeder [5]

Aerospace Research Corporation tested rotary valve feeders with sawdust. There were however major sealing problems and the abrasiveness of the wood also became an issue [17].

# 4. PREPARATION-DRYING

The drying process in gasification vaporizes the water that is not chemically bonded. After drying the temperature increases, and the chemical bonds in the material are broken resulting in gas, tar (or pyrolysis oils) and charcoal being produced.

## *4.1 Biomass Moisture content*

The moisture content of a fuel is determined by the type of biomass, its origin and treatment. Ideally fuels with low moisture content are preferred to minimise the energy loss due to evaporation [4]. Wood is porous and hygroscopic and, because of its microscopic structure, it has two different types of porosity:

- The macro-porosity created by the cavities of the conductive tissue (used for water, energy and nutrient transport between the roots and the leaves of the plant) and by the parenchymal cells containing free (or imbibition) water.
- The micro-porosity of the actual wood substance (mainly cellulose, hemicellulose and lignin), which always contains a certain amount of bound (or saturation) water.

Wood starts to lose moisture from the moment the tree is cut down. First the imbibition water evaporates from the outermost (sapwood) and, later, from the innermost (duramen) parts of the trunk. After a certain amount of time, all the free water in seasoned wood evaporates, while saturation water reaches a dynamic balance with the outward moisture, reaching a moisture content below about 20%. The transient water content inside wood is not uniform as illustrated in Figure4.1 [19].

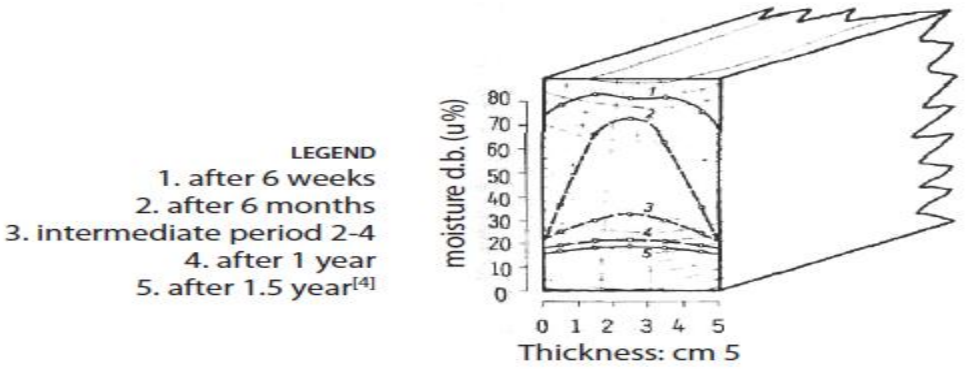


Figure 4.1: Development in radial sense, moisture content (dry basis) into a piece of beech board [19].

The typical moisture content of freshly cut wood is between 30 and 65% with some biomass fuels being as high as 90% [5, 21 and 21]. Forest products have varying moisture contents depending on the feedstock. Bark for example has a moisture content as high as 60% while woods are slightly lower at 55% [21]. Every kilogram of moisture in the feedstock takes away 2260 kJ of unrecoverable energy from the gasifier to vaporize the water. For high moisture content feedstock this loss poses operational problems and an efficiency handicap especially for energy applications [5]. High moisture content also puts a load on the cooling and filtering equipment by increasing the pressure drop across these components because of condensing liquid [4]. Even maintaining a flame inside the gasifier can prove to be difficult if the fuel is too wet. Dry biomass burns hotter and more evenly than wet biomass [21]. Not much can be done about the moisture within the cell structure of the wood but efforts can be made to drive away the external or surface moisture. A certain amount or pre-drying is therefore necessary to remove as much moisture as possible from the biomass feedstock before it is fed into the gasifier. As the moisture content to the gasifier increases, the quality of the producer gas deteriorates along with the overall system performance [22]. The production of wood gas with a reasonable heating value requires biomass with a moisture content of between 10% and 20% [3, 5]. The tolerable moisture content for gasification depends on the type of gasifier, and downdraft gasifiers cannot tolerate fuels with moisture content above 20%. Drying of biomass improves combustion efficiency, can increase steam production, usually reduces net air emissions, and improves overall operation stability [21, 22]. Moist feedstock is also likely to clog the feeding system [2].

If the fuel is to be transported, drying reduces transportation mass and hence also costs. In addition, dry biofuels are less subject to microbiological degradation in storage [21]. Roos 2008 [21] also reported that wood chips with moisture content of 45%, will permit a maximum boiler efficiency, with standard equipment, of about 74%. If the same system is used with wood having a moisture content between 10% and 15%, the efficiency can be as high as 80%. The Biomass Technology Group, [9], reported that external heating of wood chips by an engine's exhaust gas increases the apparent gasification efficiency from 75% to above 90% (by supplying a non-audited additional energy input). If sufficient insulation is used on the exhaust system the exhaust temperature can be high enough to effectively power the pyrolysis reactor.

## 4.2 Drying Biomass

The drying process requires significant energy inputs which will potentially decrease the overall system efficiency. This inefficiency can however be overcome by using waste heat from the gasifier or engine for the drying process [2, 21]. The exhaust from the drying system must be monitored for volatile organic compounds arising from the vaporisation of volatile compounds or the thermal degradation of the biomass in the dryer. There are also fire/explosion hazards associated with the drying of biomass as a result of ignition of combustible gases, if sufficient oxygen is available [2]. The combustion temperature of wood and organic vapours released during drying is 204°C-260°C, with an auto-ignition temperature of 260°C-288°C [23]. However, drying can occur at higher input air temperatures because the evaporating water vapour keeps the feedstock surface temperature lower than the air temperature. This increases the rate of drying, but also increases the risk of fire when drying [23].

### 4.2.1 Drying options

The type of drier selected depends on the fuel characteristics, moisture content, energy efficiency, emissions, operation and maintenance [21]. The design of a drier also requires the knowledge of sensible and latent heat capacities, the rate of heat transfer required and the knowledge of the heat effects associated with the chemical reactions.

There are various types of driers that are used for biomass applications, these include direct- and indirect fired rotary driers, conveyor driers, cascade dryers, flash or pneumatic driers, superheated steam driers, and microwave driers [21]. Driers are generally classified according to the medium used for drying, i.e. the stream that passes through the material that requires drying. This medium can be steam, hot air or exhaust gas. Air and exhaust gas do however have emission and fire/explosion hazards where steam driers do not, although steam dryers do produce condensate that needs to be treated. This condensate does have the potential though to be recovered and used as marketable products such as wood oils. In direct fired driers the heat transfer medium is passed directly through the material to be dried while an indirect drier makes use of tubes or a heat exchanger to dry the material indirectly through conduction. Direct fired driers are more efficient but are not suited for all materials. Indirect driers are better suited for fine or dusty materials [21].

Drying can occur either under atmospheric or vacuum condition. Under vacuum condition the boiling temperature of water is lowered and so the temperature required for drying is reduced [21]. There exists the option of open air drying but the final moisture content of this method varies between 15% and 35% depending on the fuel, the size of the material and the ambient conditions. This method is slow and weather dependant and the heap, if large, will require turning. It is not suitable for fuels with high moisture content as they tend to decompose quickly [5]. Table 4.1, below, summarises the drying options available as discussed by Roos, 2008 [21].

Table 4.1: Drying options [21]

| Classification | Options |
|---|---|
| Drying media | Flue gas, hot air or superheated steam |
| Firing | Direct/indirect fired |
| Heat transfer media | Flue gas, hot air, steam, or hot water |
| Pressure | Atmospheric, vacuum or high pressure |
| Heat source | Drier burners, boiler (flue gas or steam), recovered waste heat from system (engine exhaust gas) |

# 5. THEORETICAL APPROACH

## 5.1 GASIFIER MODEL

The design and operation of a gasifier requires an understanding of the gasification process and how its design, feedstock, and operating parameters influence its performance. The comprehension of the basic reactions is fundamental to the planning, design, operation, troubleshooting, and optimization of the gasifier system [5].

### *5.1.1 Model Assumptions*

The gasifier exit temperature was assumed to be 800°C [4, 24], and the production of ash and tars were not considered, as well as charcoal losses. Heat loss from the gasifier was not calculated. The engine's exhaust gases were represented as hot air for this model.

Additional assumptions:

- All the carbon of the feedstock is converted into gas.
- No pressure drop in the gasifier
- The produced gases behave like ideal gases
- Methane is negligible in the producer gas (trace amounts)

### *5.1.2 Model Description*

The model was constructed in Microsoft Excel together with the programming code Microsoft Visual Basic. The model comprised sub-models of each system element, each on a separate worksheet which included an input and results section. The model was based on a downdraft gasifier with ponderosa pine as the feedstock. The products were calculated from the input parameters using the global reaction for gasification (eqn. 5.1). The molar composition of the different gas species was determined, as well as the fuel/air equivalence ratio ($\phi > 1$ = rich) associated with the assumed gasifier exit temperature. The effect of moisture content on the lower heating value and gasifier efficiency was also calculated. This was done using the numerical solver in Excel.

Note: Chopra 2007 [13], Sadaka 2008 [14], Narvaez 1996 [11] and Zainal 2002 [30] define equivalence ratio as the air/fuel ratio thus $\phi < 1$ = rich. This ratio is not to be confused with the fuel/air equivalence ratio used in this dissertation.

The chemical equilibrium methodology of the non-stoichiometric equilibrium model was developed through two different approaches (i) stoichiometric model and (ii) minimization of the Gibbs free energy [25].

The chemical formula for the feedstock was defined as $C_xH_yO_z$, where x, y, and z were the atoms of carbon, hydrogen, and oxygen respectively. The formula for ponderosa pine, based on a single carbon atom, calculated from the ultimate analysis, shown in Table 5.1.1, is $CH_{1.45}O_{0.68}$ with a molar mass of 24.29g/mol [26].

Table 5.1.1: Ultimate analysis for Ponderosa Pine (%mass, dry) [26]

| Species | Carbon (%) | Hydrogen (%) | Oxygen (%) | Nitrogen (%) | Sulphur (%) | Ash (%) | HV (kJ/kg) |
|---|---|---|---|---|---|---|---|
| Ponderosa Pine | 49.25 | 5.99 | 44.36 | 0.06 | 0.03 | 0.29 | 19.66 |

The global gasification reaction can be written as follows:

$$aC_xH_yO_z + wH_2O + b(O_2 + 3.76\,N_2) \rightarrow cH_2O + dCO_2 + eCO + fH_2 + 3.76bN_2 \quad (5.1)$$

The moisture per mole of feedstock (a=1) is w (eqn. 5.3) and b is the amount of oxygen per mole of feedstock. All inputs on the left-hand side are defined at 25°C. The right-hand side, c, d, e, and f are the number of moles of the unknown species [27].

The moisture content (wet basis), MC, is per mole of biomass was used to calculate the moisture per mole of feedstock [28].

$$MC = \frac{mass\ of\ water}{mass\ of\ dry\ biomass + mass\ of\ water}(100\%) \quad (5.2)$$

$$= \frac{18w}{(1(12) + 1.45(1.008) + 0.68(16)) + 18w}$$

$$\therefore w = \frac{24.3\,MC}{18(1 - MC)} \quad (5.3)$$

Since the moisture content of the biomass was known or given, the value of w can be determined.

To find the molar values of the four unknown species of the producer gas, four equations are required. These equations are based on mass balance and equilibrium constant relationships [27]. Considering eqn. 5.1, the first three equations were formulated by balancing each chemical element.

Carbon balance:

$$x = d + e \tag{5.4}$$

Oxygen balance:

$$z + w + 2b = c + 2d + e \tag{5.5}$$

Hydrogen balance:

$$y + 2w = 2c + 2f \tag{5.6}$$

The equilibrium constants are then calculated as follows:

Chemical equilibrium is commonly calculated either by minimising the Gibbs free energy or by using equilibrium constants. In this case the remaining equation was obtained using the water-gas shift reaction, eqn. 5.7, which occurs in the reduction zone [27].

$$C + H_2O \Leftrightarrow CO + H_2 \tag{5.7}$$

Consider the reaction of components: A, B, C and D with stoichiometric coefficients: $V_A$, $V_B$, $V_C$, and $V_D$. The equilibrium mole numbers: $N_A$, $N_B$, $N_C$ and $N_D$.

$$N_A A + N_B B \overset{equilibrium}{\longleftrightarrow} N_C C + N_D D$$

At equilibrium [29]

$$(dG)_{const\ T\ \&\ P} = \sum (g_i dN_i)_{const\ T\ \&\ P} = 0 \tag{5.8}$$

Where $g_i$ is molar Gibbs values and $dN_i$ is the differential change in the number of moles.

For the stoichiometric reaction

$$v_A A + v_B B \rightarrow v_C C + v_D D \tag{5.9}$$

The stoichiometric coefficients are positive for products and negative for reactants.

From eqn. 5.8:

$$g_A dN_a + g_B dN_B + g_C dN_C + g_D dN_D = 0 \ (const\ T\ \&\ P) \tag{5.10}$$

The values for $N_i$ are not known, but the differential changes are proportional, so from eqns. 5.9 and 5.10:

$$-g_A v_A - g_B v_B + g_C v_C + g_D v_D = 0 \ (const\ T\ \&\ P) \tag{5.11}$$

For the equilibrium state of ideal gas mixture [29]:

$$g_i^0 = h_i^0 - T_{s_i}^0 \ at\ 1\ atm \tag{5.12}$$

Gibbs free energy is a function of temperature and pressure.

For enthalpy [29]:

$$h_{state,(T)} = h_{formation,(T=0K)} + h_{sensible,(T)} \tag{5.13}$$

$$h_{sensible,(T)} = \int_0^T C_{p,(T)} dT \tag{5.14}$$

The sensible enthalpy is the enthalpy difference between any given state and the reference state. The specific heat, $C_p$, is temperature dependant and represented by the equation below

$$C_p = a + bT + cT^2 + dT^3 + eT^4 \tag{5.15}$$

Where the coefficients *a-e* are found in relevant literature [29]

Therefore the sensible enthalpy becomes

$$h_{sensible,(T)} = aT + \frac{b}{2}T^2 + \frac{c}{3}T^3 + \frac{d}{4}T^4 + \frac{e}{5}T^5 \tag{5.16}$$

Note that the enthalpy of formation is given at 298K and not 0K and $C_p$ is only valid over a particular temperature range, therefore

$$h_{state,(T)} = \left(\Delta h^0_{f_{298}} - h^0_{sensible_{298}}\right) + h_{sensible,(T)} \tag{5.17}$$

And similarly the entropy is [29]

$$S_{state,(T)} = \left(\Delta S^0_{f_{298}} - S^0_{sensible_{298}}\right) + S_{sensible,(T)} \tag{5.18}$$

For pressure effects:

$$g_{i(p,T)} = g^0_{i(T)} + P_{correction,T=const} \tag{5.19}$$

$$P_{correction,T=const} \rightarrow \Delta g = \Delta h - T\Delta s$$

The enthalpy change at constant temperature is zero and the entropy is:

$$\Delta S_{T=const} = -Rln\frac{P_2}{P_1} \tag{5.20}$$

Therefore,

$$P_{correction,T=const} \rightarrow \Delta g = +RT\frac{P_2}{P_1}$$

For partial P in atm.:

$$g_{i(p,T)} = g^0_{i(T)} + RTlnP_i \tag{5.21}$$

Substitute eqn. 5.11 into eqn. 5.21:

$$-[g^0_A + RTlnP_A]v_A - [\ldots]v_B + [\ldots]v_C + [\ldots]v_D = 0 \tag{5.22}$$

Define:

$$\Delta G^* = -g^0_A v_A - g^0_B v_B + g^0_C v_C + g^0_D v_D \tag{5.23}$$

$$\Delta G^* = -RT(-v_A lnP_A - v_B lnP_B + v_C lnP_C + v_D lnP_D) \tag{5.24}$$

Substitute eqn. 5.24:

$$\therefore \Delta G^* = -R_u T ln\left[\frac{P_C^{v_C} P_D^{v_D}}{P_A^{v_A} P_B^{v_B}}\right] \tag{5.25}$$

Where $R_u$ is the universal gas constant, 8,314 kJ/(kmol.K) and $\Delta G^*$ is the standard Gibbs function of the reaction.

Then define:

$$K_{P1} = \left[\frac{P_C^{v_C} P_D^{v_D}}{P_A^{v_A} P_B^{v_B}}\right] \tag{5.26}$$

And therefore

$$K_{P1} = e^{-\Delta G^*/R_u T} \tag{5.27}$$

For $K_{P2}$ from the partial pressure relation:

$$P_i = \frac{N_i P_{total}}{N_{total}} \tag{5.28}$$

Substitute eqns. 5.9, 5. 19 and 5.21:

$$K_{P2} = \left[\frac{N_C^{v_C} N_D^{v_D}}{N_A^{v_A} N_B^{v_B}}\right]\left(\frac{P_{total}}{N_{total}}\right)^{\Delta v} \tag{5.29}$$

Where:

$$\Delta v = v_C + v_D - v_A - v_B$$

Therefore at equilibrium $K_{p1}$ must equal $K_{P2}$.

As mentioned previously the equilibrium constants are temperature dependant and therefore the temperature inside the reduction zone of the gasifier needs to be determined. This was done using an energy balance method. In this model it was calculated using an enthalpy balance of the gasification process which was assumed to be adiabatic [27]. The inlet temperature was assumed to be 298K and the exit temperature from the gasifier is T from eqn. 5.17:

$$h_{state,(T)} = \left(\Delta h^0_{f_{298}} - h^0_{sensible_{298}}\right) + h_{sensible,(T)}$$

Heat or enthalpy of formation, $H_F$, is the enthalpy change when 1 mole of compound is formed at standard state (25°C, 1 atm). The heat of reaction for pine is given as 454kJ/mol. Using stoichiometry, the conversion reaction of pine can be written as:

$$CH_{1.45}O_{0.68} + 1.029O_2 \rightarrow CO_2 + 0.675H_2O - 454\ kJ/mol \quad (5.30)$$

The heat of reaction [29]:

$$H_R = Sum\ of\ H_F\ Products - Sum\ of\ H_F Reactants \quad (5.31)$$

$$H_R = \left[H_{F_{CO_2}} + 0.675H_{F_{H_2O}}\right] - \left[H_{F_{Pine}} + 1.029H_{F_{O_2}}\right]$$

Taking the textbook values of $H_F$ of $CO_2$, $O_2$, and $H_2O$ (g) [5].

$$H_R = [-393.5 + 0.675(-241.5)] - [H_{F_{Pine}} + 1.029(0)]$$

$$\therefore H_{F_{Pine}} = -114467kJ/kmol$$

For the solid fuel the state enthalpy was calculated using the enthalpy of formation calculated from eqn. 5.31 and was found to be -114467 kJ/kmol. The sensible enthalpy changes with temperature and was calculated from a constant specific heat of 33.27 kJ/kmol.K [5]. Finally the temperature could be solved for using eqn. 5.13.

### 5.1.3 Calculation Method

The values of c, d, e and f were solved for using eqns. 5.4, 5.5, 5.6 and the equilibrium constants $K_{p1}$ and $K_{P2}$. The temperature was solved for by using eqn. 5.13. These five unknowns were solved for simultaneously using the GRG nonlinear solver in Microsoft Excel.

### 5.1.4 Model results and discussion

The varying parameters for the model were the fuel/air equivalence ratio, ϕ, and the moisture content contained in the fuel. The equivalence ratio was used for air deficient situations i.e. a rich reaction, for this reason the lean equivalence ratio values were ignored. For biomass gasification the typical value is between 3.3 and 5 [5]. The moisture content was varied from 0% to 50%. The initial pressure inside the gasifier was set at 1 atm.

The first step was to investigate the effects of fuel/air ratio on the gas molar composition of the produced gas, see Figure 5.1.1. The gasifier exit temperature was found to increase as the equivalence ratio decreased because of increases in the exothermic reactions [14]. The combustible components and the heating value of the produced gas decreased with decreases in the equivalence ratio. According to the relevant literature, at the equivalence ratios of 4, 5 and 5.9, the higher heating value of the produced gas were 6.48, 6.19 and 5.98 MJ/Nm$^3$, respectively [14]. This is however not indicated in the figure below.

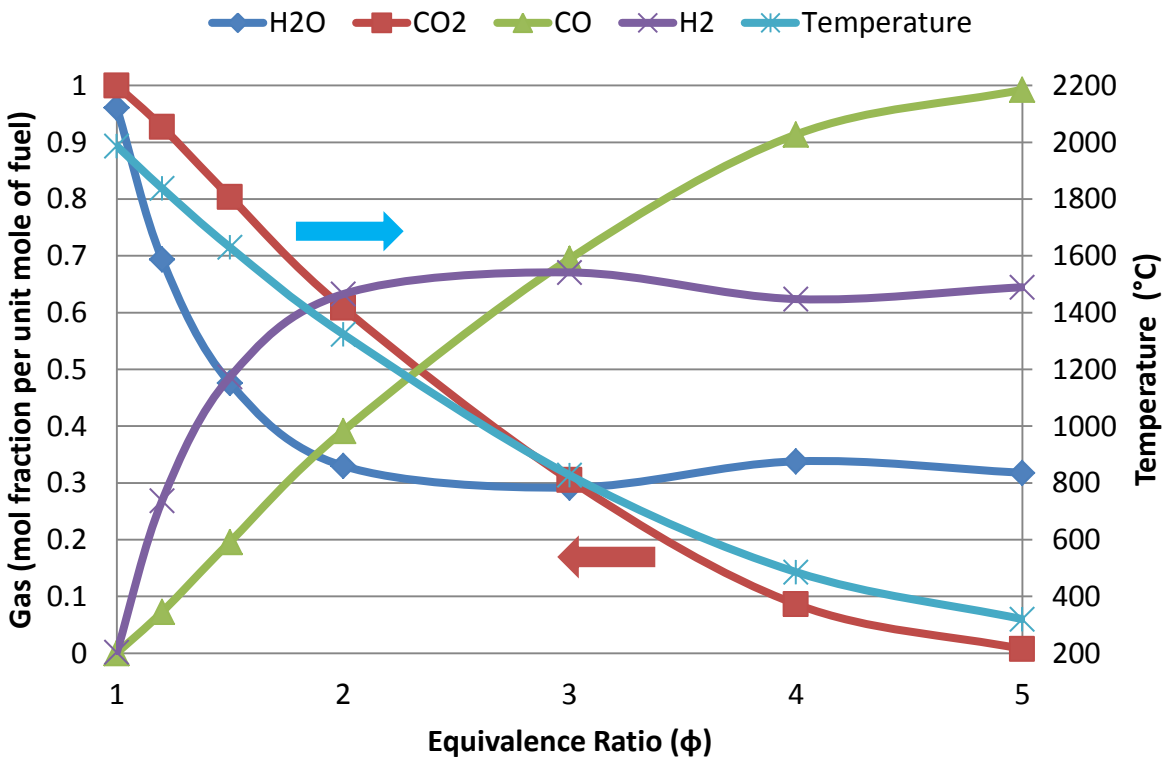


Figure 5.1.1: Product composition versus equivalence ratio, on the primary axis at moisture content of 15%. The adiabatic flame temperature is plotted on the secondary axis in °C.

It is observed from Figure 5.1.1 that the mol fraction of carbon monoxide continuously increased as the fuel/air ratio approaches 5. Hydrogen on the other hand, increased from 1 to a maximum at 3.03 and then also gradually decreased. Carbon dioxide and water decreased to roughly zero at an equivalence ratio of 5. The temperature decreased from 1987°C to 321°C with fuel/air ratio. The slight variation in the equilibrium values for hydrogen and water at high values of equivalence ratio were ascribed to the termination tolerances of the numerical solver algorithm.

Typically the gasifier exit temperature is at 800°C [19], which dictates the operating exit fuel/air ratio for the gasifier. Using the GRG solver this value was $\phi = 3.13$ at exit which is within the range for ideal and theoretical gasification (2.33-5.26) [30].

The bed temperature has the greatest influence on the performance of the gasifier as it affects the equivalence ratio, gas quality, and thermal efficiency [14]. Variation in gas composition due to equivalence ratio, moisture content and temperature will have a direct effect on engine setup and operation. The moisture content was then varied from zero to 50% to find its effects on temperature.

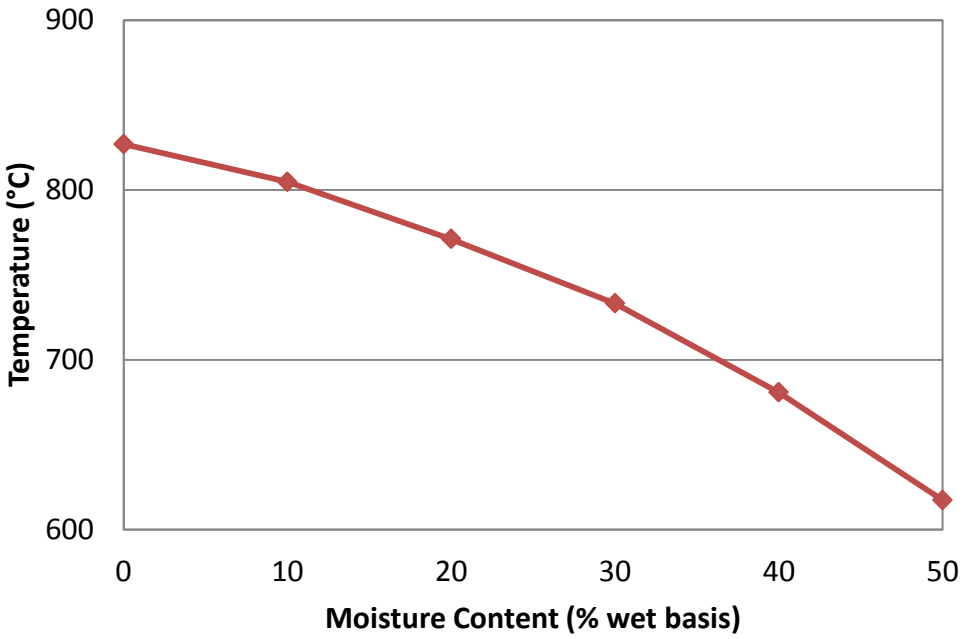


Figure 5.1.2: Temperature versus percentage moisture content of biomass feedstock at equivalence ratio $\phi = 3.13$.

Theory suggests that the exit temperature would decrease with an increase in moisture due to the energy loss needed to evaporate the water; Figure 5.1.2 reflects this theory. The effects of moisture content on the molar percentage of the gas composition was determined by setting the gasifier exit temperature to 800 °C and the equivalence ratio at 3.13 and solving for the four unknown gases and plotted in Figure 5.1.3.

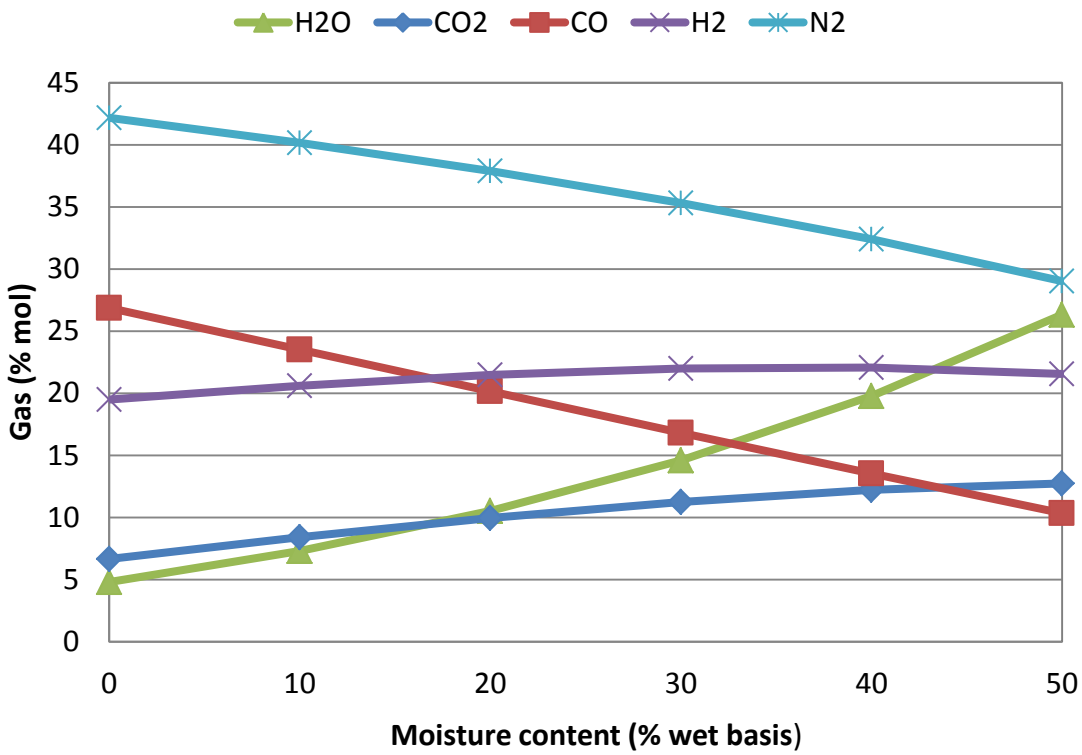


Figure 5.1.3: Product composition, % mol, versus percentage of moisture contained in the feedstock at equivalence ratio $\phi = 3.13$.

The water content in the products clearly increases with moisture content as might be expected. The hydrogen composition gradually increases from 19.5% before it decreases at a moisture content of 30%. Simultaneously, the carbon monoxide percentage reduces constantly from 26.9% to 10.3% for the same variation of moisture content. The percentage of carbon dioxide varies slightly with moisture content from 6.7% to 12.7%, reflecting the associated drop in gasifier efficiency.

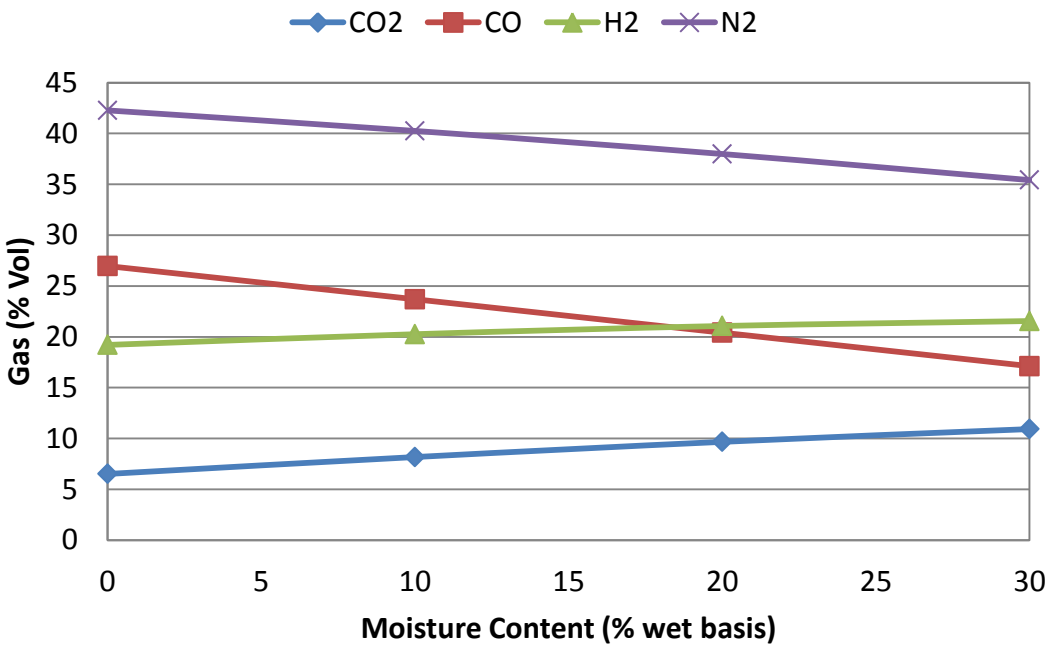


Figure 5.1.4: Product composition, % Vol, versus percentage of moisture contained in the feedstock at equivalence ratio $\phi = 3.13$.

Note: The sum of the gas, %Vol, values do not sum to 100% due to the fact that water was omitted from the figure (for clarity) and methane was not considered in the calculations.

For comparison purposes the gas composition was plotted on volume percentage versus moisture content (from 0% to 30%) in Figure 5.1.4 and compared to other authors in Table 5.1.2 (same Table as 2.1 for clarity). The gas composition of the wood gas was found to be comparable to those reported by other researchers with the exception of nitrogen which was lower than anticipated. The slight differences can be accounted for by the variation in moisture content and the type of fuel used; also methane was not considered a product in this model. All of these parameters as well as the operation equivalence ratio for the gasifier will cause the gas composition to vary.

Table 5.1.2: Wood gas product composition

| | Wood gas (%Vol) | | | |
|---|---|---|---|---|
| References | [9, 10] | [11] | [4] | [1] |
| Component | | | | |
| Moisture | Unknown | 19-25 | 12-20 | Unknown |
| Nitrogen | 50-54 | 45-66.5 | 55-60 | 45-55 |
| Carbon monoxide | 17-22 | 10-18 | 17-20 | 18-22 |
| Carbon dioxide | 9-15 | 12-15 | 10-15 | 9-12 |
| Hydrogen | 12-20 | 7-9.5 | 16-20 | 13-19 |
| Methane | 2-3 | 2.4-4.5 | 2-3 | 1-5 |
| Heating value ($MJ/m^3$) | 5-5.9 | 3.7-6.3 | 5-5.86 | 4.5-6 |

The heating value of the producer gas was calculated by the change in enthalpy with the gas when it reacted with air at 25°*C*. It is expressed in $MJ/m^3$ using the corollary that the standard volume of 1 mole of ideal gas at standard temperature and pressure is 22.4 litres [29]. The literature indicated that an increase in moisture content decreases the calorific value of the producer gas produced by gasification of a biomass feedstock [5].



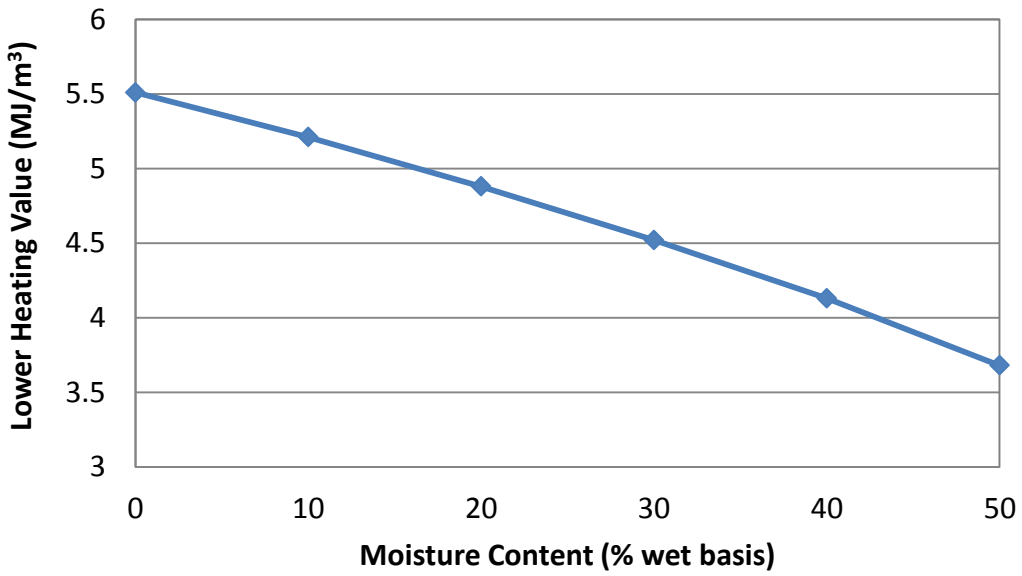


Figure 5.1.5: Lower heating value in $MJ/m^3$ of producer gas versus percentage moisture content of biomass feedstock at equivalence ratio $\phi = 3.13$ and exit temperature of 800°C.

Figure 5.1.5 shows a steady decrease in the lower heating value of the producer gas from 5.51 to 3.68 MJ/kg. This is in agreement with the values presented in Table 5.1.2.

The conversion efficiency of the gasifier:

$$\eta_{gas} = \frac{calorific\ value\ of\ gas/kg\ \ of\ fuel}{avg.calorific\ value\ of\ 1kg\ of\ fuel} \tag{5.32}$$

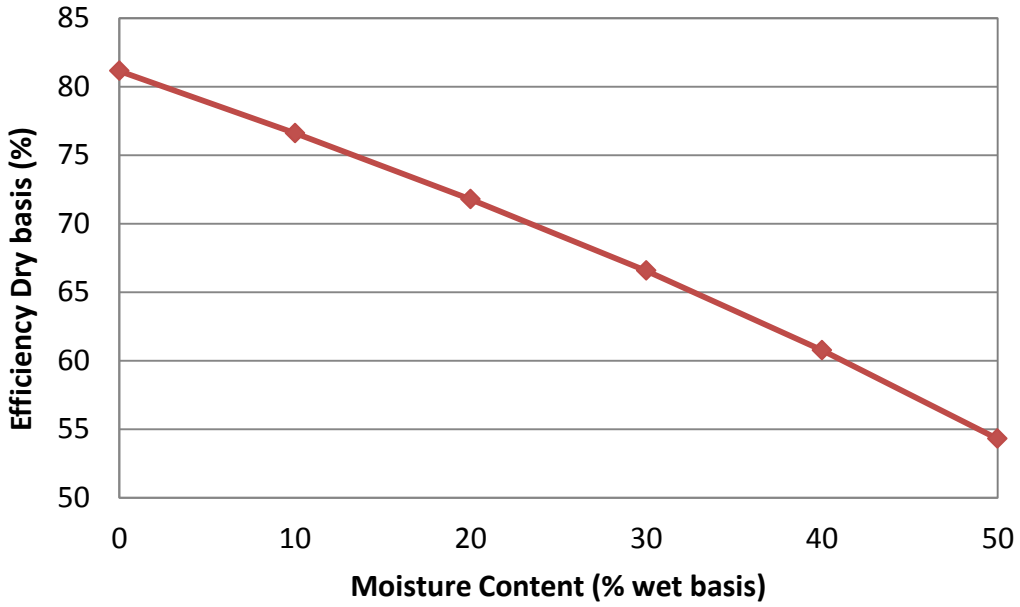


Figure 5.1.6: Effect of moisture content contained in the feedstock on gasifier efficiency at equivalence ratio ϕ = 3.13 and exit temperature of 800°C.

Figure 5.1.6 illustrates the significant decrease in gasifier efficiency from 81.1% to 54.3 % as a result of increased moisture in the biomass feedstock. This confirmed the need for drying the biomass feedstock before gasification and illustrates the relevance of this project.

### 5.1.5 Gasifier Fuel Consumption in a 20kW Gasifier

The gasifier fuel consumption was calculated using the gasifier model and the gasifier specification shown in Table 5.1.3. The calculations were based on a 20kW gasifier with an assumed efficiency of 75% and an engine efficiency of 25%, see Appendix E. These were the design specifications for the gasifier to be in this project.

Table 5.1.3: Gasifier Fuel Consumption Calculations

| Parameter | Symbol | Value | Unit |
|---|---|---|---|
| LHV of the producer gas | | 5.5 | $MJ/m^3$ |
| Biomass Heating Value (Ponderosa Pine) | | 19.66 | MJ/kg |
| Producer Gas Volume | | 2.75 | $m^3$ |
| Gasifier Conversion Efficiency (assumed) | $\eta_{Gasifier}$ | 75 | % |
| Gasifier Conversion Efficiency (predicted) | $\eta_{Gasifier}$ | 76.9 | % |
| Gasifier Power | $P_{gasifier}$ | 20 | kW |
| Engine Efficiency | $\eta_{Engine}$ | 25 | % |
| Engine Power | $P_{Engine}$ | 5 | $Kw_e$ |
| Gas Energy | | 14.8 | MJ/kg |
| Gasifier Fuel Consumption | | 1.36 | g/s |
| Density of timber yard waste | | 200 | $kg/m^3$ |
| Timber yard waste wood flow | | 24.4 | liter/h |

The fuel efficiency was calculated from the amount of gas produced and the calorific value of the wood and the gas. These values were used to calculate the gasifier consumption rate. A 20kW gasifier would consume 1.36 grams of wood per second, based on the above efficiencies and biomass properties. Chapter 8 provides a description of the type of feedstock used for this research.

### 5.1.6 GASIFIER MODEL CONCLUSION

In terms of the current project, it was desired to design a drier for a 20kW downdraft gasifier that was intended for the use with a 5kW gen-set. Assuming a 75% gasifier efficiency (predicted 76.9% by the model) it was possible to calculate a dry feed wood consumption of 1.36g/s or 4.88kg/h. The target moisture content at the exit from the drier was 10%. The feedstock was assumed to be green timber-yard waste having an inlet moisture content of around 50%. The incorporation of the drier would result in a theoretical increase of 27% in the gasifier conversion efficiency assuming that the drier heat source was derived from the gen-set engine exhaust flow.

## 5.2 HEAT EXCHANGE MODELLING

### *5.2.1 Model Description*

As with the gasifier model, the heat exchange model was also set up in Excel and coded using Visual Basic. The model was used to find the ideal method to dry the feedstock. The exhaust gas from the engine was considered as the drying medium as it was a readily available waste heat source. It could be used to dry the feedstock either directly or indirectly. Temperatures of the exhaust gas would typically be between 500°C and 700°C [31]. The use of exhaust gas for drying is an effective way of using the "waste" heat to increase the system efficiency [19]. Direct and indirect drying was investigated as well as the optimization of the drying system in order to get the most out of the exhaust gas. The energy needed for drying, the available energy and the residence time were all calculated using Excel solver.

Three options were investigated to dry the feedstock:

1. Direct drying of the biomass using the exhaust gas

The exhaust gas from the engine would be passed directly through the feedstock to assess whether the exhaust gas would have sufficient energy for drying. This option is undesirable in reality due to exhaust gas emissions and also the possibility of the exhaust gas diluting the air as it flows into the gasifier.

2. Indirect drying of the biomass using the exhaust gas

In this option the exhaust gas flows in a shell surrounding a pipe which contains the feedstock.

3. Direct dryer with forced air as an intermediary heat transfer medium

The third option uses a separate heat exchanger to heat an air supply which is then passed directly through the feedstock to dry it. The volume flow of the air could be adjusted as an independent variable.

### 5.2.2 Heat Exchange Calculation Method

General assumptions:

- Exhaust gas heat exchanger inlet temperature at 500°C
- Pressure at 1 bar
- Exhaust gas has the same properties of air
- Biomass feed pipe diameter 131.2 mm, length 2m (variable)
- The pipe has a filling ratio of 0.5
- Inlet wood moisture content 40%
- Bulk density of wood 200kg/m$^3$ [21]
- Minimal heat loss to the environment, insulation

The feedstock was assumed to be dried completely, although the literature indicates that drying to a moisture content of between 10% and 20% would be adequate. The change in temperature was calculated from the enthalpy required to heat and dry the feedstock at the assumed moisture content.

Table 5.2.1: Energy Properties [29]

| Property | Symbol | Value | Unit |
|---|---|---|---|
| Specific Heat Wood @ 25°C | $C_{pwood}$ | 1.37 | kJ/kg.°C |
| Specific Heat Water @ 25°C | $C_{pwater}$ | 4.18 | kJ/kg.°C |
| Latent Heat water at 1 bar | $Q_{water}$ | 2256.5 | kJ/kg |

The energy required for heating the wood, the water contained in it, and the latent heat of vaporisation is the energy required to dry the wood (see Table 5.2.1). The mass of the feedstock in the tube, assuming the pipe is half filled with wood, was 2.704kg.

$$Latent\ heat\ required = moisture\ content \times m_{wood} \times latent\ heat \tag{5.33}$$

$$= 2440.5\ kJ$$

$$Energy\ to\ heat\ the\ wood\ and\ water$$

$$= m_{wood}\left(0.4C_{p_{water}} + 0.6C_{p_{wood}}\right) \times (120 - 25) = 640.73\ kJ \tag{5.34}$$

$$Total\ energy\ for\ drying = 2440.52 + 640.73 = 3081.3\ kJ$$

The governing equation for convective heat transfer is [32]:

$$q = hA_{wood}\left(T_{b_{exhaust}} - T_{surface}\right) = \dot{m}C_{p_{wood}}\Delta T \tag{5.35}$$

Where the heat transfer coefficient, h, is calculated from the Nusselt number for forced convection

$$Nu_d = \frac{hd}{k} \tag{5.36}$$

Where

d – pipe diameter (m)

k – thermal conductivity (W/m.°C)

An empirical relationship commonly used to represent forced heat transfer is [32]:

The Nusselt number is calculated by

$$Nu_d = 0.023{Re_d}^{0.8}Pr^n \tag{5.37}$$

$$n = 0.4\ heating$$

$$n = 0.3\ cooling$$

The Reynolds number, $Re_d$, is calculated by

$$Re_d = \frac{\rho U_m d}{\mu} \tag{5.38}$$

Where

ρ – drying medium density (kg/m$^3$)

$U_m$ – mean gas flow velocity (m/s)

μ - drying medium viscosity (kg/m.s)

The mean velocity in this case is defined as

$$U_m = \frac{\dot{m}_{gas}}{\rho A_{pipe}} \tag{5.39}$$

The mean velocity was calculated with the assumption that half the pipe was filled with feedstock and therefore the drying medium only flows in half the area of the pipe. The mass flow rate and density of the exhaust gas was calculated in Appendix E.

In a tube, the flow is considered turbulent if the Reynolds number exceeds 2300 [32].

$$Re_d > 2300\ Turbulent\ for\ tube\ flow$$

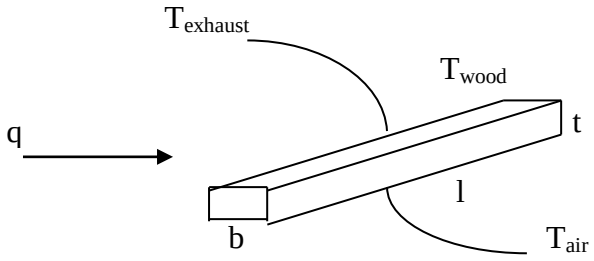


Figure 5.2.1: Heat transfer to a woodchip

Microsoft Excel was used with the governing heat transfer equations to calculate the temperatures and energy supplied for drying. Where figure 5.2.1(above), illustrates the heat transfer to a piece of wood.

### *5.2.3 Direct drying of the biomass using the exhaust gas*

The energy provided by the exhaust gas or air must be greater than the energy required to heat and dry the wood. To gain the basic understanding of the heat transfer to the feedstock an empirical approach was used. The exhaust gas properties were drawn from Holman 2010 [32] and tabulated in Table 5.2.2 as well as the thermal conductivity of wood.

Table 5.2.2: Exhaust Gas Properties at 450°C and 1atm

| Property | Symbol | Value | Unit |
|---|---|---|---|
| Density | ρ | 0.588 | $kg/m^3$ |
| Prandtl | Pr | 0.680 | |
| Viscosity | μ | 2.797E-05 | kg/m.s |
| Thermal Conductivity | $k_{wood}$ | 0.12 | W/m.°C |

Therefore the velocity in the feed pipe is:

$$U_m = 4.45 m/s$$

And

$$Re_d = 6053.5 \ > (2300 \ implies \ turbulent \ for \ tube \ flow)$$

$$Nu_d = 21.73$$

Therefore from eqn. 5.36

$$h = 39.75 \ W/m^2 \ .℃$$

The heat transfer to the wood from the exhaust gas was calculated using the bulk temperature of the exhaust gas and the total surface area of the wood, see Table 8.1. This must match or exceed the enthalpy required to heat and dry wood. In this case the exit temperature of the exhaust gas and the surface temperature were unknown. Using the above equation and excel solver the unknowns were calculated.

From eqn. 5.35

$$T_{exit} = 101.02 \ ℃$$

$$and \ T_{surface} = 287.09 \ ℃$$

From which the heat transfer from the exhaust gas to the wood was calculated.

$$\therefore q = 3606.7 \ W$$

This is the heat transfer rate from which the residence time could be calculated. This was done by dividing the mass of wood, in the assumed pipe size, by the gasifier wood flow. The wood mass flow was calculated previously from the gasifier fuel consumption rate.

$$\dot{m}_{wood} = 0.081 \ kg/min$$

$$\Delta t = \frac{m_{wood}}{\dot{m}_{wood}} \tag{5.40}$$

$$= \frac{2.704}{0.081} = 33.2 \ minutes$$

This is the residence time that the wood would be exposed to in the heat transfer medium; the time will ultimately depend on the feed rate of the biomass. The required residence time for drying based on the energy balance was calculated as:

$$\Delta t = 14.3\ minutes$$

It is important to note that as the length or diameter of the pipe changes the mass and thus the residence time will change.

The energy supplied by the exhaust gas is thus:

$$energy\ supplied = \frac{3606.73}{1000} \times 33.2 \times 60$$

$$= 7189.9\ kJ$$

$$\therefore energy\ supplied \gg energy\ required$$

The above calculations reveal that it is a feasible proof of concept to use the exhaust gas to dry the wood. However, it would be undesirable to ventilate the entire biomass feed system with toxic exhaust gas and therefore other options were considered whereby the engine exhaust heat could be used indirectly to heat and dry the biomass.

The wood was to be fed using a screw feeder inside a tubular housing. Therefore the option existed to dry the wood by heating the feed pipe itself. To save space and manufacturing costs, a shell and single tube heat exchanger could be used to provide the energy required. The exhaust gas would flow in the shell with the wood inside the tube. The heat transfer is therefore from the exhaust gas to the tube wall and from the wall to the air in the tube and then from the air to the wood.

### *5.2.4 Indirect drying of the biomass using the exhaust gas enclosing the feed pipe*

Option 2 uses the same general assumptions as in the previous section and the heat transfer was calculated as a single shell and tube heat exchanger

Option 2 additional assumptions:

- Shell diameter 140 mm, length 2m
- Air at 25°C
- Exhaust gas at bulk temperature of 400°C

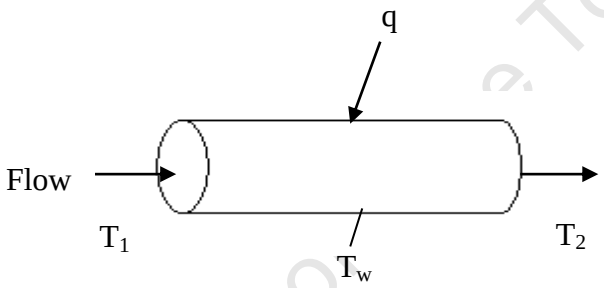


Figure 5.2.2: Tube Profile for gas flow

Figure 5.2.2 illustrates the heat transfer through a tube. The temperature of the air exit, exhaust gas exit and wall temperatures were unknown. The heat transfer was again calculated using empirical relationships for tube flow.

The heat transfer for flow inside a pipe was determined from the flow conditions with properties evaluated at the bulk temperature. In this case the bulk temperature was not known, and the exit temperatures were unknown. The convection heat transfer coefficient in the tube depends on the temperature difference between the tube wall and the air inside the tube. This temperature difference depends on the overall energy balance. Since the temperatures of the exit and the wall (see Figure 5.2.3) were not known they were solved for using Excel Solver.

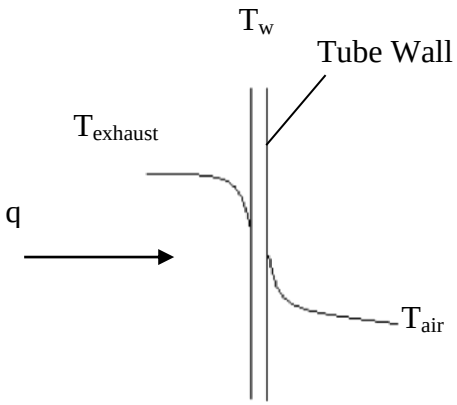


Figure 5.2.3: Heat transfer through tube wall

Table 5.2.3: Properties of exhaust gas at 400°C [32]

| Property | Symbol | Value | Unit |
|---|---|---|---|
| Density | ρ | 0.488 | $kg/m^3$ |
| Viscosity | μ | 3.4E-05 | kg/m.s |
| Thermal Conductivity | k | 0.054 | W/m.°C |
| Prandtl | Pr | 0.685 | |

In this case the flow area was different since the exhaust gas was flowing in the annular area between the shell and tube.

$$A = \frac{\pi}{4}\left({D_{shell}}^2 - {d_{tube}}^2\right) = \frac{\pi}{4}(0.140^2 - 0.1312^2)$$

$$= 0.00187\ m^2$$

Therefore the mean velocity was now

$$U_m = 9.53\ m/s$$

The Reynolds number was calculated using the critical dimension as the outside diameter of the tube.

$$Re_d = 19158.3$$

$$\therefore Turbulent\ flow\ is\ applicable$$

$$Nu_d = 52.71$$

The convection heat transfer coefficient for the outside of the tube was thus

$$\therefore h_o = 21.53\ W/m^2\ .℃$$

The air moves at the same speed as the wood flow. Thus one can assume laminar flow of the air in the tube and free convection from the wall of the tube to the air contained in it. Therefore for the inside of the tube [32]

$$h_i = 1.32\left(\frac{\Delta T}{d}\right)^{1/4} \tag{5.41}$$

Where

$$\Delta T = T_w - T_\infty$$

With

$$T_w - \ tube\ wall\ tempearature$$

$$T_\infty - air\ temperature$$

Heat transfer from exhaust gas to the wall must equal the heat transfer from the wall to the air.

$$q_{outside} = h_o A_o\left(T_{b_{exhaust}} - T_w\right) \tag{5.42}$$

Where

$$A_o = \pi d_o L$$

$$T_{b_{exhaust}} = \frac{T_{1_{exhaust}} + T_{2_{exhaust}}}{2}$$

Similarly

$$q_{inside} = h_i A_i\left(T_{b_{air}} - T_w\right) \tag{5.43}$$

Where

$$A_i = \pi d_i L$$

$$T_{b_{air}} = \frac{T_{1_{air}} + T_{2_{air}}}{2}$$

Equate the heat transfer equations for inside and outside the tube

$$q_{outside} = q_{inside}$$

$$h_o A\left(T_{b\,exhaust} - T_w\right) = h_i A\left(T_w - T_{b\,air}\right) \tag{5.44}$$

Then using solver to solve for the unknown temperatures, the results are tabulated in Table 5.2.4.

Table 5.2.4: Calculated Temperatures for shell and tube configuration

| Symbol | Value | Unit |
|---|---|---|
| $T_{2exhaust}$ | 251.9 | °C |
| $T_{2air}$ | 104.4 | °C |
| $T_w$ | 289.9 | °C |

The heat transfer was then calculated using the temperatures in Table 5.2.4.

$$q = 1525.9W$$

And the energy supplied was calculated as

$$energy\ supplied = 3041.8\ kJ$$

$$\therefore energy\ supplied \ll energy\ required$$

This configuration is therefore clearly not feasible. Changing the pipe length increased the heat transfer required to dry the wood because more wood (mass) was now contained in the pipe, heat transfer is directly proportional to the mass of wood. By increasing the residence time the required heat transfer rate could be achieved although this value is more than double than that of the previous setup. The residence time calculated from the energy balance is

$$\Delta t = 33.7\ minutes$$

Since it was proved previously that using the exhaust gas directly is feasible, an option exists to use a separate heat exchanger to heat the air and pass this air directly over the wood. This would permit the free convection heat transfer inside the biomass pipe to be replaced with forced convection, which will improve the energy transfer significantly. For this design multiple tubes and passes can be used with forced convection inside the tubes.

### *5.2.5 Direct dryer with forced air as an intermediary heat transfer medium*

Option 3 additional assumptions:

- Exhaust gas flows through 40mm pipe
- Forced convection in the tubes
- Feeder pipe length 2m
- 1 Shell pass, multiple tube passes
- Constant friction losses through the pipes ∴ constant velocity
- Air bulk temperature of 200°C

The exhaust gas was evaluated the same as previously and thus has the same values as in Table 5.2.3.

Area for exhaust gas flow was calculated as

$$A_{exhaust} = 0.00126\ m^2$$

Therefore the mean velocity was

$$U_{m_{exhaust}} = 7.89\ m/s$$

For optimum heat transfer from the exhaust gas in the shell to the tubes and thus the air contained in the tubes the mass flow of the air was assumed to be the same as the exhaust mass flow [32].

$$\dot{m}_{exhaust} = \dot{m}_{air} \tag{5.45}$$

The combined cross sectional area of the tubes must match the exhaust gas flow area. Then changing the number of tubes will change the tube diameter and the length of the tubes required to achieve the heat transfer necessary to dry the wood.

$$A_{tubes} = \frac{n\pi {d_{tube}}^2}{4} = A_{exhaust} \tag{5.46}$$

Using eqn.5.46 the effective number of tubes and diameters can be explored. The results are tabulated in Table 5.2.5.

The heat transfer area in this case must include the surface area of all the tubes and the Reynolds number was calculated using the critical dimension as the tube diameter (12mm).

Table 5.2.5: Calculated Heat Exchanger configurations

| Tubes | $d_{tube}$ | Velocity | Required Length | Heat Transfer Area | $q_{supplied}$ |
|---|---|---|---|---|---|
| # | mm | m/s | m | $m^2/m$ | kJ/m |
| 1 | 40.0 | 7.9 | 11.6 | 1.45 | 266.6 |
| 2 | 28.3 | 7.9 | 6.7 | 1.19 | 459.6 |
| 4 | 20.0 | 7.9 | 3.9 | 0.98 | 789.2 |
| 6 | 16.3 | 7.9 | 2.9 | 0.88 | 1080.7 |
| 8 | 14.1 | 7.9 | 2.3 | 0.81 | 1349.5 |
| 10 | 12.7 | 7.9 | 1.9 | 0.76 | 1602.3 |
| 12 | 11.6 | 7.9 | 1.7 | 0.73 | 1843.0 |
| 14 | 10.7 | 7.9 | 1.5 | 0.69 | 2074.0 |
| 16 | 10.0 | 7.9 | 1.3 | 0.67 | 2296.9 |
| 20 | 8.9 | 7.9 | 1.1 | 0.64 | 2723.3 |

The heat transfer area is defined as

$$A_t = n\pi dL \tag{5.1}$$

Where

$n - number\ of\ tubes$

$d - tube\ diameter$ (m)

$L - tube\ length$ (m)

The properties of air were calculated using the assumed air temperature and displayed in Table 5.2.6.

Table 5.2.6: Properties of air at 200°C and 1atm [32]

| Property | Symbol | Value | Unit |
|---|---|---|---|
| Density | ρ | 0.746 | $kg/m^3$ |
| Viscosity | μ | 2.757E-05 | kg/m.s |
| Thermal Conductivity | k | 0.039 | W/m.°C |
| Prandtl | Pr | 0.682 | |

The heat transfer from the exhaust gas to the tubes must match the heat transfer from the wall to the air in the tubes. The wall temperature and the exit temperatures for the exhaust gas and air were unknown. These values were solved for using Excel solver and equating the heat transfer equations (eqn. 5.44), see Table 5.2.7.

Table 5.2.7: Calculated Temperatures for Heat Exchanger

| Symbol | Value | Unit |
|---|---|---|
| $T_{2exhaust}$ | 176.7 | °C |
| $T_{2air}$ | 338.6 | °C |
| $T_w$ | 241.9 | °C |

## 5.2.6 *Heat Exchanger Optimisation*

The temperatures in Table 5.2.7 were calculated on a heat transfer per meter length basis. The diameters of the tubes were then varied to calculate the length required to achieve the desired energy for drying. The following graph shows the net energy for various configurations.

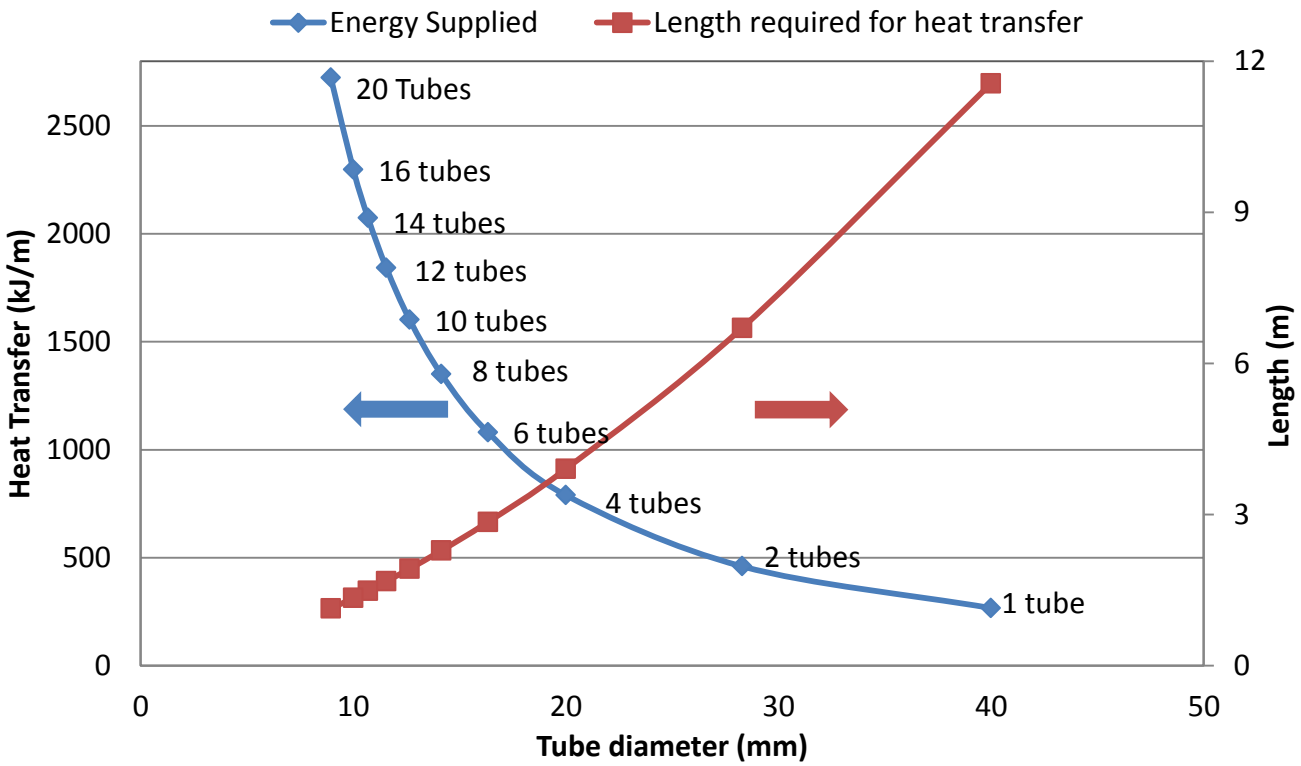


Figure 5.2.4: Illustration of the effect of change in tube diameter and number of tubes on primary axis. The secondary axis shows the effective length required to achieve the heat transfer for the respective configurations.

Figure 5.2.4 illustrates the effect of diameter and number of tubes on heat transfer per meter, due to the change in heat transfer area. The secondary axis illustrates the need to increase the tube length to obtain the required heat transfer. Sixteen tubes at a diameter of 10mm (standard size) and a length of over 1.3m were chosen for this application (Figure 5.2.5). Due to the manipulation required for the tubes, a 10mm standard size was preferred. Thicker tubes would make bending clearly more difficult whereas smaller tubes would increase cost.

The heat transfer for the above arrangement was then:

$$q = 1531.7\ W$$

And the energy supplied is thus

$$energy\ supplied = \ 3095.7\ \ kJ$$

$$\therefore energy\ supplied > energy\ required$$

For this arrangement there exists the option to change the tube length to increase the heat transfer.

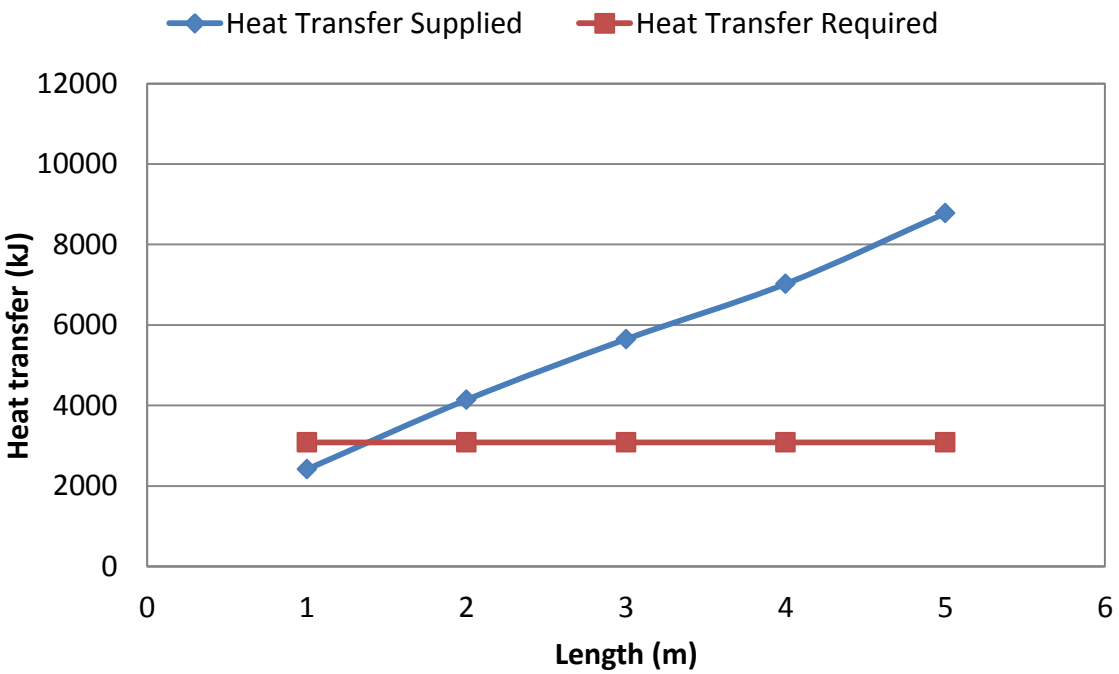


Figure 5.2.5: Illustrates the relationship between heat transfer and tube length

As shown previously, any length over 1.3m for this configuration will supply sufficient energy for drying. In order to compensate for heat loss to the environment a slightly longer length was chosen. The length of the tube has the greatest effect on heat transfer and

therefore the energy supplied. However, due to manufacturing cost, space constraints and friction losses in the pipe, the length of the tube was limited. The heat transfer required can be achieved with 16, 10mm tubes that are each 2.2m long. This results in a heat transfer of 4479.9 kJ, which means the heat transfer is approximately 30% more than what was required.

The above calculations apply to the heat exchanger i.e. the exhaust gas to the air. From this, the air exit temperature could be calculated and the heat transfer could be calculated from the air to the feedstock. This calculation is similar to the exhaust gas over the wood with the exception of the air properties (Table 5.2.8). Thermal conductivity of wood is also included in the table.

Table 5.2.8: Air Properties at 190°C and 1atm [32]

| Property | Symbol | Value | Unit |
|---|---|---|---|
| Density | ρ | 0.747 | $kg/m^3$ |
| Prandtl | Pr | 0.683 | |
| Viscosity | μ | 2.514E-05 | kg/m.s |
| Thermal Conductivity | $k_{wood}$ | 0.12 | W/m.°C |

Therefore the mean velocity was now

$$U_m = 4.45\ m/s$$

The heat transfer to the wood from the air was calculated using the bulk temperature of the air and the total surface area of the wood.

$$\therefore T_{exit} = 64.4\ ℃$$

$$and\ T_{surface} = 267.6\ ℃$$

$$Nu_d = 21.7$$

$$\therefore h = 39.8\ W/m^2\ .℃$$

$$\therefore q = 3937.4\ W$$

The energy supplied for the optimum configuration is then

$$energy\ supplied = 7848.9\ kJ$$

$$\therefore energy\ supplied \gg energy\ required$$

Therefore the calculations reveal that it is feasible to use the above mentioned configuration to dry the wood, with 60% more energy supplied than what is needed.

### *5.2.7 Heat Exchange Conclusion*

The hot air inside the tube and the feeding (motion) of the feedstock by the screw feeder improves the heat transfer allowing reduced residence time. Theoretically if the tubes were 1.3m long there would be sufficient energy to dry the wood. However due to external heat loss the tube length was increased to 2.2m to compensate for these losses. Also to further minimise the losses the shell of the heat exchanger was insulated, see Appendix C. Care needs to be taken to not get the biomass too hot and start pyrolysis reactions. The feed rate was to ensure that the feedstock would not be exposed to the hot air for long enough that pyrolysis would start. A counter flow arrangement was used in the heat exchanger to ensure that the air would be at its maximum temperature when leaving the heat exchanger.

In summary, the final heat exchanger design comprised a shell and tube counter flow heat exchanger with 16 10mm tubes each 2.2m long.

# 6. COMMERCIALLY AVAILABLE GEK GASIFIER

## 6.1 The GEK Gasifier

The GEK gasifier forms part of the GEK Power Pallet that is commercially available from All Power Labs, Berkely, USA [7]. It is a complete biomass power generation solution that converts woody biomass to electricity or heat. The Power Pallet comprises the GEK multi-stage gasifier, spark fired industrial engine, generator, and electric controller. TOTTI or Tower of Total Thermal Integration is claimed to be an innovative "waste heat" capture and recycling system. Traditionally hot output wood gas from the gasifier has been problematic, requiring cooling components and extra space. The GEK TOTTI uses the "waste gasifier heat" and engine exhaust heat for new useful inputs in the gasification process, see Figure 6.1 This system improves tar conversion, fuel flexibility and general efficiency of the Power Pallet system [7].

The customary reactor for the GEK is an Imbert type downdraft reactor. The standard 3" (76.2mm) hearth and nozzle configuration are claimed to run 5-20hp engines or 3kW to 12kW of electrical load.

## 6.2 GEK Gasifier Claim

The TOTTI system results in higher cracking and combustion temperatures for improved conversion, increased tolerance for high moisture content fuels, and improved gasifier efficiency. Due to the nature of this dissertation only the Auger Feed Drying Bucket part of the system was analysed. The Auger Feed Drying Bucket uses output wood gas to dry the incoming fuel by vaporising the water contained in the fuel. The dryer is said to deliver good performance on regular wood chip fuels with up to 30% moisture content.

## 6.3 GEK Gasifier Critique

In Chapter 5 a shell and tube heat exchanger arrangement (option 1) was analysed and found to be insufficient for drying the wood. The GEK Drying Bucket represents the same concept as the shell and tube heat exchanger except there are some changes in the parameters, see Figure 6.1.

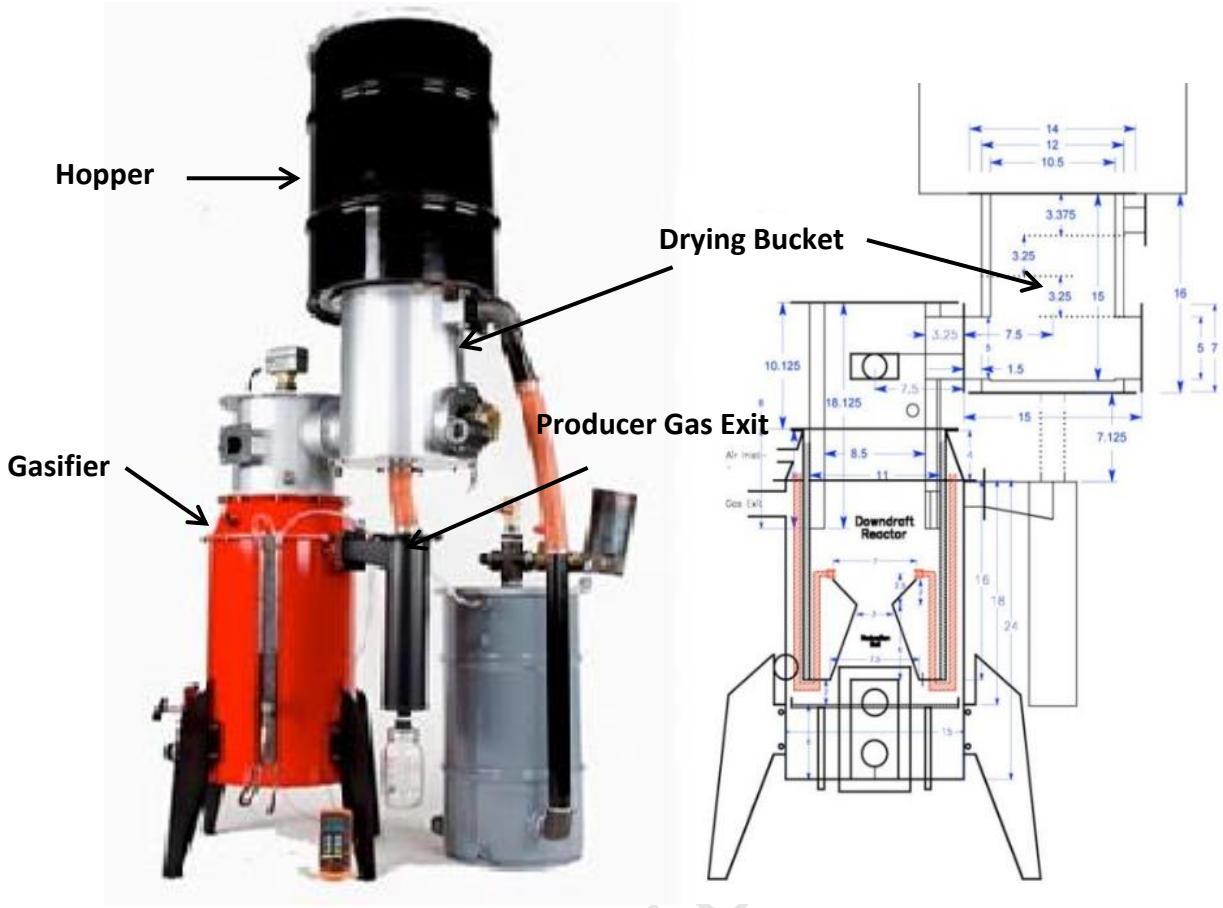


Figure 6.1: GEK Gasifier with Hot TOTTI [7]

The design uses a bucket surrounded by a shell in which the output wood gas from the gasifier flows. The claim is that the gas is sufficient to dry the wood through the wall of the bucket. Table 6.1 below shows the parameters of the Auger Feed Drying Bucket.

Table 6.1: Auger Feed Drying Bucket Parameters

| Parameter | Symbol | Value | Unit |
|---|---|---|---|
| Bucket Diameter | $D_b$ | 266.7 | mm |
| Bucket Height | $H_b$ | 381 | mm |
| Shell Diameter | $D_s$ | 266.7 | mm |
| Flow Area | A | 0.017 | $m^2$ |
| Mass of wood | M | 2.13 | kg |
| Wood gas Mass Flow | m | 0.01 | kg/s |

The calculations were based on a 20kW gasifier therefore resulting in a wood consumption rate of 1.43g/s. The mass flow of the wood gas was calculated from the GEK website using a density of 0.95kg/$m^3$. The temperature of the wood gas was assumed to be 500°C with

allowance for some heat loss in the system and the temperature of the air in the bucket is assumed to be initially at 25°C. The mass of wood in the bucket was calculated as previously in Chapter 5.

From the mass of the wood the energy required for drying wood of 30% moisture content was then:

$$energy\ required = 1888.38\ kJ$$

The calculation method for the heat transfer of a shell and tube followed the method outlined in Chapter 5 where the heat transfer from the wood gas to the bucket wall was the same as the heat transfer from the bucket wall to the air.

$$q_{outside} = q_{inside}$$

And

$$q = hA(T_b - T_w)$$

Using solver to solve for the unknown temperatures, the results are tabulated below.

Table 6.2: Calculated Temperatures for GEK bucket dryer configuration

| Symbol | Value | Unit |
|---|---|---|
| $T_{wood\ gas\ exit}$ | 197.47 | °C |
| $T_{air\ in\ bucket}$ | 70.36 | °C |
| $T_w$ | 206.01 | °C |



From the above calculation it is already clear that the system will not be able to dry the wood. The temperature does not reach the required vaporization temperature for water of 100°C and was only 70°C.

In terms of heat transfer the energy supplied by the wood gas was:

$$q = 160.52W$$

$$energy\ supplied = 239.59\ kJ$$

$$\therefore energy\ supplied \ll energy\ required$$

The energy supplied was significantly less than what was required to dry the wood. Even if the residence time of the feedstock inside the bucket were increased it would take four hours to dry under these conditions. The theory of the GEK Auger Feed Drying Bucket is correct in principle but the surface area and heat transfer area are insufficient as shown in the above calculations.

# 7. GOOD DESIGN PRACTICE AND SAFETY

## 7.1 Potential Hazards

There are numerous health and environmental hazards associated with the operation of a gasifier system of which toxic gas, fire, and explosive hazards form the main elements. These hazards should not be taken lightly or underestimated.

### 7.1.1 Toxic Hazards

Carbon monoxide is an extremely toxic and dangerous gas as a result of its propensity to combine with the haemoglobin of the blood and therefore prevent oxygen transport and absorption in the body. CO is produced in the operation of the gasifier and therefore it is necessary to ensure that the room is either well ventilated or the gasifier is operated outdoors. CO exposure symptoms can range from mild headaches at 200ppm to unconsciousness or death at 12800 ppm. Prolonged exposure to syngas is believed to cause tiredness, irritability, and difficulty in sleeping [33].

### 7.1.2 Fire Hazards

One of the unavoidable hazards of a project of this nature is the presence of hot surfaces (> 500°C) and the risk of fires, and the associated hazards thereof. There is a risk of sparks in the feeder or flames when refuelling. All of these can cause serious burns if the proper precautions are not taken [10]. Another cause of fire associated with biomass feedstock is the condensation of resins that are released from the material during drying. If the resin is allowed to condense it may attract dust. This resin dust mixture is extremely flammable and can build up and ignite at a later stage. The greatest risk of fire is when dry, hot, feedstock leaves the dryer and comes into contact with fresh air. The longer the feedstock is exposed to high temperatures the lower the moisture content but the greater the risk of fire [24].

### 7.1.3 Explosion Hazards

An explosion can occur if combustible gas is mixed with sufficient amounts of oxygen/air. Possible reasons for this are:

- Oxygen/air leaks into the gas system. In general, air leaking into the gasifier does not lead to an explosion. If the leak is in the lower section of the gasifier, this will result

in partial combustion of the gas causing the gas outlet temperature to be higher and the quality of the gas to decrease.

- Oxygen/air entering when refuelling can cause an explosive mixture when mixed with the pyrolysis gases. The refuelling unit in this project was equipped with a gate valve to prevent this problem.
- Oxygen/air leaking into a cold gasifier still containing gas. Therefore cold gasifiers should always be ventilated before start-up [10].
- Hydrogen leak from the syngas – mitigated by operation at sub atmospheric pressures

### 7.1.4 Environmental Hazards

The exhaust gas from a biomass drying system may require treatment as it can contain sulphur dioxide ($SO_2$), nitric oxide ($NO_x$), carbon monoxide (CO), and particulate matter [24]. Ash and condensate in the form of water vapour are formed during the gasification process. The condensate can be polluted by tar, which is difficult to dispose of without having adverse effects on the environment. Ash on the other hand is not considered an environmental hazard [10].

### 7.1.5 Other potential hazards

The other hazards that can be encountered in the operation of the gasifier system are related to the test engine being used. These range from hot surfaces to dangerous moving parts. Other moving parts also include the screw feeder as well as the chain drive used for the agitators.

## 7.2 Precautions taken

- The dryer and gasifier must be designed to minimize the risk of fire and should be equipped with a fire suppression system.
- Fire detection equipment should be installed in the vicinity of the dryer and gasifier. Shutoff valves should be installed for the air and fuel supply.
- A fire dump can be utilized to prevent smouldering material from reaching the fuel supply.
- All air/gas inlets to and from the heat exchanger/gasifier should be equipped with a double block device for isolation or intervention.
- Exhaust ports should be located close to the ventilation or extraction system.

- Gas alarms in exposed areas (carbon dioxide/monoxide sensors)
- Pipes reaching 500°C must be all-welded to insure a gas tight seal and fitted with heat shields.
- Pressure and temperature sensors included in the safety circuit should be duplicated for redundancy
- Escape routes to fresh air should be clearly marked out from gasifier and engine room
- Moving parts should have safety guards and equipped with emergency stop
- Safety switches and load sensors on rotating parts with intrinsic fail-safe design
- Sensors and safety devices should be checked regularly
- The appropriate personal protective equipment must be worn
- Insulation was placed where possible
- Warning signs indicated hazards
- Unauthorised personal may not operate any part of the system
- Provide an operating manual

# 8. FEEDSTOCK ANALYSIS

## 8.1 Feedstock Description

The feedstock used for analysis and feeding was pine timber-yard waste obtained from P.J. Van Reenen Timbers, Sedgefield, South Africa, in June 2012 and stored indoors in refuse bags. Timber-yard waste is different to standard wood chips in that it consists of various different components of the tree, namely; wood chips, wood shavings and more often than not, bark fragments.

## 8.2 Feedstock Physical Properties

The amount of feedstock contained in the feed pipe at any given time was assumed to fill half the volume of the pipe. The average wood dimensions were measured, Table 8.1. The bulk density was measured, from this data it was possible to estimate the number of shavings contained within the feeder pipe as well as the total surface area of the wood shavings. It is important to note that this is purely an average for calculation purposes, the actually feedstock used varies greatly in size and shape, see Figures 8.1 and 8.2.

Table 8.1: Feedstock average dimensions

| Parameter | Symbol | Value | Unit |
|---|---|---|---|
| Wood length | l | 0.120 | m |
| Wood width | b | 0.015 | m |
| Wood thickness | t | 0.002 | m |
| Tube Volume | $V_{tube}$ | 0.027 | $m^3$ |
| Volume occupied by wood | $V_{wood}$ | 0.014 | $m^3$ |
| Wood shaving Volume | $V_{shavings}$ | 0.0000036 | $m^3$ |
| Number of shavings | # chips | 3755.4 | |
| Total Surface Area | Area Chips | 6.76 | $m^2$ |
| Mass of wood | $m_{wood}$ | 2.704 | kg |

## *8.3 Moisture Content Experiment*

A sample of timber-yard waste was placed in a beaker in an oven and dried in air to a constant weight at 105°C [34]. The mass of the sample was measured before and after drying to determine the moisture content contained in it. Examples of each of the samples are shown in Figure 8.1 and 8.2.

Figure 8.1: Feedstock sample: bark (left), wood chips (right)

Figure 8.2: Feedstock sample: wood shavings (left), unsorted sample (right)

Two samples were left outdoors in the rain to assess the climate/weather effect on moisture content. The results revealed a moisture content of 65.6% and 64.9% for each sample. This is higher than the literature value for forest products of 60% due to hydroscopic nature of the samples.

The moisture content of 10 samples was determined for the entire sample of timber-yard waste as well as its different constituents. The experiments were performed three weeks after the date of delivery of the feedstock. The time from when the tree was cut down to the time of delivery was unknown but anecdotal information indicated that it was no more than a few days. The average moisture content of the timber-yard waste samples were 53.7% with a standard deviation of 1.6%. The high standard deviation was due to the inconsistency of the samples. Note that the shavings, which were easily sorted, have a lower standard deviation. The reason for the high moisture content of the samples was presumed to be because of the high presence of bark. The moisture content of 10 bark samples were determined to validate the reason for the high moisture content. The bark had an average moisture content of 64.8% (standard deviation of 0.9%). This is higher than the literature value of about 60% and is likely due to the species of wood and the climate. It was clear that the presence of bark in the timber yard waste led to the high moisture content. The moisture content of wood chips and shavings from the timber-yard waste were also determined in isolation and found to have a moisture content of 46.3% (standard deviation 0.9%) and 49.7% (standard deviation 0.5%) respectively.

Thermogravimetric analysis (TGA) experiments were conducted on various feedstock samples but due to the size of the samples the results were inconclusive. The method shown above is a clearer representation of the moisture content of the bulk of the sample that was used for test throughout the project.



## *8.4 Feedstock Handling Analysis*

As highlighted in the literature section, the single most important aspect of a gasifier system is the reliable flow of the feedstock. A screw feeder was chosen to feed the wood because of its low cost, low power consumption, low maintenance requirements, and its ability to meter the feedstock. The practical concerns of feeding the above mentioned feedstock were analysed prior to the design of the feeder. These concerns were: bridging/arching, compacting, maintenance requirements and feed rate.

The initial, prototype feeder used was a wire screw of 40mm outside diameter and 40mm pitch with a wire diameter of 5mm. Through various configurations and experimentation a number of key issues were highlighted when dealing with the feedstock. These included:

- The screw feeder bored a hole through the biomass (rat hole), this was expected.
- The material did not flow down an incline due to friction and only flowed when the angle was greater than 60°
- The material quickly bridged above the screw feeder inside the hopper
- The larger pieces of material wedged at the pipe exit (arching)
- The nature of the screw feeder caused the feedstock to compact often compressing the spring

The wire feeder was modified by attaching washers to it with a larger feed pipe being used to accommodate the washers. The washers made a significant difference to the reliability of the feed and prevented a rat hole from being formed. They also assisted with preventing the feedstock from compacting at the transition from the hopper to the tube. Bridging however did occur in the hopper. This was because the opportunity for arching still presented itself in the area where the hopper joins the screw feeder trough, thus highlighting the need for straight vertical walls.

The hopper was modified to a single, rectangular column, with the screw feeder at the bottom.

- The hopper occasionally emptied itself and was therefore unreliable.
- The increased height of the column required to maintain the hopper volume led to bridging.
- It was discovered that the friction between the rig walls and the biomass material also increased the probability of bridging.
- A weight was placed on top of the biomass and the material fed through without interruption but without any noticeable difference in the feed rate.
- It was concluded that some sort of an agitator was needed to prevent bridging.

An agitator/feeder idea was conceived from the design of a rotary feeder. In this case, wooden dowels were equally spaced on a wooden shaft in two planes (Figure 8.3).

Figure 8.3: Photo of experimental agitator

The agitators prevented bridging by collapsing the bridge when they were rotated. Figure 8.4 illustrates the feedstock bridging on the stationary agitators, highlighting the flow issues associated with this feedstock.

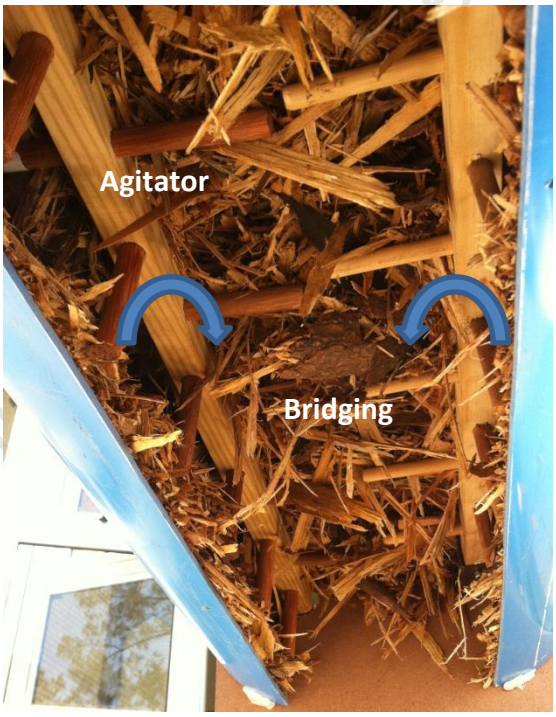


Figure 8.4: Image of the feedstock bridging on the agitator

Having established a proof of concept, the volume would need to be increased to the desired amount and the agitator would also need to be automated. Two agitator shafts rotating in opposite directions were used to increase the volume, see Figure 8.4. Mild steel shafts were used as opposed to wooden shafts and they were geared and coupled to a motor.

## *8.5 Feedstock Analysis Conclusion*

Every biomass fuel has different characteristics, especially related to flow characteristics. There is no single system that will successfully feed all biomass fuels and for this reason each fuel needs to be assessed individually and the feeding system then designed accordingly. In this case the biomass used in this project consisted of three distinct fuels; chips, shavings and bark.

The agitation concept that was conceived worked extremely well at preventing bridging in the hopper and aided in the feeding of the biomass feedstock. The screw however needed to be further assessed on a larger scale as a wire screw would be too flexible over a 3m length. The washers used also aided in the feeding and it was planned to use a similar component in the final design.

Overall, the timber yard waste had a higher moisture content than presumed or suggested by the literature. The average moisture content of the timber-yard waste samples were 53.7% with a standard deviation of 1.6%. The residence time was increased to allow for suitable drying however as the literature suggests, any moisture content between 10% and 20% would be adequate for gasification. The heat exchanger was sized for drying from 40% to 0% moisture content.

# 9. DESIGN

A modular design approach was taken for this project where the system was designed in three separate sections and then merged to form a single entity. The sections include the fuel handling section (hopper), feeding section, and the drying section (heat exchanger) which together makes up the complete pre-treatment system as shown in Figure 9.1.

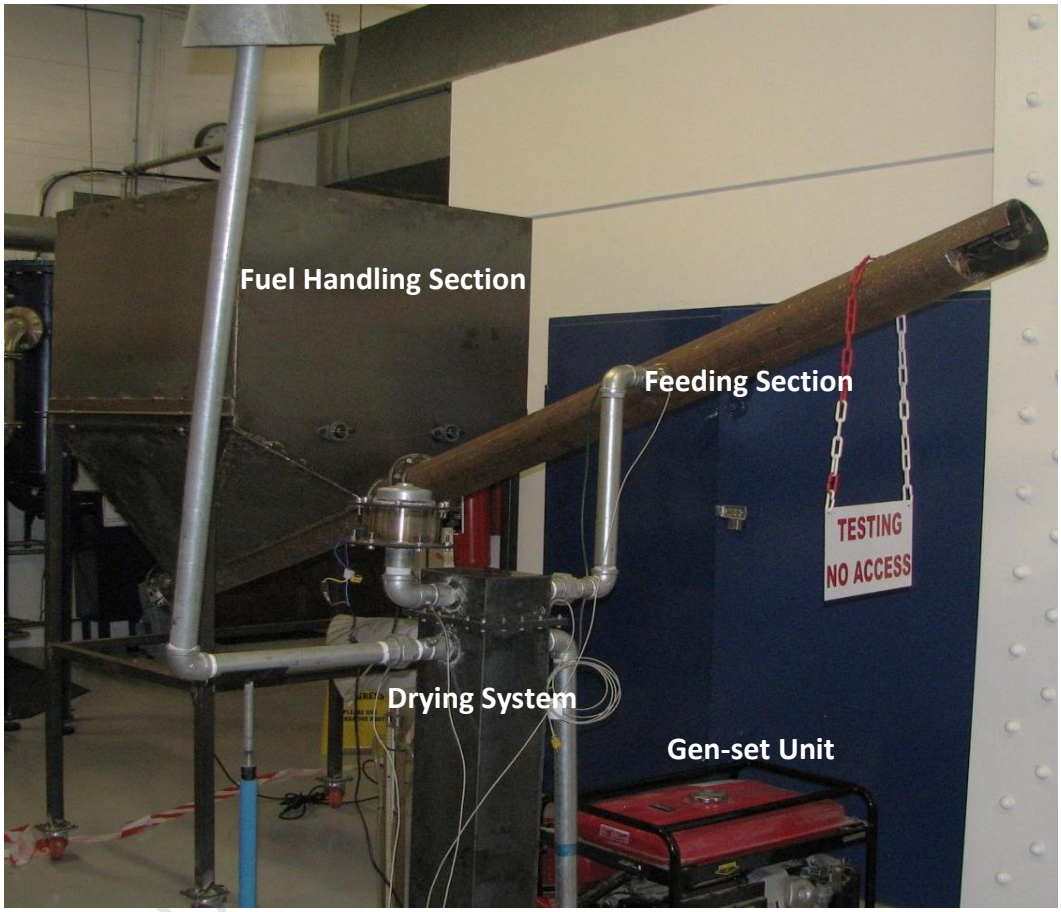


Figure 9.1: Photo of pre-treatment system

## *9.1 Fuel Handling System*

The gasifier was to be batch-fed from a one cubic meter hopper tapered to a nominal 130mm pipe which forms the trough for the screw feeder. The advantage is this is a low cost simple design and construction. The disadvantage of batch feeding is the need for manual labour to fill and empty the hopper as well as irregular gas generation due to the opening of the gasifier for feeding (contamination). This can be overcome however by diligent observation and refilling of the hopper. Batch feeding allows the appropriate time for the feedstock to dry. To minimize the refuelling needs the hopper was designed to be one cubic meter with the feeder

pipe inclined at 20° so that the feedstock could be fed directly into the top of the gasifier which stood at 1.8m and is 3.2m long. An auger/screw feeder was chosen to feed the wood due to its simplicity and cost benefits as highlighted in the literature review; also using ta screw feeder allows the option of drying the feedstock in the feeder pipe.

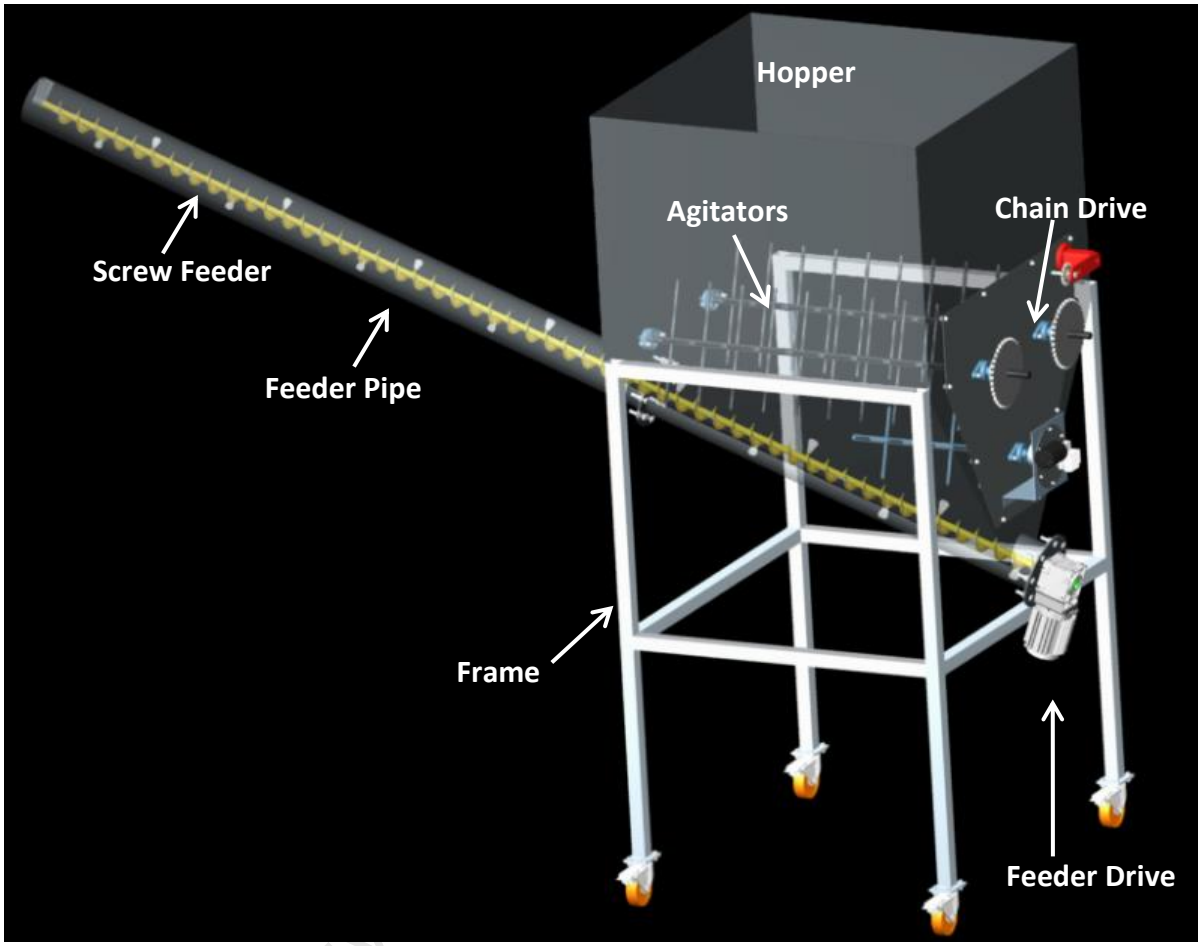


Figure 9.2: Rendered image of fuel handling system

Figure 9.2, above, shows the major components for the fuel handling section and the feeding section.

The literature review and experimental work highlighted the problems of compacting, arching bridging and rat holing associated with woody biomass. Basu 2010 [5] suggested using a variable pitch screw, variable diameter screw or a wire screw. Experimentation showed that a wire screw compressed easily with this type of feedstock and was also not sufficiently rigid over a 3 meter length. Compacting was further minimised by using a screw with a large clearance between the flights and the pipe.

The screw dimensions and drive were chosen based on the screw feeder calculations in Appendix A. The screw (Figure 9.3) had an outside diameter of 60mm, a pitch of 60mm and a blade thickness of 2mm.

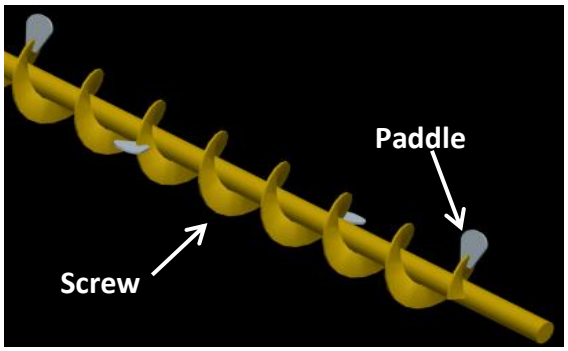


Figure 9.3: Rendered image of screw with paddles

The screw was housed inside a 130mm inside diameter pipe and driven by a 0.25kW SEW Eurodrive motor with a variable speed controller, see Figure 9.4. The calculated power required for this size screw feeding the specified feedstock was 0.18kW with a total torque of 103.5N.m for the required feed rate (see Appendix A).


Figure 9.4: SEW Eurodrive variable speed controller (left), Eurodrive motor (right)

Experimentation and literature also indicated the need for agitation inside the hopper. Three agitators were mounted inside the hopper and driven by a chain drive to prevent the feedstock from bridging, see Figure 9.5. The drive consisted of two 38 tooth driven 10B sprockets and a driver sprocket of 19 teeth driven by a modified automotive windscreen wiper motor. An idler sprocket was used to tension the chain and allow two of the agitators to rotate in the opposite direction with the third agitator being coupled to the motor.

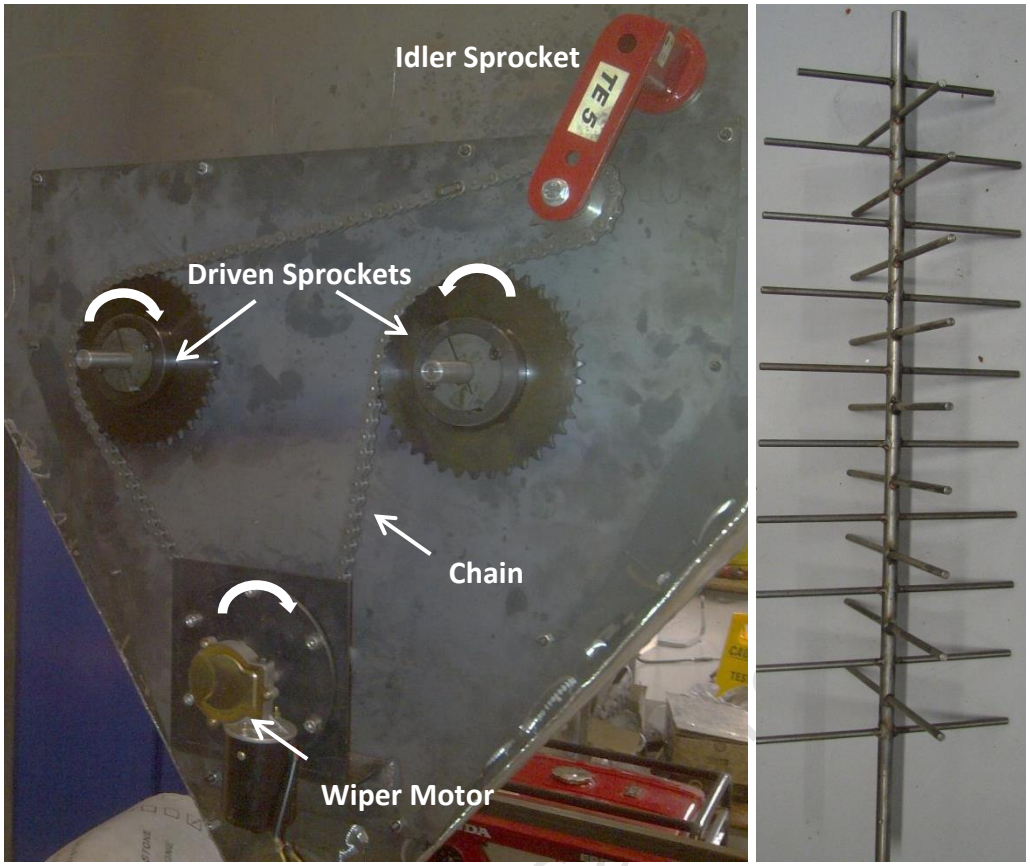


Figure 9.5: Chain drive (left), Agitator (right)

A hanger bearing with brass bush was located at the outlet and supported from above to prevent wear of the shaft, see Figure 9.6. The outlet of the pipe was also cut to aid in the discharge of the feedstock and minimise arching, see Figure 9.6.

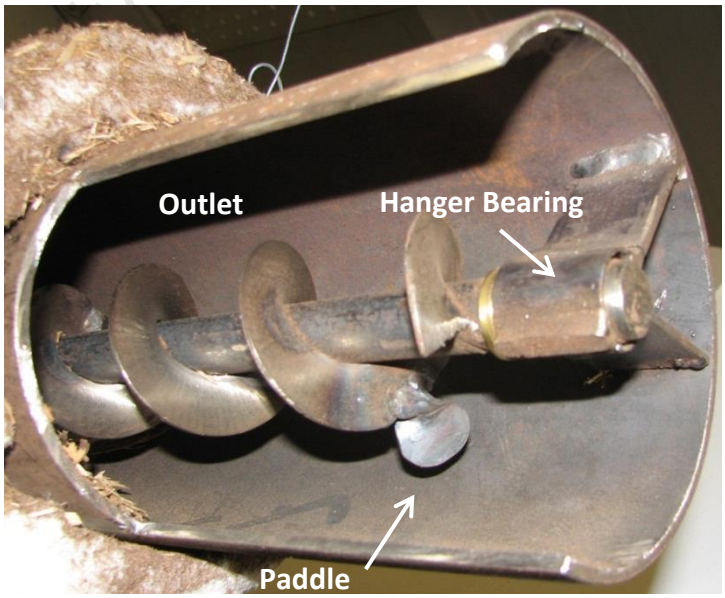


Figure 9.6: Outlet with hanger bearing

Paddles were welded onto the screw at intervals inside the hopper with one paddle located at the outlet end of the feeder (see Figure 9.3 above) to aid in flow and prevent the feedstock from compacting or forming rat holes.

The hopper was bolted onto a support frame with trolley wheels bolted onto the feet of the frame to allow for easy manoeuvrability of the unit.

## *9.2 Drying System*

The scheme described in Chapter 5 was used to calculate the best option for drying the wood. The model revealed that 16 tubes of 12mm outside diameter with a 1mm wall thickness would be sufficient for the heat exchanger. The tubes were stainless steel due to the material's resistance to corrosion and they were cheaper than copper tubing.

A shell and tube counter flow heat exchanger design was selected with a single pass for the exhaust gas and also for the air. The air would flow inside the tubes and the exhaust gas in the shell around the tubes. The critical aspect of this design was to minimize the flow area of the exhaust gas thus increasing the velocity and therefore the heat transfer and therefore match the design assumption.

A staggered tube arrangement was chosen over an in-line arrangement as this resulted in an 11% increase in heat transfer due to the reduced area between the tubes (see Figure 9.7).

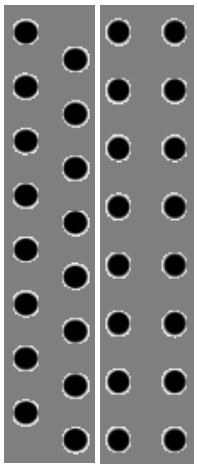

Figure 9.7: Staggered (left) versus in-line (right) tube arrangement

Note: Only the area around the holes was considered for the external flow calculations.

The tubes were bent into a U-shape arrangement and fitted to a bulkhead plate using Swagelok NPT fittings, see Figure 9.8. Ideally the tubes should have been welded to the plate but due to the fact that a permanent fixture was not desired and the welding constraints of using 32 fittings this option was avoided.

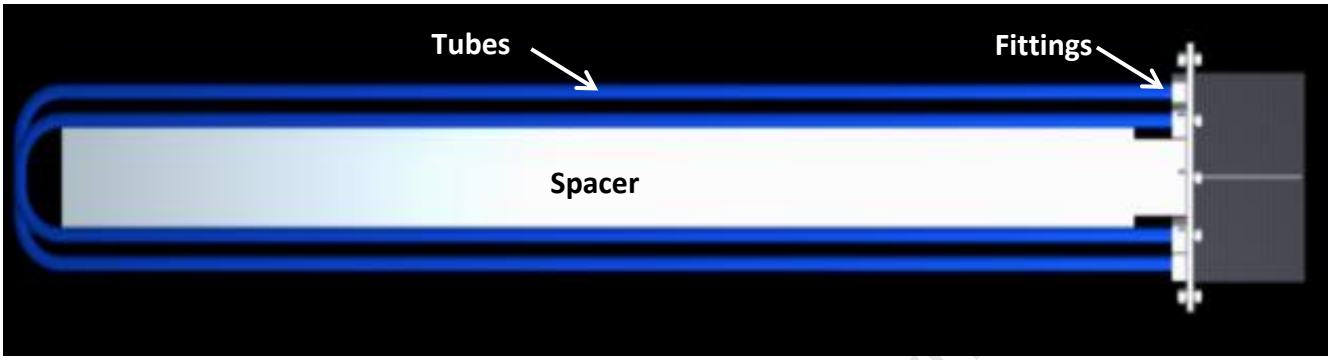


Figure 9.8: Rendered view of the U-shaped tube arrangement

The excess area in the staggered arrangement was minimised by using a spacer to fill the gap between the inlet and exit sections of the shell, see Figure 9.8 and 9.9.

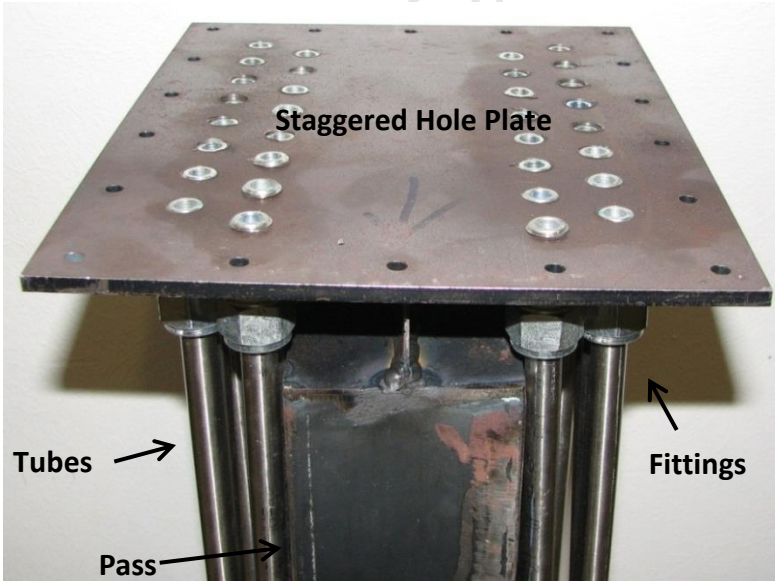


Figure 9.9: Photo of the spacer (to fill unused void space) and the tube bank

All the tubes needed to be bent exactly the same due to the tight tolerencing required to reduce the flow area. For this reason a jig was made to aid in the bending but further manipulation of the tubes was still required.

The exhaust gas was supplied by the engine as specified in Appendix E. The air was to be driven by a blower at roughly the same flow rate as the exhaust gas while overcoming the

losses in the heat exchanger (Appendix B). A blower could be used to either blow air into the drying section or pull hot air through the system. Considerably more power is needed to pull the air than to push it because the gas is less dense. In addition suction requires the fan to handle higher temperatures [6].

A 1.2 kW modified vacuum cleaner fan, with a rotor diameter of 120mm running at 2500rpm, was chosen as the drier fan to drive the air through the system due to its simplicity, extremely low cost when compared to other commercially available blowers and its ability to overcome the losses associated with the system (see Appendix B), see Figure 9.10.

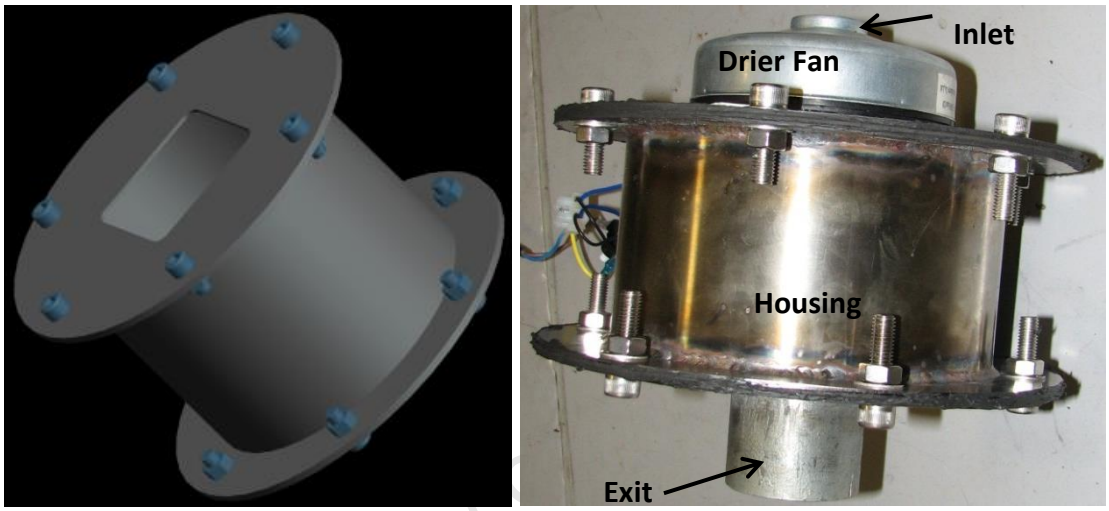


Figure 9.10: Rendered view of drier fan housing (left) Photo of drier fan in housing (right)

The drier fan unit was mounted in a housing that easily attached to the plumbing system. A gate valve was installed below the drier fan to control the air flow rate through the system, see Figure 9.11

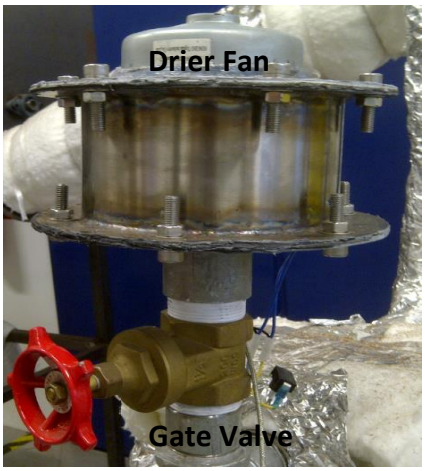


Figure 9.11: Photo of drier fan and gate valve situated below the fan

Three 1.3 kW electric heaters were purchased to load the generator unit so that the temperature of the exhaust gas reached a representative operating level of 500°C. The gen-set maximum generator power rating was 9.6kW so the drier fan was also run off the generator thus loading it at 5.1 kW.

The feeder pipe, heat exchanger and associated pipework were all insulated with fiberglass blanket to ensure minimal heat loss to the surrounding environment. The insulation calculations are shown in Appendix C.

## *9.3 Software and Hardware controllers*

The system was controlled and various parameters measured using National Instruments design software called LabVIEW and the necessary hardware. The variable speed drive was programmed and controlled through LabVIEW. If the screw feeder "jammed" the motor was programed to reverse for a given time period (10 seconds) in the hope of dislodging jammed feedstock. After the given time period, the motor rotated again in the forward direction with increased power. LabVIEW was programmed to perform this function when the current drawn by the motor increased above a given value (0.8A) indicating that the drive had stalled. LabVIEW was also used to view the temperatures read by the various thermocouples using the NI 9213 input module.

The hardware used and the body/brain block diagram used for programming is shown in Appendix D while Figure 9.12 displays the front panel view of the system in LabVIEW.

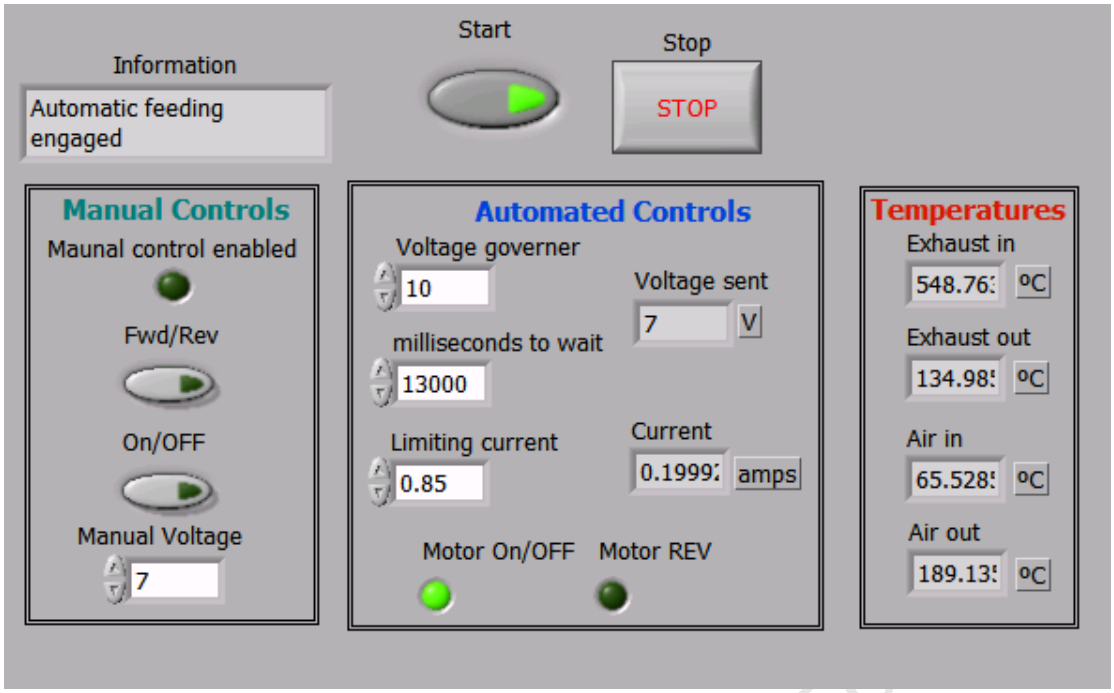


Figure 9.12: Automation Front Panel in LabVIEW

The system also included a manual control as shown on the left of Figure 9.12 as well as an emergency stop button for safety. An information box was displayed in the top left of the panel to allow the operator to know exactly what cycle the system was in at a given time.

# 10. EXPERIMENTAL DETAILS AND TESTING

## *10.1 Feeding*

The designed feeding system designed was discussed in Chapter 9. Testing was done to determine the feed rate of the screw feeder feeding at a 20° incline. The use of paddles on the screw was analysed to see if they positively increased the flow rate. The hopper was filled with the feedstock (described in Chapter 8) with feeding executed at various motor speeds to determine the optimum feed rate. The drive speed was set in LabVIEW by changing the voltage supplied to the variable speed drive. The feed rate was then determined by measuring the mass of wood collected at the outlet of the feeder in a measured time period.

## *10.2 Drying*

Chapter 9 showed all the major components in the drying section. The generator engine was started along with the drier fan and heaters and allowed to run until the desired exhaust gas (> 500°C) and air exit (> 200°C) temperatures were achieved. This took about 25 minutes. The temperatures were measured using multiple K-type thermocouples at various locations in the drying system and displayed using LabVIEW. Drying was performed while the feeder was running. Wet feedstock was loaded in the hopper. The moisture content of the fuel at the exit of the feeder pipe was measured and compared to the feed material in the hopper to determine effectiveness of the drier. The moisture content before and after drying was measured using the same method as described in Chapter 8. The feed rate of the screw feeder and the flow rate of the air were varied to investigate the effect on the drier effectiveness. The pressure drop across the heat exchanger tube bank (air flow) was measured using a U-tube manometer filled with mercury.

# 11. Results and Discussion

## 11.1 Feeding

The first test was to determine the feed rate of the screw feeder at different motor speeds. The voltage was varied from 6V to 10V in increments of 1V. The values of the feeder speed and average feed rate for each voltage is plotted in the bar graph illustrated in Figure 11.1.

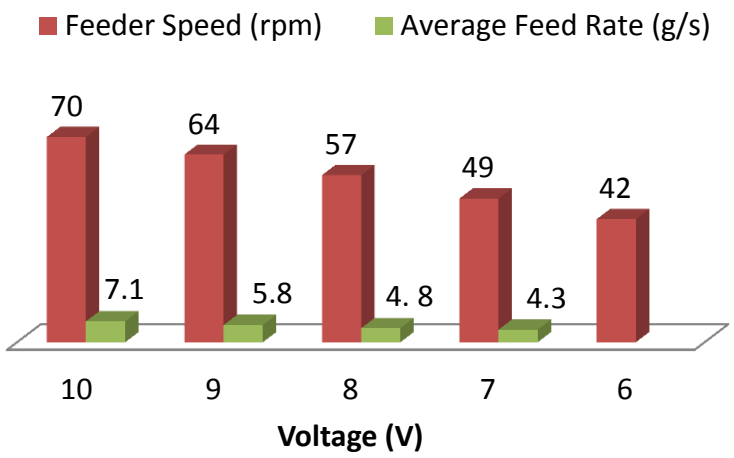


Figure 11.1: Illustration of the effect of feeder speed on feed rate.

Common sense dictated that the faster the screw feeder rotates the better the feed rate. However, it is important to note that the difference in the mass flow between 7 and 10 volts was 65% and 43% in rpm. At 6 volts and below the screw feeder would "jam" as the motor was not providing enough power and torque to reliably feed the feedstock.

The slowest feed rate of 4.3g/s was more than the required feed rate, based on the gasifier consumption rate of 1.36g/s. Therefore, the screw can be operated at far lower speeds but then the chance of the screw jamming greatly increases – or operated intermittently.

There were start-up issues when the screw feeder was engaged. The hopper needed to be empty or only slightly full when the screw feeder was engaged as the motor did not have enough torque to turn the screw when a large batch of wood was compacted on it. This issue was unfortunately not resolved but merely minimised with the agitators which limited the amount of wood that fell onto the screw when the hopper was filled. The agitators worked well to prevent the wood from bridging/arching inside the hopper.

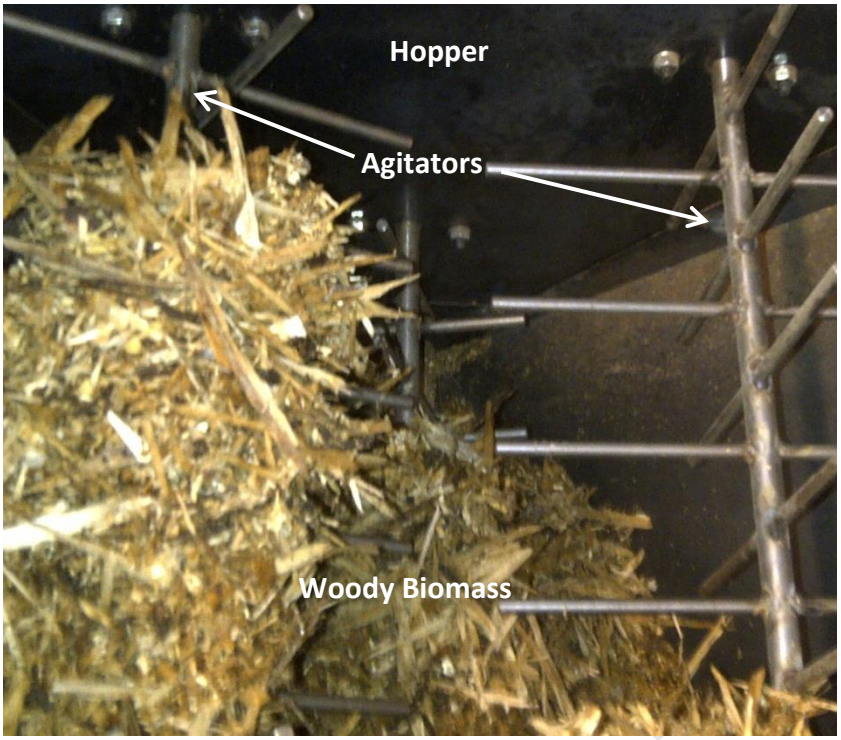


Figure 11.2: Photo of agitators inside the hopper

Figure 11.2 is a photo of the agitators inside the hopper. Note the wood resting on the agitator on the left until the agitators are engaged.

The fact that the screw feeder was inclined upward also meant that at faster speeds the feedstock motion was increased and thus due to gravity some particles would actually move back along the screw feeder. This was viewed in the hopper section of the feeder and was accentuated by the paddles which tossed the wood into the air. The paddles in the pipe section increased the severity of compacting inside the pipe and also caused bulk rotation of the shavings without driving them forward. Too many paddles likewise increased the torque required by the motor and did not allow the wood to travel along the screw. Care needed to be taken for the orientation and placement of the paddles ensuring that they faced the right direction and did not negate the effect of the screw feeder. The exact positioning of the paddles could be determined by computational fluid mechanics as assessing the orientation manually would require a great deal of grinding and welding, this was however outside the scope of the project. It also appeared as if the larger shavings travelled relatively slowly along the outer peripheral of the pipe.


Figure 11.3: Photo illustrating a rat hole and the effect of the paddles

The paddles did however prevent the screw from forming rat holes (Figure 11.3) or they collapsed the rat holes. They did increase the feeder efficiency but only when placed in certain positions. Since the paddles did not help when they were placed across the full length of the feeder, they were therefore placed only in the hopper section, the transition section from the hopper to the pipe and at the outlet.

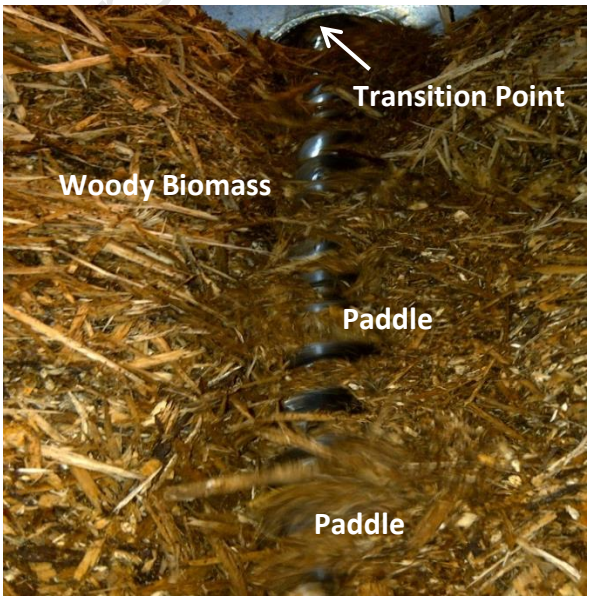


Figure 11.4: Photo illustrating the transition point and placement of some paddles.

The paddle at the transition point limited the chance of the feedstock from compacting in this area, see Figure 11.4. The transition point was generally the main area where the feedstock would compact and cause the screw to "jam".

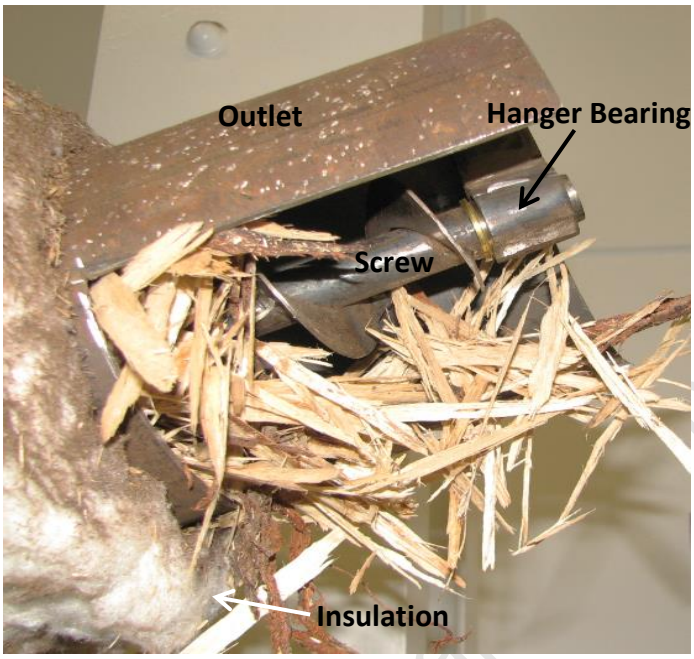


Figure 11.5: Photo of feeder outlet

At the outlet the paddle aided in breaking the bridge as the wood flowed out the exit, see Figure 11.5.

The feeder took roughly 15 minutes to feed wood from the hopper to the outlet. This value would vary though depending on how full the hopper was and the speed of rotation of the screw. The more fuel in the hopper the greater the feed rate. It was also observed that the hopper did not empty completely. This was due to the screw feeder being smaller than the pipe in which it was mounted as the smaller particles would settle in the trough of the feeder. The initial discharge from the outlet was generally the larger would shavings and only later the smaller wood chip particles would start to emerge.

Figure 11.6: Photo of troublesome large piece of wood

The feeder did occasionally "jam" for no visible reason but this was easily rectified with the programming of the motor to reverse then go forward with increased power and thus dislodging any wood particle that may have got stuck. Occasionally a large piece of wood would find its way into the feeder and easily "jam" the screw, see Figure 11.6. Therefore light screening was necessary to ensure these excessively large pieces were removed.

## *11.2 Drying*

Initial drying tests were performed at various feed rates with the gate valve completely open. The same feed rates as in Chapter 11.1 were used for drying. The initial moisture content of the feedstock was over 50% for each test sample. The temperatures that were reached inside the heat exchanger are shown in Table 11.1.

Table 11.1: Measured Heat Exchanger Temperatures

| Location | Label | Temperature | Unit |
|---|---|---|---|
| Exhaust in | $T_0$ | 556 | °C |
| Exhaust out | $T_1$ | 135 | °C |
| Air in | $T_2$ | 65 | °C |
| Air out | $T_3$ | 186 | °C |

The air temperature entering the heat exchanger was measured by a thermocouple situated after the drier fan and therefore was higher than ambient temperature due to the heat generated by the drier fan motor. The temperatures shown in Table 11.1 were significantly

lower than the temperature values used in the mathematical model. Although the model did not account for heat loss in the system, the values were still lower than anticipated (25 minutes would not have attained steady state heat of the heat exchanger). The desired velocity through the system was 7.9m/s according to the heat exchanger model. Upon measuring the velocity of the air through the system with a digital anemometer it was seen that the velocity was in fact 43.8m/s. This is far greater than what was used for the calculations of heat transfer. The heat exchanger model was then altered using this new velocity for air flow while keeping the calculated exhaust gas flow to find out the changes in temperature, see Table 11.2.

Table 11.2: Revised Heat Exchanger model temperatures

| Location | Temperatures | | Unit |
|---|---|---|---|
| | Old | New | |
| $T_{2exhaust}$ | 191 | 150 | °C |
| $T_{2air}$ | 315 | 197 | °C |
| $T_w$ | 228 | 137 | °C |

The change in velocity greatly affects the temperatures in the heat exchanger and this fits well with heat transfer theory. The air was not exposed to the heat from the exhaust for long enough to allow the temperatures to reach over 300°C. The increased air flow is however good for heat transfer which is a function of velocity. The calculated heat transfer from the increased velocity was 7935kJ which was 61% more energy than what was required; roughly double the original value of 30%.

Note that the new calculated values for the air and exhaust exit temperatures were within the range of experimental error and the differences could be accounted for by heat loss in the system. Also the air temperature was now below the temperature required for pyrolysis (> 204°C) and the auto-ignition temperature of wood (260°C).

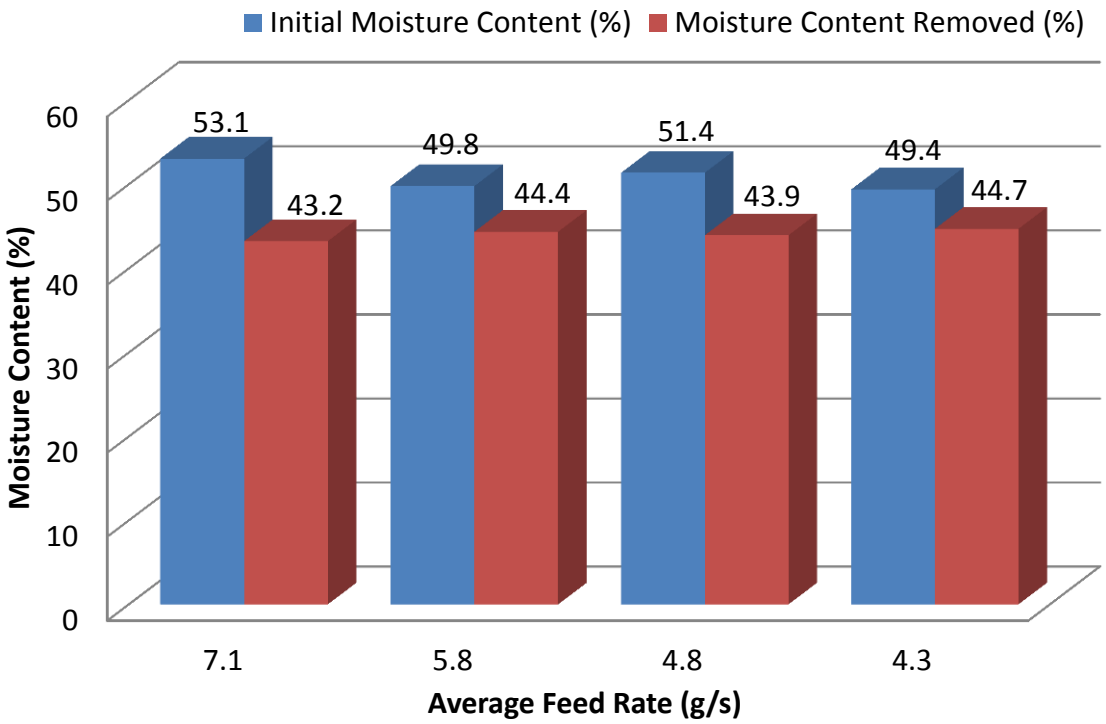


Figure 11.7: Graph depicting the effect of feed rate on percentage moisture content that was removed

Figure 11.7 illustrates the effect of feed rate on the drying performance. The moisture content shown on the graph is the percentage of moisture that was evaporated from the feedstock. Therefore for each test run the dryer was able to reduce the moisture content of the woody biomass to below 10%. As anticipated, the slower the feed rate provided a greater the residence time of the feedstock inside the dryer and a better the dryer performance. However, at 4.8g/s the trend was slightly inconsistent but this was within experimental precision. The variation can be accounted for by the irregular feeding rate as well as the varying composition of the feedstock as discussed in Chapter 8.

The uncertainty analysis for Figure 11.7 was based on a repeatability variation of 1 gram that was found during the experimental measurements. The precision of the measuring instrument was ±0.1 gram. Overall, the uncertainty associated with the moisture content experiments was determined as 3.5 grams or 7.9%. This was considered to be within the accepted region of experimental error (< 10%). It is also important note that there could also be a slight variation in the moisture content of the feed stock due to the relative humidity of the surroundings on the day of testing.

The next test was to investigate the transient effect of taking dry samples at different time intervals while feeding. The feeder speed was set at maximum with the gate valve fully open. The first sample was taken as the feedstock fed through the drier and then 10 and 20 minutes after that.

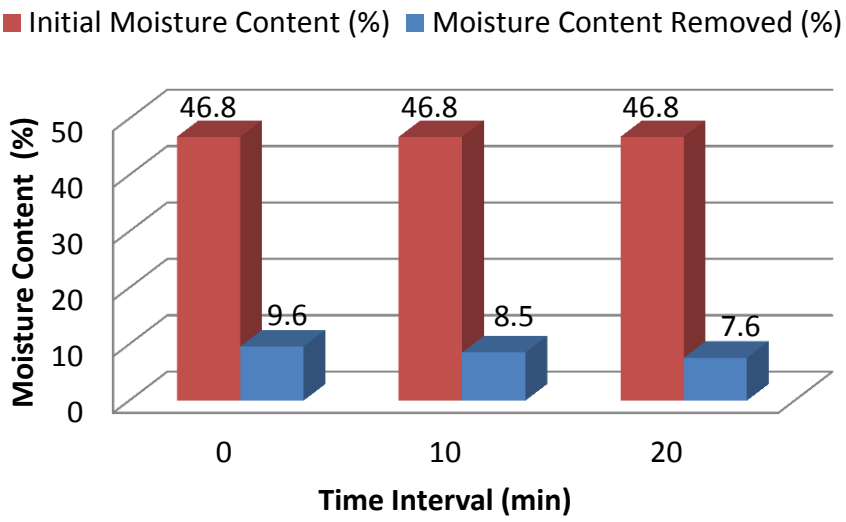


Figure 11.8: Illustration on the effect of taking samples progressively at different times

The initial moisture content of the feedstock sample was 46.8%. After 10minute time intervals dry samples were measured to determine their final moisture content. The time intervals only had a small effect on the drier performance; 2% for a 20 minute increase in time, see Figure 11.8, This meant that increasing the running time of the system beyond 20 minutes would result in a negligible increase in drying capability. This consequence was because as the hot air (still had drying capability) flowed into the hopper section, steam was emitted at the transition point, meaning drying took place not only in the pipe section.

The effect of increased residence time of the feedstock inside the pipe section was the investigated. The feedstock was fed through the drier at the maximum feed rate with the gate valve fully open until the feed material reached the outlet. The feeder was then turned off for 10 minutes and then a dry sample was taken. This was then repeated for hold times of 5, 10 and 15 minutes.

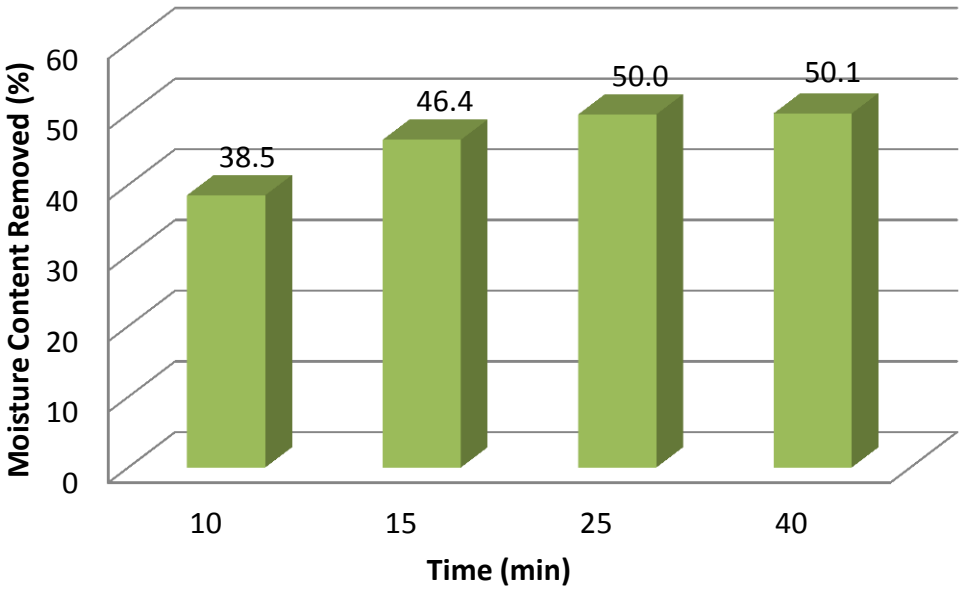


Figure 11.9: Bar graph displaying the effect of increased residence time in the dryer and percentage moisture content evaporated

As suspected the increased residence time increased the amount of moisture that was evaporated from the feedstock, see Figure 11.9. For a residence time of 15minutes, 50.1% moisture was evaporated from the wet biomass resulting in a final moisture content of 1.3%. The residence time of 10 and 15 minutes resulted in very similar drying capacities and it was discovered that a residence time of just less than 20 minutes would dry this feedstock sample adequately. Therefore the residence time of the feedstock in the drier has a substantial effect on the dryer performance and due to that fact that gasifier would be batched fed this aspect of drying is very relevant.

The practical effects of throttling the air flow in the system were then investigated to validate the change in velocity and its relationship to heat transfer. The gate valve was partially closed in various positions to throttle the air into the heat exchanger with the values showing the percentage that the gate valve was open, 100% being fully open. The throttling caused changes in the air velocity and thus the temperatures in the system, these results are illustrated in Figure 11.9.

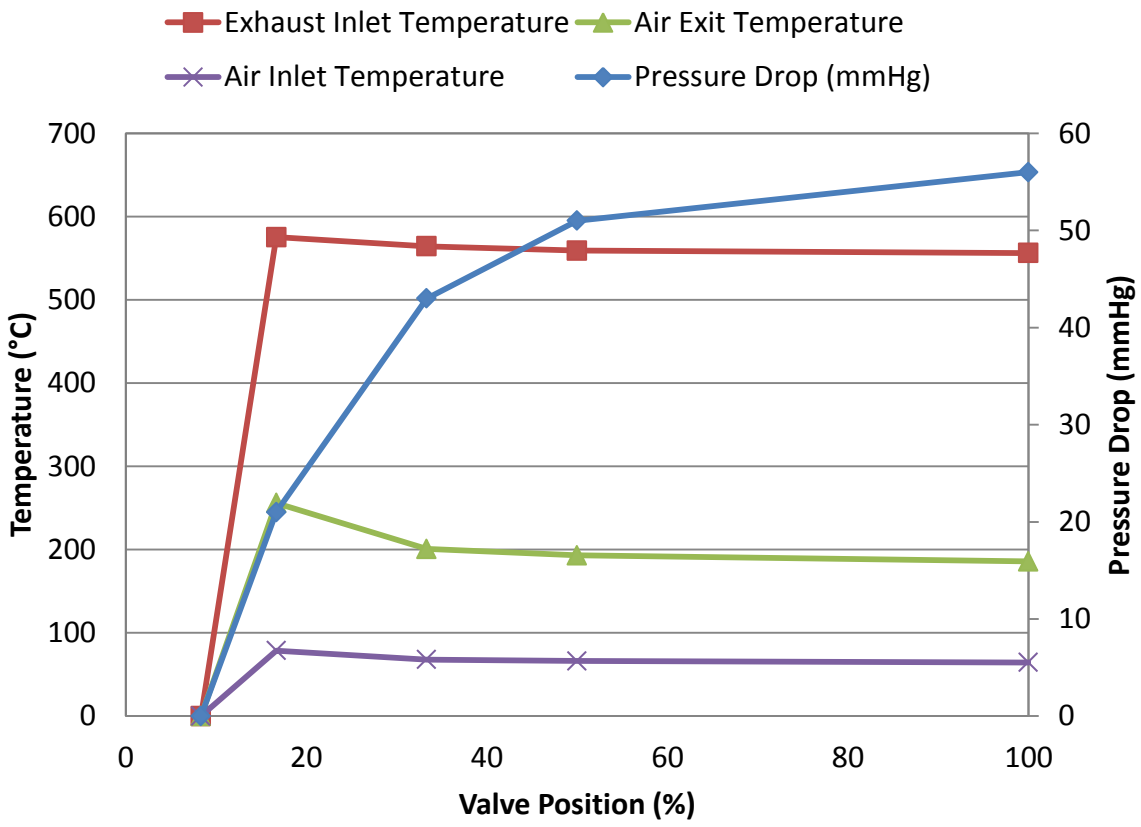


Figure 11.10: Illustration of the relationship between throttling the air and the heat exchanger temperatures.

As the air was throttled using the temperatures increase due to the decreased air velocity. This effect was however not only as a result of the velocity but also due to the increased work of the drier fan and thus the increased load on the generator. This is clearly seen by the increased air and exhaust temperatures into the heat exchanger. When the valve was open at 8.33% the drier fan stalled due to it being over loaded. The losses in the system were significantly increased and air was blown back and out the drier fan.

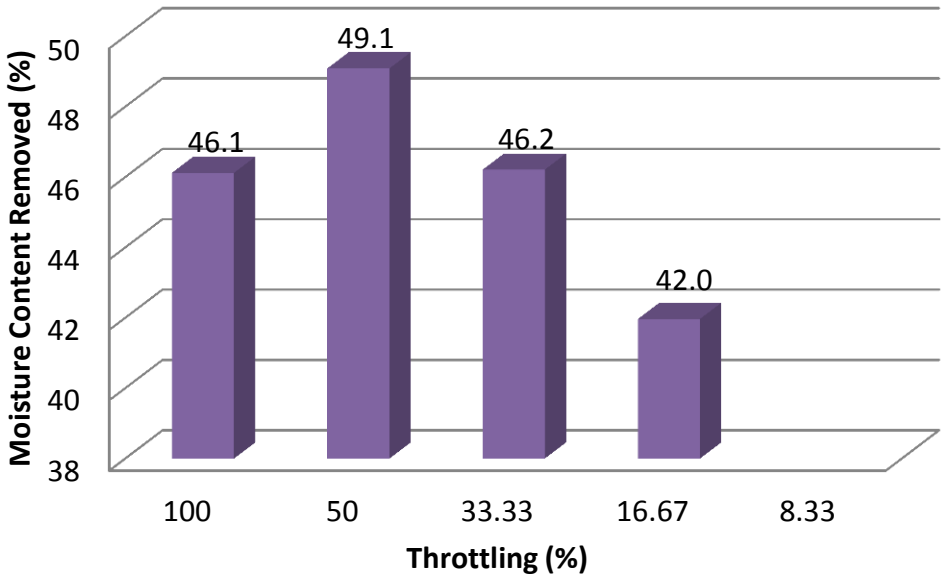


Figure 11.11: Illustration on the effect of throttling the air supply on percentage moisture content evaporated

As shown in Figure 11.11, the ideal operating condition for the drier was when the gate valve was 50% open, causing to a 3% greater drier performance compared to other throttling results. This was seen as the optimum balance between air temperature and velocity for drying the woody biomass.

## *11.3 System optimization*

The various tests allowed the ideal operating conditions to be identified to optimise the systems performance. The system was run with the gate valve 50% open, the voltage set at 7V giving a feed rate of 4.3g/s.

With this setup the drier was able to completely dry the feedstock with a moisture content of 53%. According to the gasifier model in Chapter 5 this would yield an increase from 54% to 81% in the gasifier conversion efficiency with the assumption that the exhaust gas used was "waste" heat which was not included in the energy review.

# 12. CRITICAL ANALYSIS

It is important to highlight some of the experimental/design issues arising from the system setup.

Firstly the feeder was not 100% reliable. The torque supplied from the motor was slightly lower than what was required to feed continuously. Increased torque on the screw feeder would minimise the risk of the screw jamming and also allow the feeder to feed when the hopper was full without the concern of the feedstock compacting on the screw. The incline of the feeder caused gravity to slightly negate the feeding although the feed rate was still suitable for the desired setup.

The heat loss in the system was ignored in the heat exchanger model. The flow area of the exhaust gas was greater than what was originally estimated. Minimising it would improve the heat exchanger performance. The reason for the lower flow rate was due to the tight tolerencing required for 16 tubes. Ideally the tubes should have been welded to the plate. However, use of standard pipe fitting was chosen for this prototype on account of the flexibility of experimenting with the number of pipes and dealing with leaks.

The feeder pipe internal wall finish may warrant further consideration as a rough finish hinders the flow of the feedstock through it in time. The drying in the pipe will cause the metal to oxidise and thus increase the surface roughness inside the pipe.

# 13. CONCLUSION

This thesis focused on the design, development, and comprehensive testing of a woody biomass gasification pre-treatment system. The literature review revealed a tendency of biomass gasification designers to experiment first before basing their design on the successes and failures of previous designs. A reliable, semi-automated feeding system was designed and built and allowed the feedstock to be successfully fed from a hopper to the top of a gasifier. The feeder occasionally would "jam" but this issue was rectified by programming the feed drive to reverse for a given time period and then move forward again. Paddles were welded on the auger in an effort to increase the feeding efficiency. The paddles only aided the feeding when placed in specific locations but did prevent rat holes from forming. The agitators that were mounted in the hopper worked adequately to prevent the biomass from bridging.

The model was based on a downdraft gasifier with ponderosa pine as the feedstock and indicated the ideal operating parameters for the specified gasification setup. At a gasification bed exit temperature of 800°C, the associated equivalence ratio was calculated at 3.13 which was within the typical theoretical range for gasification equivalence ratio. The effect of moisture content and temperature was also studied through the model. The model also suitably calculated the effect of moisture content on the lower heating value of the product gas and gasifier efficiency as well as the gas products.

Different methods of drying the wood were investigated and the calculations led to the design of a 16 tube shell and tube heat exchanger. The heated air was then used as a direct drying medium to reduce the moisture of the biomass fuel. The average moisture content of the timber-yard waste samples were 53.7% with a standard deviation of 1.6%. The heat exchanger proved to be extremely successful, drying feedstock with a moisture content of over 50%, to a target below 10%. This was well above the recommended maximum moisture content of feedstock for gasification of 15%. The system effectively increased the caloric value of the wood gas from 3.68MJ/kg to 5.52MJ/kg and the gasifier conversion efficiency from 54% to 81%. The results in this dissertation show the necessity for more consideration to be paid to the pre-treatment system and not merely the gasifier itself.

# RECOMMENDATIONS

The system performed satisfactorily but it could be improved by a few modifications or changes. As discussed in the critical analysis, the torque of the motor driving the screw feeder was lower than what was needed for reliable feeding and therefore a more powerful motor would be better suited for this application.

The low feed rates required mean that a smaller hopper could be used which would reduce the tendency for the feedstock to compact on the screw when the hopper was filled. A level sensor should be installed in the hopper to notify the operator when refuelling is needed.

Heat loss calculations could be incorporated into the model so that all the losses in the system could be more accurately accounted for.

The system was manufactured from mild steel due to this material's low cost. Mild steel however, rusts (oxidises) easily due to the high temperatures and moisture associated with the dryer. If a commercial dryer was to be developed, stainless steel should be considered. The hopper walls and the feeder pipe can be coated with Teflon or by painting to increase the smoothness and prevent corrosion or abrasion and reduce friction.

Additional automation could be incorporated into the system by automating and programming the agitators to run after certain time intervals.

It is also advisable that a certain level of feedstock screening be done to remove any problematic pieces of wood that would cause feeding issues.

# 14. REFERENCES


1. Kumararaja, L. 2009. *Development of gasifier suitable for non-woody bioresidues for electric power generation*. Project report. Department of Science, Technology and Environment, Govt. of Puducherry, Puducherry.
2. Cummer, K.R. and, Brown, R.C. 2002. *Ancillary Equipment for Biomass Gasification.* Biomass and Bioenergy. Vol. 23, pp. 161-168.
3. Mousdale, D.M. 2008. *Biofuels, biotechnology, Chemistry, and Sustainable Development.* CRC Press. Print ISBN 978-1-4200-5124-7.
4. Rajvanshi, A.K. 1986. *Biomass Gasification. Alternate Energy in Agriculture.* Vol. 2, ed. D, pp. 83-102.
5. Basu, P. 2010. *Biomass Gasification and Pyrolysis: Practical Design and Theory*. Elsevier.
6. Reed, T.B. and, Das, A. 1994. *Handbook of Biomass Downdraft Gasifier Engine Systems.* Biomass Energy Foundation, Zürich. 2nd ed.
7. GEK Gasifier Experimenters Kit. Available: http://gekgasifier.com/ [2012, October 5].
8. Henrich, E. 2007. *The status of the FZK concept of Biomass gasification.* University of Warsaw, Poland.
9. Knoef, H.A.M. 2005. *Handbook of Biomass Gasification.* BTG Biomass Technology Group. Enschede, Netherlands. ISBN: 90-810068-1-9
10. FAO Forestry Paper. 1986. *Wood Gas as Engine Fuel*. Mechanical Wood Products Branch. Forest Industries Division. Paper 72. ISBN 92-5-102 436-7.
11. Narvaez, I., Orio, A., Aznar, M.P., and Corella, J. 1996. *Biomass Gasification with Air in an Atmospheric Bubbling Fluidized Bed. Effect of Six Operational Variables on the Quality of the Produced Raw Gas*. Industrial & Engineering Chemistry Research. Vol. 35, pp 2110-2120.
12. Stiegel, G.J. and, Maxwell, R.C. 2001. *Gasification Technologies: the path to clean, affordable energy in the 21st century.* US Department of Energy, Technology Laboratory, Pittsburgh, USA.
13. Chopra, S. and, Jain, A.K. 2007 *A review of fixed bed gasification systems for biomass*. Ph.D. Thesis. School of Energy Studies for Agriculture, Ludhiana, India.
14. Sadaka, S. 2008.*Gasification*. Sun Grant Bio Web. Accessed 22-07-2012.

15. Jain, A. 2006. *Design Parameter for Rice Husk Throatless Gasifier*. Agricultural Engineering International: the CIGR Ejournal, Manuscript EE 05 012. Vol.8.
16. Bridgwater, A.V. 1994. *The Technical and Economic Feasibility of Biomass Gasification for Power Generation.* Fuel. Vol. 74, pp. 631-653.
17. Nevill, J.D. 2001. *Biomass Gasification Feed System Design and Evaluation.* Texas Tech University. Master of Science in Mechanical Engineering Thesis.
18. Carson, J.W. and, Petro, G. *How to Design Efficient and Reliable Feeders for Bulk Solids.* Jenike & Johanson Incorporated, http://www.jenike.com/TechPapers/ accessed 25.04.2012.
19. Francescato, V., Antonini, E. and, Bergomi, L.Z. 2008. *Wood Fuels Handbook.* AIEL–Italian Agriforestry Energy Association.
20. Ragland, K.W., Aerts, D.J., and Baker, A.J. 1991. *Properties of Wood for Combustion Analysis.* Bioresource Technology. Vol. 37, pp 161-168.
21. Roos, C.J. 2008. *Biomass Drying and Dewatering for Clean Heat and Power.* Northwest Combined Heat and Power Application Center.
22. Brammer, J.G. and, Bridgwater, A.V. 2001. *The Influence of Feedstock Drying on the Performance and Economics of a Biomass Gasifier-engine CHP System.* Biomass and Bioenergy. Vol. 22, pp. 271-281.
23. Amos, W.A. 1998. *Report on Biomass Drying Technology. National renewable Energy Laboratory.* Colorado. U.S. Department of Energy. NREL/TP-570-25885.
24. Karlsson, E. *Modelling of a Highly Efficient Gasifier Engine System for Small-Scale CHP*. Department of Chemical Engineering, Lund University, Sweden. Available: www.chemeng.lth.se/exjobb/E487.pdf
25. Antonopoulos, I.S., Gkouletsos, A., Karagiannidis, A. and, Perkoulidis, G. 2011. *Modelling of a Downdraft Gasifier Fed by Agricultural Residues.* 1st International Conference on: "Waste Management in Developing Countries and Transient Economies".
26. Gaur, S., and Reed, T.B. 1995. *An Atlas of Thermal Data for Biomass and Other Fuels.* National Renewable Energy Laboratory. A National Laboratory of the U.S. Departement of Energy Managed by the Midwest Research Institute for the U.S. Departement of Energy.
27. Jarungthammachote, S. And, Dutta, A. 2006. *Thermodynamic Equilibrium Model and Second Law Analysis of a Downdraft Waste Gasifier.* Energy Field of Study, School

of Environment, Resources and Development, Asian Institute of Technology, Thailand.

28. Koroneos,C., and Lykkidou, S. 2011. *Equilibrium modelling for Downdraft Biomass Gasifier for Cotton Stalks Biomass in Comparison with Experimental Data.* Journal of Chemical Engineering and Materials Science. Vol. 2(4), pp. 61-68.
29. Cengal, Y.A. and, Boles, M.A. 2002. *Thermodynamic, an Engineering Approach.4$^{th}$ed.* New York: McGraw-Hill Higher education.
30. Zainal, Z.A., Rifau, A., Quadir, G.A. and, Seetharamu, K.N. 2002. *Experimental Investigation of a Downdraft Biomass Gasifier. Biomass and Bioenergy.* Vol. 23, pp. 283-289.
31. Henriksen, U., Kofoed, E., Gabriel, T., Koch, T., and Christensen, O. 1991. *Gasification of Straw.* Biomass for Energy, Industry and Environment. Elsevier. Vol. 4, pp. 797-801.
32. Holman, J.P. 2010. *Heat Transfer*. 10th ed. New York: McGraw Hill.
33. MSDS Carbon Monoxide. 2009. Praxair Material Safety Data Sheet. Available: http://www.praxair.com/
34. Stahl, R., Henrich, E., Gehrmann, H.J., Vodegel, S. and, Koch, M. 2004. *Definition of Standard Biomass. RENEW - Renewable Fuels for Advanced Power Trains.*SES6-CT-2003-502705.
35. Roberts, A.W. 2001. *Design Considerations and Performance Evaluation of Screw Conveyors.* Centre for Bulk Solids and Particulate Technologies, The University of Newcastle, Australia.
36. Douglas, J.F., Gasiorek, J.M. and, Swaffield, J.A. 2001. *Fluid Mechanics*. 4th ed. Pearson Education Limited.

# APPENDIX A: FEEDER CALCULATIONS

Screw conveyors can be separated into two broad categories, the U-shaped trough type and the fully enclosed conveyor with a tubular casing, Figure A.1. The U-shaped trough type is widely used in industry but restricted to low angles of elevation, low speeds and low fill ratios. The fully enclosed tubular screw conveyor is more versatile. They operate over a wide range of speeds and angles of elevation up to the vertical. Their disadvantage is the limitation in conveying distance as they need to operate without intermediate support bearings. This however can be overcome by using shaft-less screws which employ helical flights of heavy cross section supported on plastic, wear resistant liners attached to the inside surface of the casing [35]. Practical limitations of the tubular type screw feeder require a substantial clearance between the flight and the casing; this has been shown to be advantageous rather than detrimental to performance. It is acceptable to allow the screw flight to project beyond the casing at the lower or intake end, this projection is referred to as the "choke". It is necessary to immerse the screw in the feedstock at least to the level of the lower end of the casing; otherwise the conveyor will not elevate the material [35]. There should be a close correlation between the speed of the feeder and the rate of discharge [18].

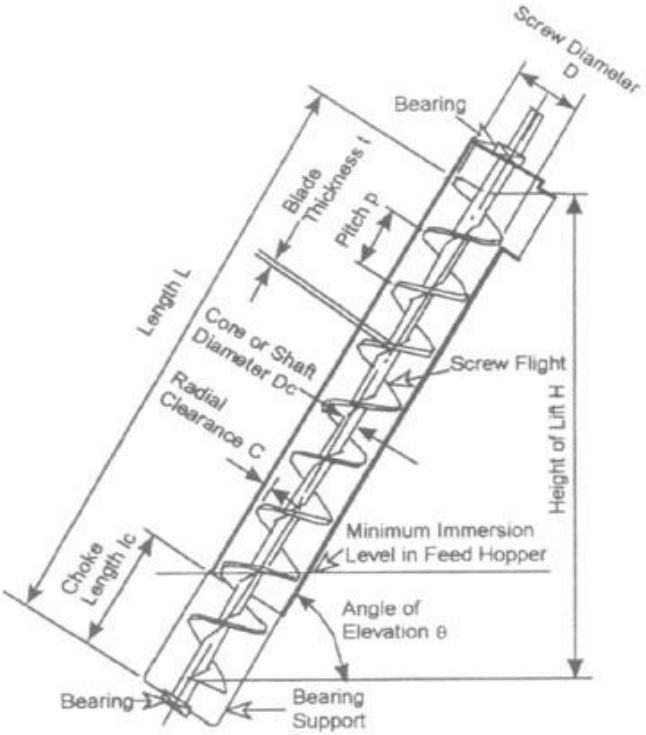


Figure A.1: Enclosed screw conveyor [35]

The throughput of an enclosed screw is influenced by the rotational motion of the bulk material during transportation and the fill ratio of the screw. As the rotational speed increases, the rotational motion decreases up to a limiting value, making for more efficient conveying action. Although, when a gravity feed system is employed into the screw intake, the feed rate cannot match the potential conveying capacity, and a reduction in fill ratio occurs. The result is for the throughput of the screw conveyor to reach a limiting value as illustrated in Figure A.2.

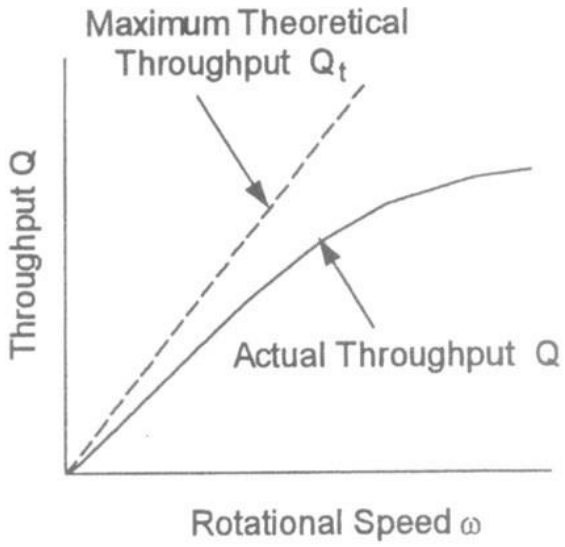


Figure A.2: Screw conveyor throughput [35]

The volumetric throughput of a screw conveyor is given by

$$Q = Q_t \eta_v \tag{A.1}$$

Where

$$Q_t = r\omega D^3 \tag{A.2}$$

And

$$r = \frac{1}{8}\left[\left(1 + 2\frac{C}{D}\right)^2 - \left(\frac{D_c}{D}\right)^2\right]\left[\frac{p}{D} - \frac{t}{s}\right] \tag{A.3}$$

Where

$Q_t$– maximum theoretical throughput with conveyor running 100% full and the bulk material moving axially without rotation ($m^3/s$)

$\eta_v$ – volumetric efficiency

D – screw diameter (m)

$D_c$ – core or shaft diameter (m)

p – pitch (m)

ω – angular velocity of screw feeder (r/s)

C – radial clearance (m)

$t_s$ – thickness of screw blade (m)

The volumetric efficiency of a screw conveyor is the product of two components as specified:

$$\eta_v = \eta_{vR}.\eta_F \quad \text{A.4}$$

Where

$\eta_{VR}$ – conveying or vortex efficiency accounting for the rotational motion

$$\eta_v = \eta_{vR}.\eta_F \quad \text{A.5}$$

$$\eta_F =' Fullness' efficiency = \frac{h_{av}}{p}$$

$h_{av}$ – average height of material on the screw surface

**Effect of conveyor diameter – corresponding speeds**

Corresponding speeds are given by non-dimensional specific speed number $N_s$ defined by:

$$N_s = \frac{\omega^2 R_o}{g} \quad \text{A.6}$$

Where

$R_o$ – outer radius (m)

g – gravitational acceleration ($m/s^2$)

N – rotational speed (rev/min)

**Mass throughput – influence of bulk density**

The mass throughput of a screw conveyor (kg/s) is given by:

$$Q_m = \rho Q \quad \text{A.7}$$

ρ – bulk density ($kg/m^3$)

**Effective radius**

In order to determine the conveying efficiency, the variation of the path helix angle λ needs to be determined as a function of the radius and rotational speed of the conveyor. The analysis of the screw conveyor is simplified by grouping the rotational mass and resultant forces at the effective radius $R_e$ defined by:

$$R_e = \frac{2}{3}\left[\frac{{R_o}^3 - {R_i}^3}{{R_o}^2 - {R_i}^2}\right] \quad \text{A.8}$$

Where

$R_o$ – outside radius of screw flight (m)

$R_i$ – inside radius of screw flight (m)

The helix angle of the screw flight corresponding to $R_e$ is:

$$\alpha_e = \tan^{-1}\left[\left(\frac{p}{\pi D}\right)\left(\frac{R_o}{R_e}\right)\right] \quad \text{A.9}$$

**Conveying efficiency**

The conveying efficiency is given by:

$$\eta_{VR} = \frac{\tan\lambda_e}{\tan\alpha_e + \tan\lambda_e} \quad \text{A.10}$$

Where

The angle $\lambda_e$ increases with speed of rotation reaching, asymptotically, a limiting value defined as:

$$as\ N_s \to \infty, \lambda_e \to 90^\circ - (\alpha_e + \emptyset_s) \quad \text{A.11}$$

That is, $\lambda_e$ approaches a constant value defined by the helix angle of the screw and the friction angle of the bulk solid in contact with the screw surface.

$\emptyset_s$ – friction angle for screw surface

**Influence of casing and screw friction**

The performance of the screw conveyor is significantly influenced by the friction generated between the feedstock and the screw and casing surfaces. Figure A.3 and A.4 compare the conveying efficiencies for a vertical screw conveyor for a range of friction angles for casing and screw surface respectively.

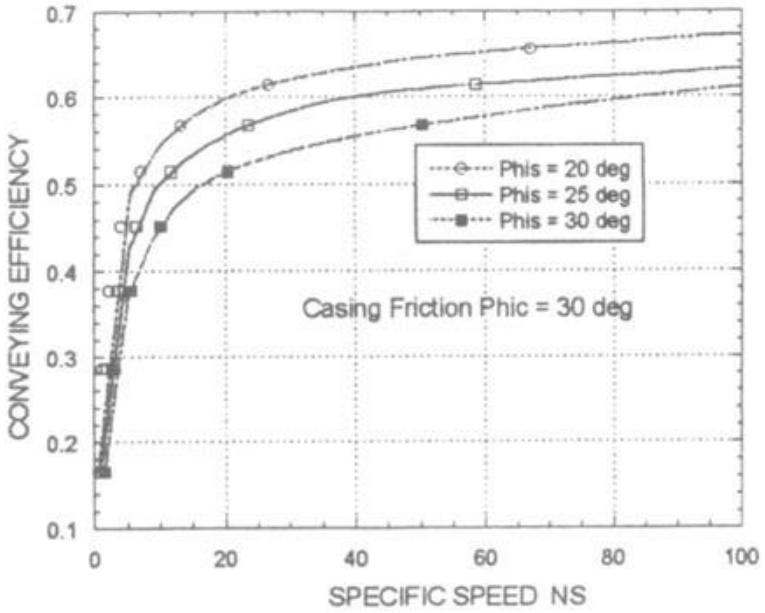


Figure A.3: Effect of casing friction on conveying efficiency [35]

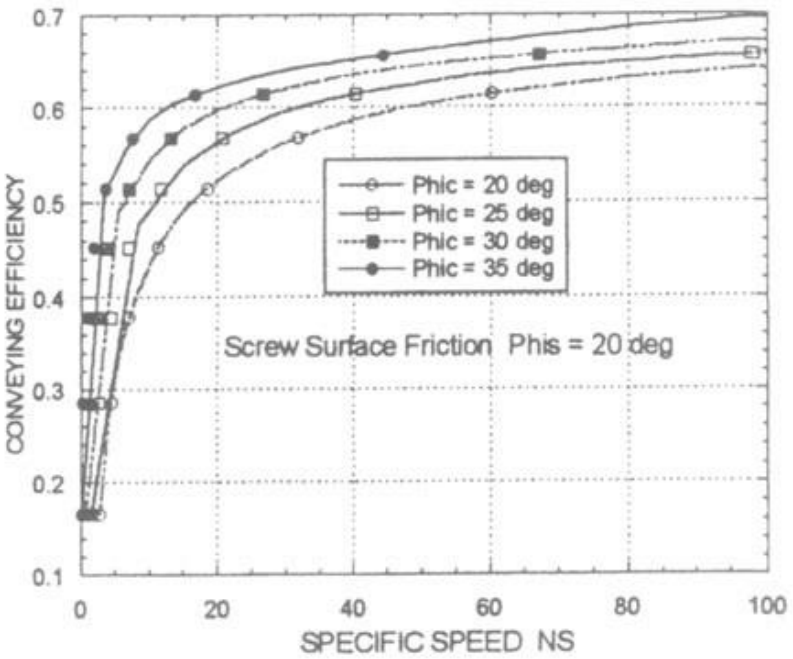


Figure A.4: Effect of screw surface friction on conveying efficiency [35]

**Screw conveyor at certain angle of elevation**

The helix angle of a path is independent of the screw speed and is given by:

$$\lambda = 90° - (\alpha + \phi_s) \quad \text{A.12}$$

The conveying efficiency is then:

$$\eta_{VRh} = \frac{1}{\tan \alpha_e \tan(\phi_s + \alpha_e) + 1} \quad \text{A.13}$$

Where the subscript 'h' denotes horizontal position

**At an inclination angle**

Using an empirical approach:

- The conveying efficiency is calculated as before (eqn. A.10)
- Calculate the conveying efficiency for a horizontal conveyor
- Interpolate the conveying efficiency for inclination angle θ using the following:

$$\eta_{VR\theta} = \eta_{VRh} - (\eta_{VRh} - \eta_{VR}) \sin \theta \quad \text{A.14}$$

**Force Analysis**

The force and velocity components acting on particles in a screw feeder are shown in Figure A.5.

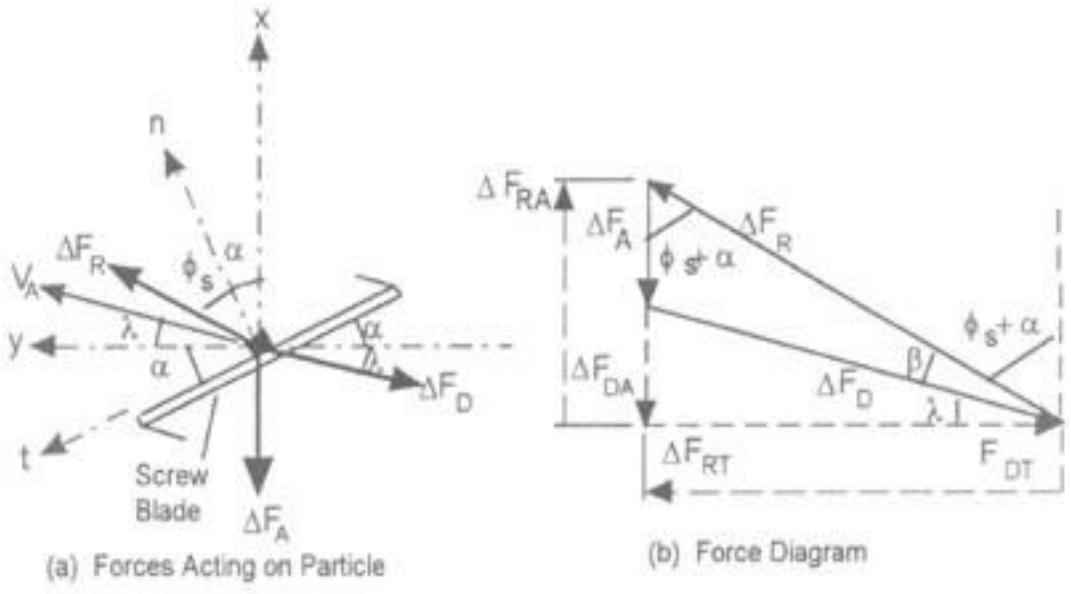


Figure A.5: Forces acting on bulk particle in contact with screw surface [35]

A particle in contact with the casing exerts a force $\Delta F_N$ against the casing, mainly as a result of the centrifugal pressure. This pressure gives rise to the normal pressure $p_n$ acting at the casing. A frictional drag force $\Delta F_D$ acts in the direction opposing the absolute velocity as shown in Figure A.5(a).

$$\Delta F_D = \mu_c \Delta F_N \quad \text{A.15}$$

Where

$\mu_c$– is the coefficient of friction for the particle on the casing surface.

The weight of bulk material retained on each pitch is:

$$W = \pi\left({R_o}^2 + {R_i}^2\right) p \rho g \eta_F \quad \text{A.16}$$

The axial force is:

$$\Delta F_{RA} = W(\sin\theta + \mu_E \cos\theta) \quad \text{A.17}$$

Where

$$\mu_E = \mu_C(1 + K_\theta \eta_F \quad \text{A.18}$$

$\mu_E$– equivalent friction coefficient to allow for drag of the casing walls during motion

$$K_\theta = 0.4 \; to \; 0.6 \quad \text{A.19}$$

$K_\theta$ – pressure ratio, value depends on consolidation of bulk solid

**Screw Torque**

The screw torque per pitch due to the bulk solid on the flight face can be determined from the following:

$$T_{sp} = \frac{2}{3}\frac{L}{p}\Delta F_{RA} R_e \tan(\alpha_e + \phi_s) \quad \text{A.20}$$

Where

L – is the length of the screw conveyor (m)

**Shaft Torque**

The normal pressure due to bulk solid on the shaft is:

$$\sigma_n = K\rho g p \eta_F \quad \text{A.21}$$

K accounts for the pressure distribution around the shaft as can be assumed to be 0.4

And then the torque due to the bulk solid moving relative to the shaft is:

$$T_{SH} = 2\pi {R_i}^2 \sigma_n \frac{L}{p} \quad \text{A.22}$$

The total torque is then:

$$T = T_{sp} + T_{SH}\ (N/m) \quad \text{A.23}$$

**Power**

$$P = \frac{0.105TN}{\eta_d}\ (kW) \quad \text{A.24}$$

Where

$\eta_d$– is the drive efficiency

Table A.1 and A.2 show the parameters chosen for the screw feeder and the calculations based on the equations shown in this chapter. The primary inputs were the required feed rate and the basic screw dimensions that were chosen based on the experimental work. The calculations were done in Excel for easy optimization of the screw feeder. Of particular interest is the performance with respect to throughput, torque and power.

Table A.1: Screw feeder parameters and calculations

| Parameter | Symbol | Value | Unit |
|---|---|---|---|
| Screw diameter | D | 0.060 | m |
| Core Diameter | $D_c$ | 0.020 | m |
| Pitch | P | 0.060 | m |
| Radial clearance | C | 0.035 | m |
| Blade thickness | $t_s$ | 0.002 | m |
| Volumetric Efficiency | $\eta_V$ | 0.355 | |
| Max throughput | $Q_t$ | 0.002 | $m^3/s$ |
| Volumetric throughput | Q | 0.001 | $m^3/s$ |
| Conveying Efficiency | $\eta_{VR}$ | 0.710 | from graph |
| Fullness Efficiency | $\eta_F$ | 0.500 | assume half |
| Average height of material | $h_{av}$ | 0.030 | assume half |
| Specific Speed | $N_s$ | 0.005 | 0.004803658 |
| Outer radius | $r_o$ | 0.030 | m |
| Gravity | g | 9.810 | $m^2/s$ |
| Rotational Speed | N | 15.000 | rpm |
| Rotational Speed | r | 0.023 | |
| Rotational Speed | ω | 1.571 | rad/s |
| Mass throughput | $Q_m$ | 0.155 | kg/s |
| Density | ρ | 200.000 | $kg/m^3$ |
| Length | L | 3.200 | m |
| Height of Lift | H | 1.094 | m |
| Angle of elevation | θ | 20.000 | deg |
| Angle of elevation | | 0.349 | radians |
| Traveling Speed | v | 0.015 | m/s |

Table A.2: Screw feeder parameters and calculations continued

| Parameter | Symbol | Value | Unit |
|---|---|---|---|
| Axial force per pitch | $\Delta F_{RA}$ | 2.721 | N |
| Equivalent friction coefficient | $\mu_e$ | 0.419 | |
| Friction coefficient on Surface | $\mu_c$ | 0.349 | 20 |
| Weight of material on pitch | W | 3.698 | N |
| Flight radius | Ro | 0.030 | m |
| Shaft radius | $R_i$ | 0.010 | m |
| Pressure ratio | $K_\theta$ | 0.400 | |
| Effective Radius | $R_e$ | 0.667 | m |
| Torque per Pitch | $T_{SP}$ | 24.592 | N.m |
| Helix angle flight | $a_e$ | 0.014 | radians |
| Screw surface friction | s | 0.350 | assumed |
| Torque due to material | $T_{sh}$ | 78.897 | N.m |
| Normal Pressure | $\sigma_n$ | 23.544 | Pa |
| Pressure distribution | K | 0.400 | |
| Total torque | $T_{total}$ | 103.489 | N.m |
| Power | P | 0.181 | kW |
| Drive Efficiency | $\eta_d$ | 0.900 | |
| Axial Pressure on blade | $\sigma_a$ | 58.860 | Pa |
| Required throughput | $Q_r$ | 0.000 | $m^3/s$ |
| | $\eta_F$ | 0.064 | calculated |
| | $C_{Fo}$ | 1.000 | |
| | $C_F$ | 0.080 | |
| Helix Angle | $\lambda_e$ | 1.206 | calculated |
| | $\eta_{VR}$ | 0.995 | |
| | $\eta_{VRh}$ | 0.995 | use graph |
| | $\eta_{VR\theta}$ | 0.710 | |

# APPENDIX B: FAN SELECTION

The fan/blower needed to be selected to drive the air through the heat exchanger and over the feedstock. From the heat exchanger calculations the flow rate required was already known, 0.0117m$^3$/s (Chapter 5). This was calculated that on the assumption that the velocity through the tubes is constant. In practice this is not the case and the air will incur friction losses as it flows through the tubes. The pressure drop across the tube bank was calculated by calculating the pressure drop through the tube length, 2.2m [36].

**Tube Area**

$$A = \pi d^2/4 \qquad \text{B.1}$$

$$= \pi(0.01)^2/4 = 7.85 \times 10^{-5} m^2$$

**Mean velocity**

$$v = \frac{Q}{A} \qquad \text{B.2}$$

$$= 0.0117/7.85 \times 10^{-5} = 9.30\ m/s$$

**Reynolds number (from Chapter 5)**

$$Re = 2517.05$$

$$Re_d > 2300\ Turbulent\ flow$$

**Darcy equation**

$$h_f = \frac{4fl}{d}\frac{v^2}{2g} \qquad \text{B.3}$$

$h_f -$ *head los due to friction* (m)

$l -$ *length of pipe* (m)

$v -$ *velocity* (m/s)

$d -$ *pipe diameter* (m)

$g -$ *gravitational constant* (m/s$^{-2}$)

The Blasius equation was used to calculate the friction factor, *f*, using an empirical relation for turbulent flow.

$$f = \frac{0.079}{Re^{1/4}} \qquad \text{B.4}$$

$$= \frac{0.079}{(2517.05)^{1/4}} = 0.0112$$

**Head loss due to pipe fittings**

$$h = K(v^2/2g) \qquad \text{B.5}$$

Table B.1: Head loss for various pipe fittings [36]

| Fitting | Loss coefficient K |
|---|---|
| Return Bend | 2.2 |
| 90° Bend | 0.9 |
| Pipe entry/exit | 0.5 |

The separation loss, K, is defined in terms of equivalent length of straight tube, of the same diameter of that including the fitting that would results in the same frictional loss as that incurred by flow separation through the fitting. From the Darcy equation:

$$l_e = \frac{Kd}{4f} \qquad \text{B.6}$$

Where

$l_e - \ equivalent\ length$ (m)

$K - loss\ coefficient$

$d - \ \ tube\ diameter$ (m)

$f - friction\ factor$

Table B.2: Equivalent length for various fittings

| Entry | Return Bend | Exit | Total |
|---|---|---|---|
| $l_e$(m) | $l_e$(m) | $l_e$(m) | $l_e$(m) |
| 0.113 | 0.4988 | 0.113 | 0.163 |

Then from eqn. B.3

$$h_f = \frac{4f(l + l_e)}{d}\frac{v^2}{2g}$$

$$\therefore h_f = \frac{4 \times 0.0112 \times (2.2 + 0.163)}{0.01}\frac{9.30^2}{2 \times 9.81} = 46.48m$$

Need to consider the pipe from the Heat exchanger to the feeder pipe, length 1m.

**Pipe Area for 40mm diameter**

$$A = 0.001257m^2$$

**Reynolds number**

$$Re = 12762.$$

**Head loss**

$$h_f = 3.092m$$

And finally the pressure drop as the air flows through the pipe containing the wood. The pipe diameter is 131.2mm and it was assumed that it was half filled with wood (which are settled at the bottom) thus the following calculations were based on half the diameter of this pipe and a length of 2m.

**Pipe Area for 131.2mm diameter**

$$A = 0.00338m^2$$

**Reynolds number**

$$Re = 6734.11$$

**Head loss**

$$h_f = 0.415m$$

The total head loss that the fan would need to overcome to keep the desired flow rate is:

$$h_{total} = 48.41m$$

$$= 354.41Pa$$

The load curve below is calculated from the given flow conditions for the plumbing of the system by varying the flow rates.

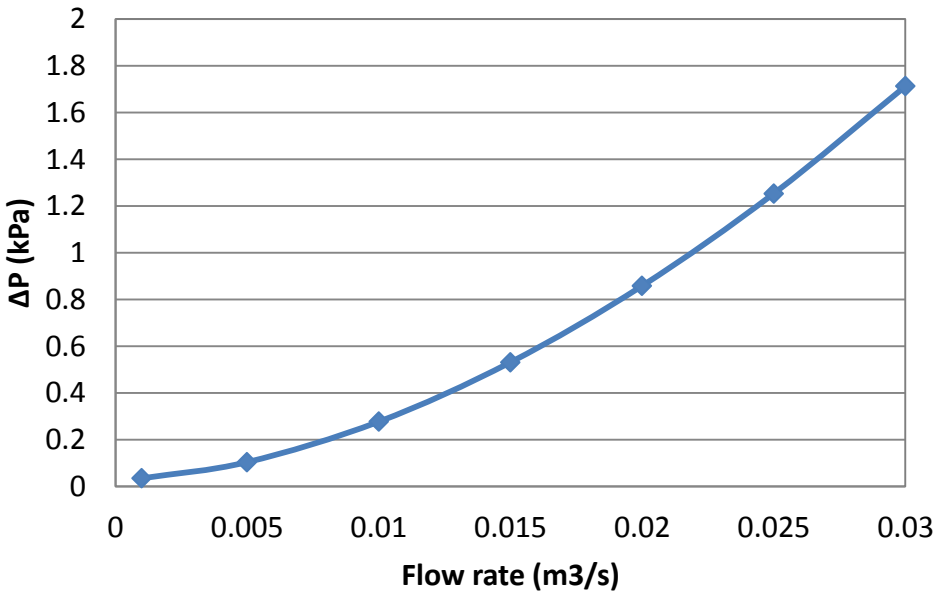


Figure B.1: Calculated load curve for air flow through the system

Based on the calculated load curve, Figure B.1, a suitable device was selected to overcome the pressure drop of the system and achieve the flow rate. A centrifugal fan was preferred for this application because of its ability to deal with pressure increase. A vacuum cleaner fan was chosen due to its ability to overcome pressure losses and maintain a constant velocity.

# APPENDIX C: INSULATION CALCULATIONS

There existed a need for insulation of the heat exchanger to prevent heat loss to the environment. The heat transfer through the cylinder walls were based on convection and thus depended on the material used. For the purpose of these calculations conduction was not considered [32].

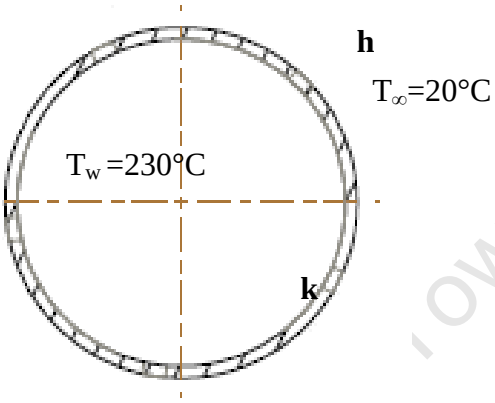


Figure C.1: Critical thickness

$T_w - Tube\ wall\ Temperature$ (°C)

$T_\infty -\ Room\ temperature$ (°C)

**Natural Convection (Empirical Calculations)**

Outside Diameter, $OD = 131.2mm$, is to be maintained at 270°C

$$T_f = \frac{230 + 20}{2} = 125℃ = 398K$$

$$\beta = \frac{1}{T_f} \qquad \text{C.1}$$

$$= \frac{1}{415} = 0.00251$$

$$k_{air} = 0.0350\ (interpolated\ [32])$$

$$\nu = 28.24 \times 10^{-6} (interpolated\ [32])$$

$$Pr = 0.6866\ (interpolated\ [32])$$

$$Gr_L = \frac{g\beta(T_w - T_\infty)(L)^3}{\nu^2} \quad \text{C.2}$$

$$= \frac{(9.8)(0.00350)(270-20)(2)^3}{(28.24\times10^{-6})^2} = 3.57\times10^{10}$$

$$\frac{D}{L} \geq \frac{35}{{Gr_L}^{1/4}} \quad \text{C.3}$$

$$0.0656 \leq 0.0805$$

Therefore cylinder cannot be treated as a flat plate

$$\therefore GrPr = \frac{g\beta(T_w - T_\infty)(D)^3}{\nu^2}Pr \quad \text{C.4}$$

$$= \frac{(9.8)(0.00251)(230-20)(0.1312)^3}{(28.24\times10^{-6})^2}0.6866$$

$$= 1.01\times10^7$$

**From Holman Table 7.1 [32]**

$C = 0.53$

$m = 1/4$

$$Nu = C(GrPr)^m \quad \text{C.5}$$

$$= 0.53(1.01\times10^7)^{\frac{1}{4}} = 29.85$$

$$h = Nu\left(\frac{k}{D}\right) \quad \text{C.6}$$

$$= 29.85\left(\frac{0.0350}{0.1312}\right) = 7.96\ W/m^2$$

**Critical Insulation Thickness**

Insulation material - Glass fibre

$k = 0.038\ W/m.℃$

Maximum insulation radius

$$r_o = \frac{k}{h} \qquad \text{C.7}$$

$$= \frac{0.038}{7.96} = 0.0048m$$

$$\approx 5mm$$

Now, the value of the critical radius is less than the outside diameter of the pipe (131.2mm), so addition of any fibreglass insulation would cause a decrease in the heat transfer to the room. In practice, the total heat loss will be influenced by radiation as well as convection from the outer surface of the insulation.

# APPENDIX D: CONTROL SYSTEMS AND LABVIEW

Appendix D deals with the control systems used in LabVIEW as well as the brain/body block diagram used for programming the system.

The hardware includes:

- NI CompactDAQ 4-slot Chassis (NI cDAQ-9174)
- C series 32-Ch,5V/TTL Bidirectional Digital I/O Module (NI 9403)
- 32-Ch ±200mV to ±10V, 16-Bit, 250kS/s Analogue Input Module (NI 9205)
- 16-Ch Analogue Output Module (NI 9264)
- 16-Ch Thermocouple Input Module (NI 9213)
- K-type thermocouples
- SEW variable speed drive
- Desktop computer and auxiliary components



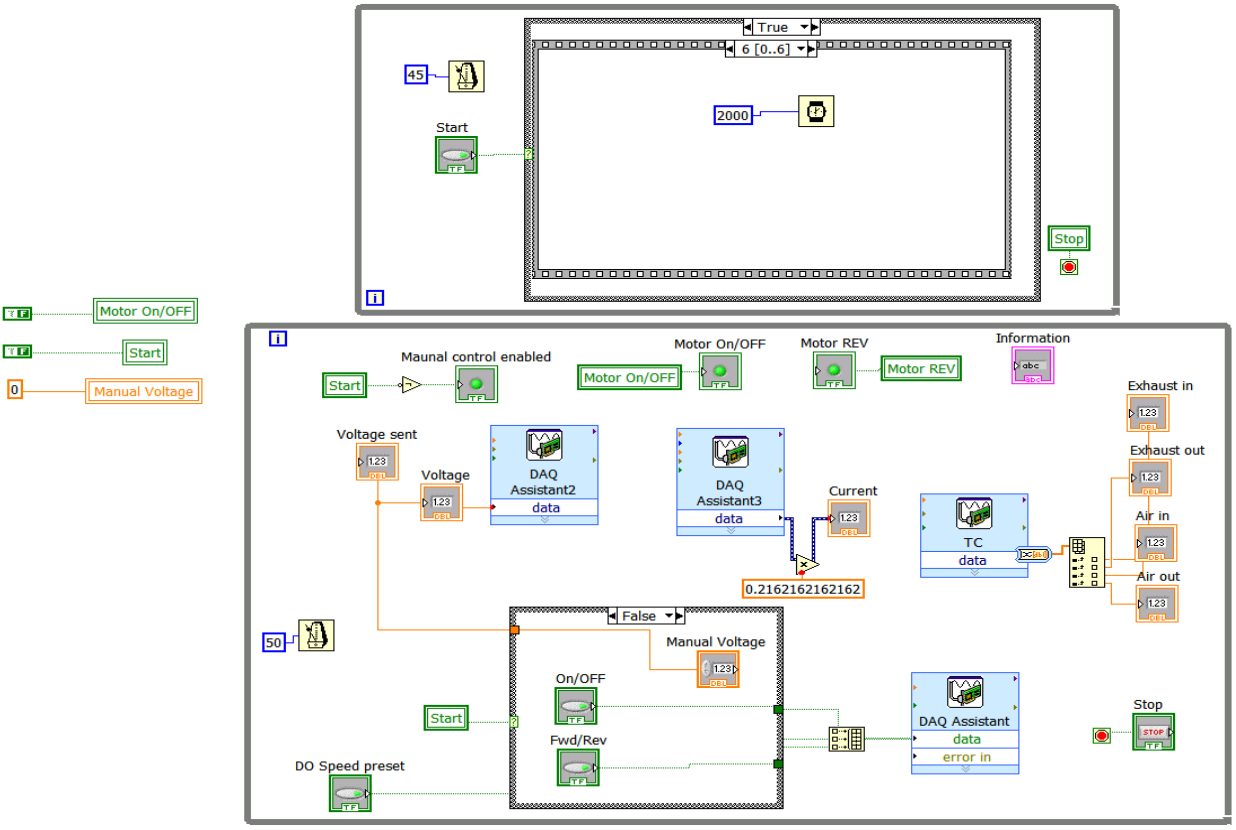


Figure D.1: Brain/body block diagram in LabVIEW

The brain shown in the top of Figure D.1 controls the body shown in the bottom of the figure. Inputs were displayed in the front panel of LabVIEW and outputs were sent from LabVIEW to the various control modules and to the drive. In this system the voltage was sent to control the speed of the motor while the current, voltage and temperatures readings were received as inputs.

# APPENDIX E: GEN-SET SPECIFICATIONS

The gen-set specifications are shown below in Tables E.1 and E.2 along with a mass flow calculation of the exhaust gas.

Table E.1: Engine Specifications

| | | | |
|---|---|---|---|
| Model | | GX 390 K1 | |
| Engine Size | | 0.389 | Litres |
| Engine Speed | n | 3600 | rpm |
| Bore x Stroke | | 88 x 64 | mm |
| Engine Type | | 4 stroke | |
| Max. Output | P | 9.6 | kW |

Table E.2: Calculated Operational Parameter Assumptions

| | | | |
|---|---|---|---|
| Volumetric Efficiency | $\eta_{vol}$ | 85 | % |
| Engine in-cylinder Temperature | $T_{in\text{-}cyl}$ | 120 | °C |
| Intake Pressure Drop | | 80.55 | mm H2O |
| Intake Pressure | $P_{intake}$ | 99.18 | kPa |

Table E.3: Generator Specifications (AC output)

| | | | | | |
|---|---|---|---|---|---|
| Model | | EP6500CXS | | | |
| Type | | R | S | LD | |
| Rated Voltage | V | 220 | | 120/240 | V |
| Rated Frequency | f | 50 | | 60 | Hz |
| Rated Ampere | I | 22.7 | 25 | 45.8/22.9 | A |
| Rated Output | | 5000 | | 5500 | VA |
| Max. Output | | 5500 | | 6500 | VA |

**Engine Volumetric intake:** 0.389 *l* engine at 3600 rpm

$$0.389 \times (Liters) \times \frac{3600}{60}\left(\frac{rpm}{s}\right) \times \frac{1}{2}(4\ stroke) \times 0.85\ (efficiency)/1000 \qquad \text{E.1}$$

$$Q_{exhaust} = 0.00992\ m^3/s$$

$$\rho = \frac{99.18 \times 1000}{287 \times (120 + 273)} = 0.879\ kg/m^3$$

**Engine inlet mass flow:**

$$\dot{m} = \rho Q_{exhaust} = 0.00872\ kg/s \qquad \text{E.2}$$

# APPENDIX F.1: HOPPER DRAWINGS

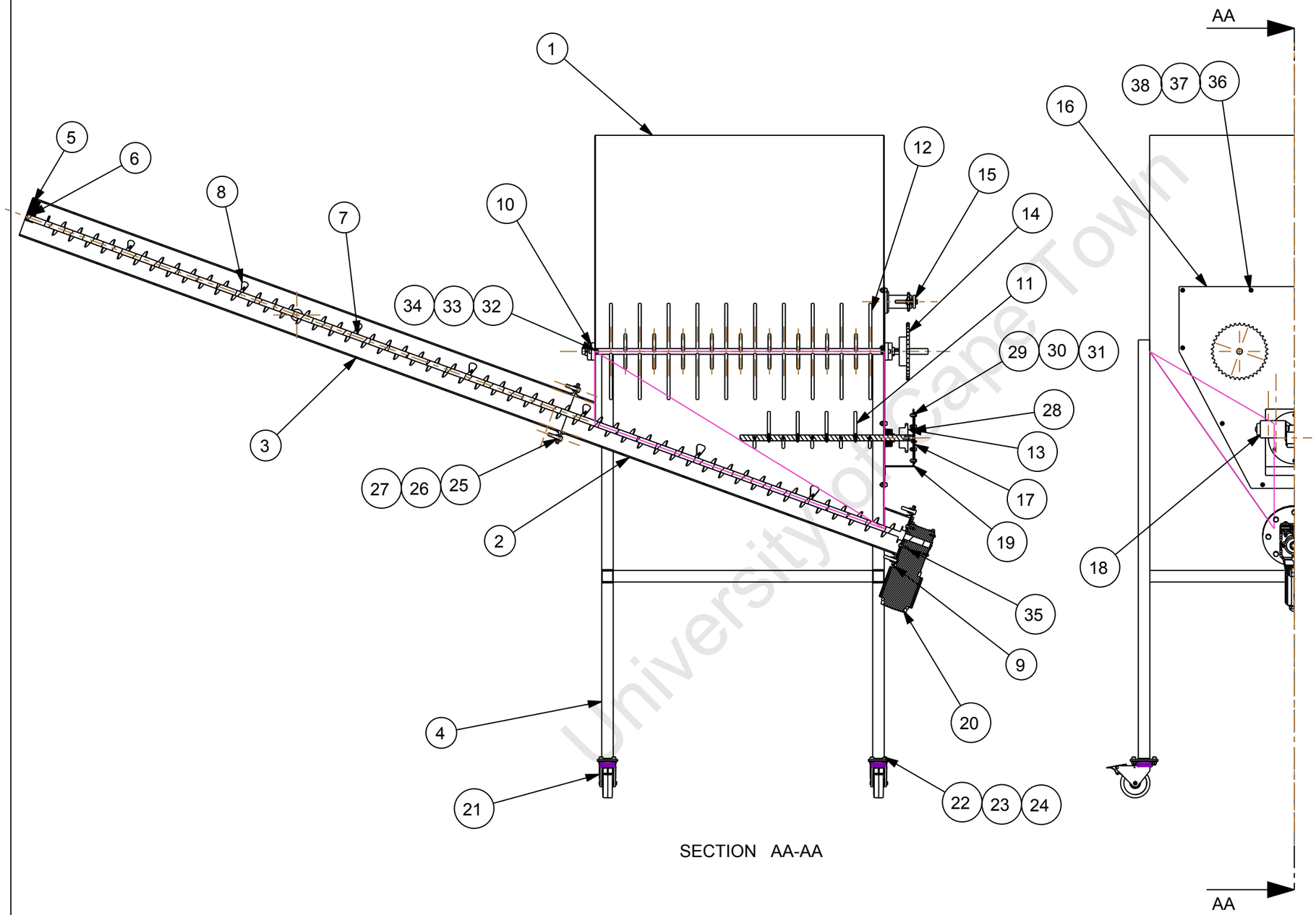


SECTION AA-AA

Note: Trough welded to Hopper assembly.
Hanger located at pipe exit, welded from top.
Chain mount welded to hopper mount.

| Item | Name | Qty | Material | Remarks |
|---|---|---|---|---|
| 38 | M8 Hex Nut | 10 | Mild Steel | Std. Part |
| 37 | M8 Washer | 10 | Mild Steel | Std. Part |
| 36 | M8 by 20mm Cap Head | 10 | Mild Steel | Std. Part |
| 35 | M6 by 40mm Hex Bolt | 4 | Mild Steel | Std. Part |
| 34 | M8 Hex Nut | 10 | Mild Steel | Std. Part |
| 33 | M8 Washer | 10 | Mild Steel | Std. Part |
| 32 | M8 by 25mm Cap Head | 10 | Mild Steel | Std. Part |
| 31 | M6 Hex Nut | 6 | Mild Steel | Std. Part |
| 30 | M6 Washer | 6 | Mild Steel | Std. Part |
| 29 | M6 by 30mm Cap Head | 6 | Mild Steel | Std. Part |
| 28 | M5 by 30mm Cap Head | 3 | Mild Steel | Std. Part |
| 27 | M10 Hex Nut | 16 | Mild Steel | Std. Part |
| 26 | M10 Washer | 16 | Mild Steel | Std. Part |
| 25 | M10 by 40mm Hex Bolt | 16 | Mild Steel | Std. Part |
| 24 | M8 Hex Nut | 16 | Mild Steel | Std. Part |
| 23 | M8 Washer | 16 | Mild Steel | Std. Part |
| 22 | M8 by 20mm Cap Head | 16 | Mild Steel | Std. Part |
| 21 | Trolley Wheels | 4 | As Supplied | Std. Part |
| 20 | Srew Feeder Drive | 1 | As Supplied | SEW Eurodrive |
| 19 | Chain Mount | 1 | Mild Steel | Welded |
| 18 | Wiper Motor | 1 | As Supplied | |
| 17 | Wiper Motor Mount | 1 | Mild Steel | |
| 16 | Hopper Mount | 1 | Mild Steel | |
| 15 | Jockey Sprocket Unit | 1 | As Supplied | 10B |
| 14 | Driven Sprocket | 2 | As Supplied | 38 tooth 10B |
| 13 | Driving Sprocket | 1 | As Supplied | 19 tooth 10B |
| 12 | Agitator 2 | 2 | Mild Steel | Weld Assembly |
| 11 | Agitator 1 | 1 | Mild Steel | Weld Assembly |
| 10 | Ø20 Flange Bearing | 5 | As Supplied | Std. Part |
| 9 | Screw Mount | 1 | Mild Steel | |
| 8 | Paddles | 21 | Mild Steel | Welded |
| 7 | Screw | 1 | Mild Steel | Weld Assembly |
| 6 | Bush | 1 | Brass | |
| 5 | Hanger | 1 | Mild Steel | Welded |
| 4 | Support | 1 | Mild Steel | Weld Assembly |
| 3 | Pipe | 1 | Mild Steel | Weld Assembly |
| 2 | Trough | 1 | Mild Steel | Weld Assembly |
| 1 | Hopper | 1 | Mild Steel | Weld Assembly |

University of Cape Town
Department of Mechanical Engineering

Title
Feeder Assembly

| Dimensions in mm Tolerance U.O.S. | Scale | Date | Sheet | of |
|---|---|---|---|---|
| | 0,065 | 7 July 2012 | 1 | 32 |
| | Drawn By | | Drawing Number | |
| 0.1 | WG Randall | | F001 | |

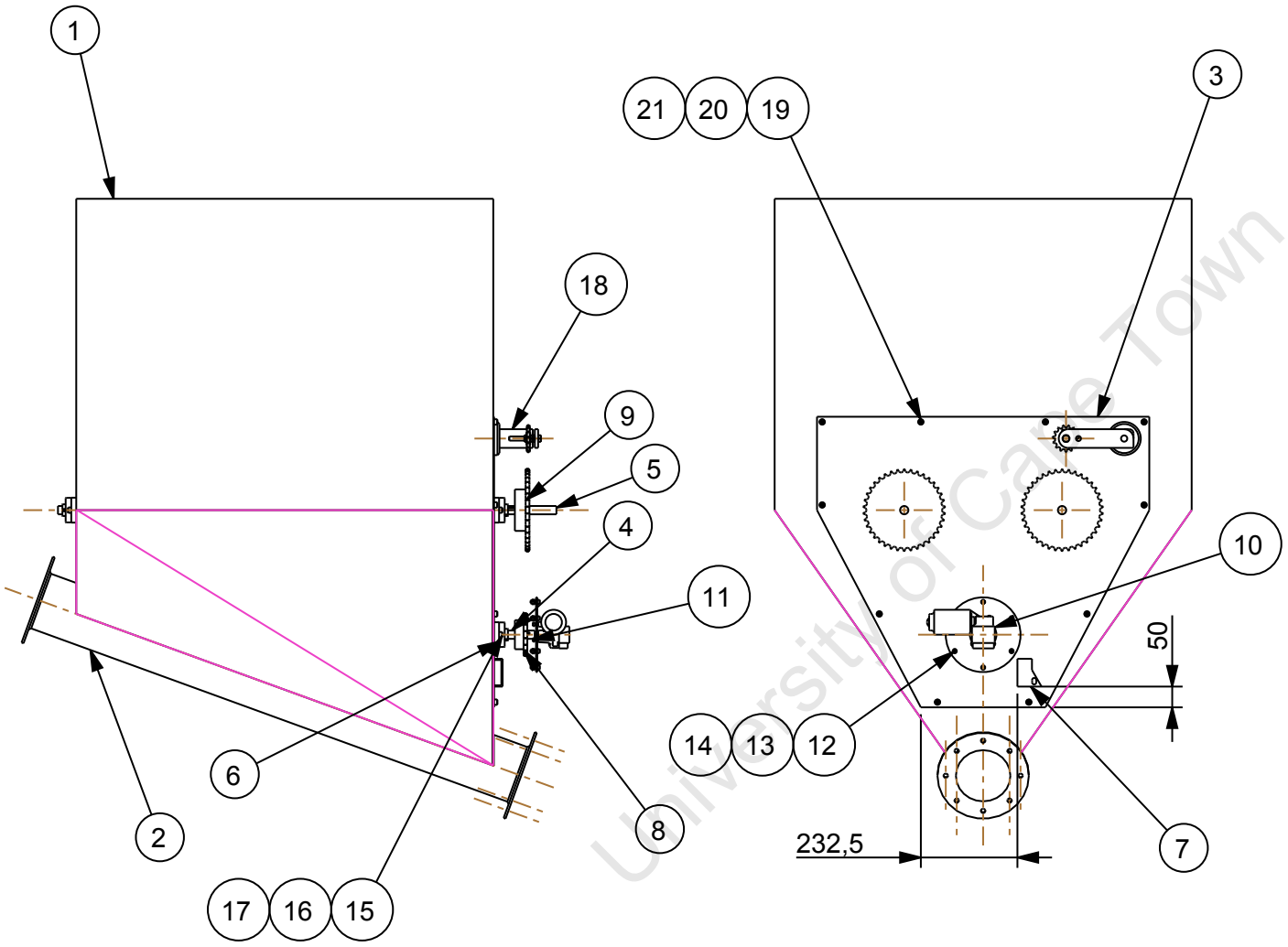


Note: Chain Mount welded to Hopper Mount
Trough Assembly welded to Hopper Assembly

| Item | Name | Qty | Material |
|---|---|---|---|
| 21 | M8 Hex Nut | 10 | Mild Steel |
| 20 | M8 Washer | 10 | Mild Steel |
| 19 | M8 by 25mm Cap Head | 10 | Mild Steel |
| 18 | Jockey Sprocket Unit | 1 | 10B |
| 17 | M8 Hex Nut | 10 | Mild Steel |
| 16 | M8 Washer | 10 | Mild Steel |
| 15 | M8 by 25mm Cap Head | 10 | Mild Steel |
| 14 | M6 Hex Nut | 6 | Mild Steel |
| 13 | M6 Washer | 6 | Mild Steel |
| 12 | M6 by 30mm Cap Head | 6 | Mild Steel |
| 11 | M5 by 30mm Cap Head | 3 | Mild Steel |
| 10 | Wiper Motor | 1 | As Supplied |
| 9 | Driven Sprocket | 2 | 38 tooth 10B |
| 8 | Driving Sprocket | 1 | 19 tooth 10B |
| 7 | Chain Mount | 1 | Mild Steel |
| 6 | Ø20 Flange Bearing | 5 | As Supplied |
| 5 | Agitator 2 | 2 | Weld Assembly |
| 4 | Agitator 1 | 1 | Weld Assembly |
| 3 | Hopper Mount | 1 | Mild Steel |
| 2 | Trough | 1 | Weld Assembly |
| 1 | Hopper | 1 | Weld Assembly |

University of Cape Town
Department of Mechanical Engineering

Title
Chan Mount Assembly

| Dimensions in mm Tolerance U.O.S. | Scale | Date | Sheet | of |
|---|---|---|---|---|
| 0.1 | 0,060 | 7 July 2012 | 2 | 32 |
| | Drawn By: WG Randall | | Drawing Number: F002 | |

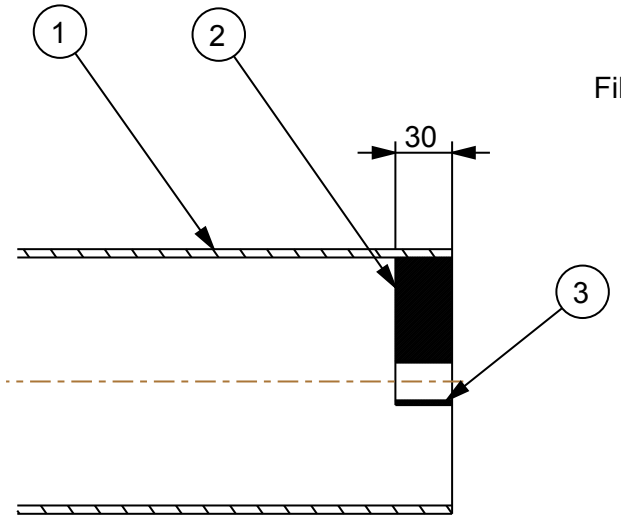


SECTION A-A

Fillet Weld

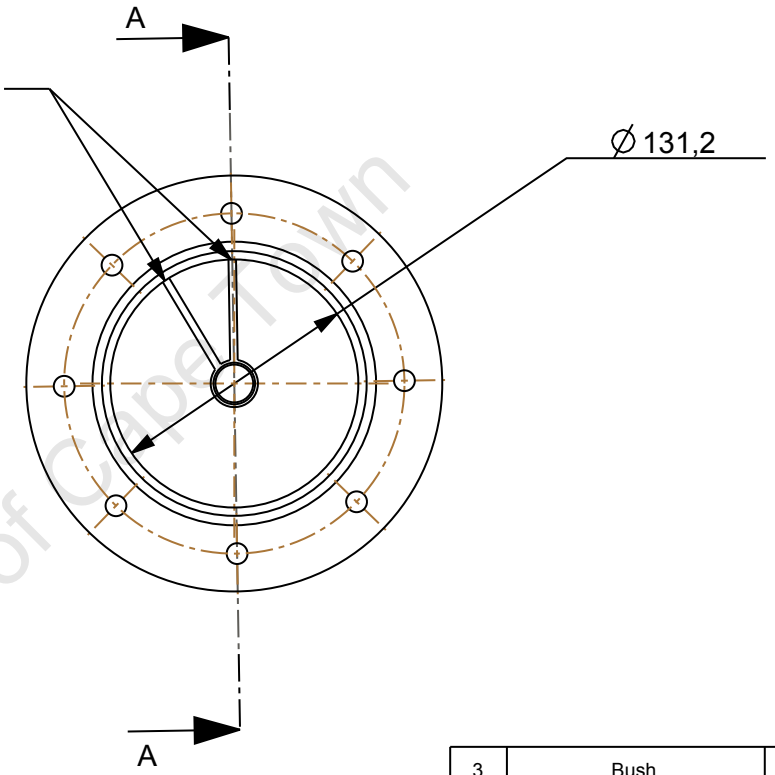


Note: Hanger welded to tube as indicated



| Item | Name | Qty | Material |
|---|---|---|---|
| 3 | Bush | 1 | Brass |
| 2 | Hanger | 1 | Mild Steel |
| 1 | Tube | 1 | Mild Steel |

University of Cape Town
Department of Mechanical Engineering

Title: Hanger Assembly

| Dimensions in mm Tolerance U.O.S. | Scale | Date | Sheet | of |
|---|---|---|---|---|
| 0.1 | 0,250 | 21 July 2012 | 3 | 32 |

| Drawn By | Drawing Number |
|---|---|
| WG Randall | F003 |

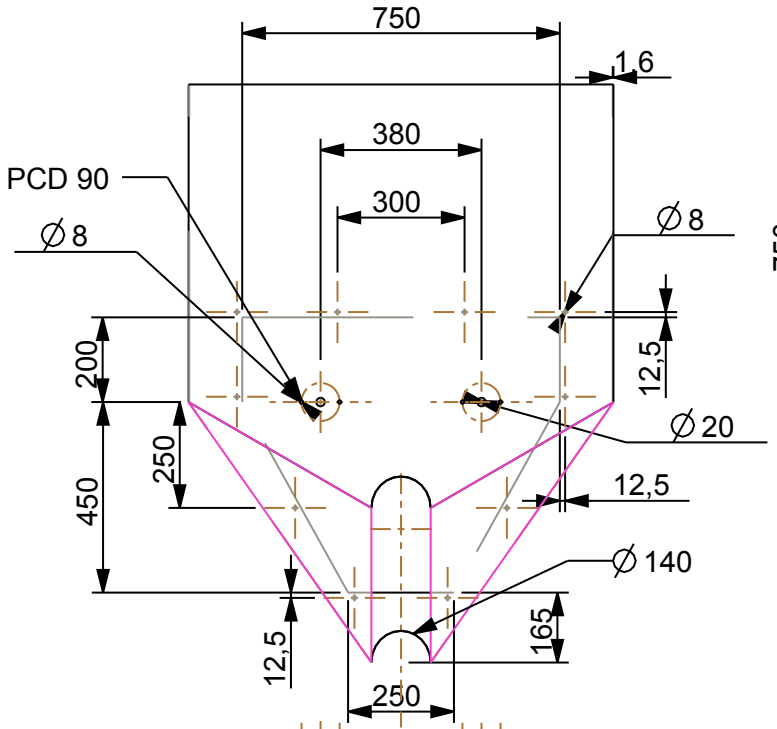


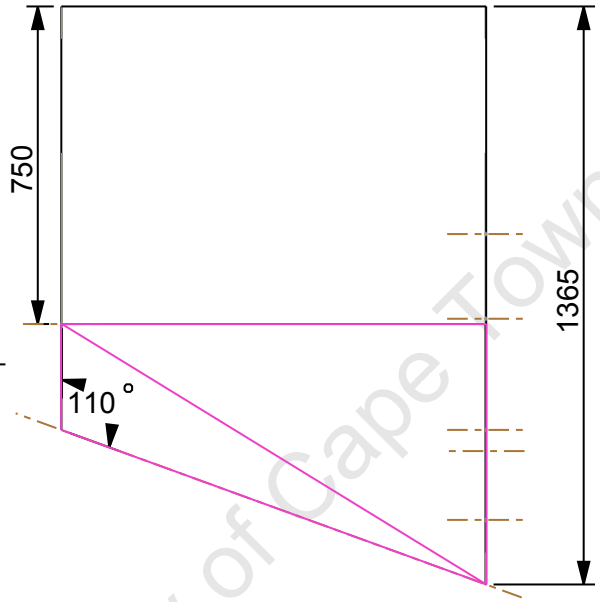


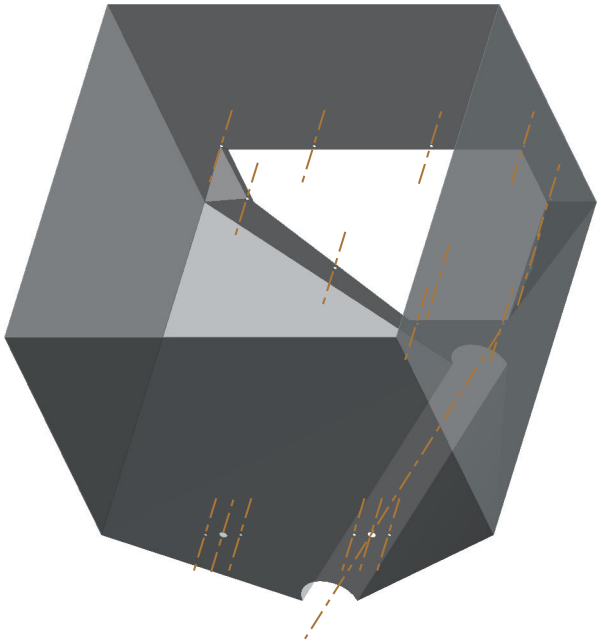

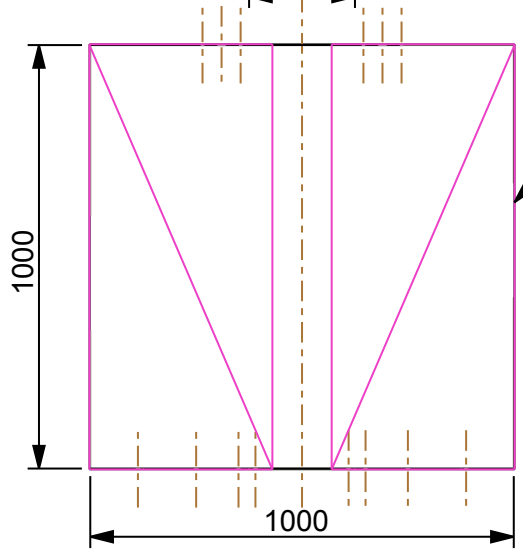


Note: Taper from 1m to 140mm



| | Mild Steel | 1 | Welded |
|---|---|---|---|
| Item | Material | Qty | Remarks |

University of Cape Town
Department of Mechanical Engineering

Title
Hopper Welded Assembly

| Dimensions in mm Tolerance U.O.S. | Scale | Date | Sheet | of |
|---|---|---|---|---|
| | 0,056 | 16 May 2012 | 4 | 32 |
| | Drawn By | | Drawing Number | |
| 0.1 | WG Randall | | F004 | |

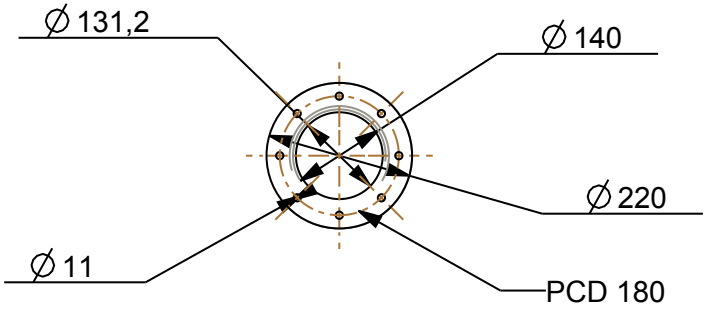


Note: Flanges welded at the ends of the trough.
Trough welded to hopper

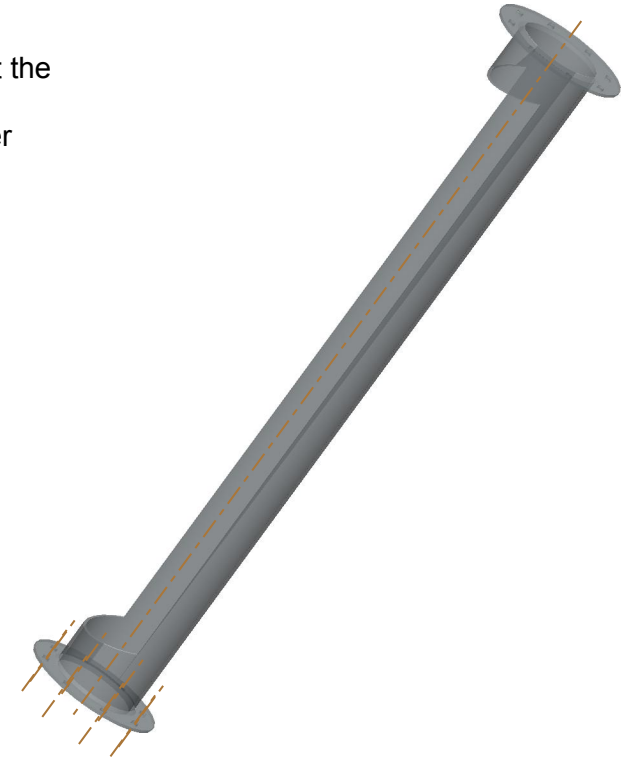

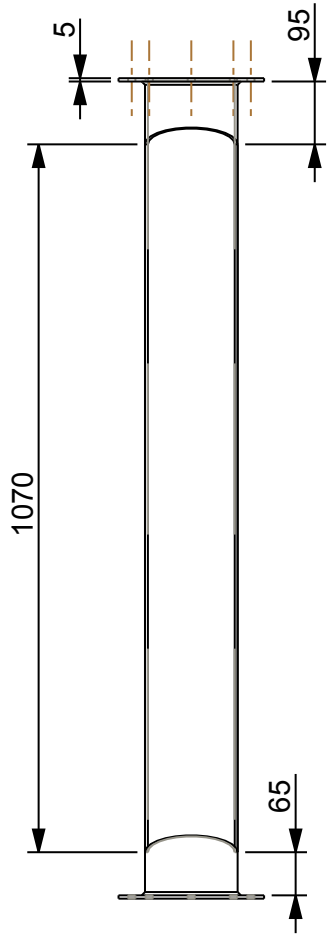


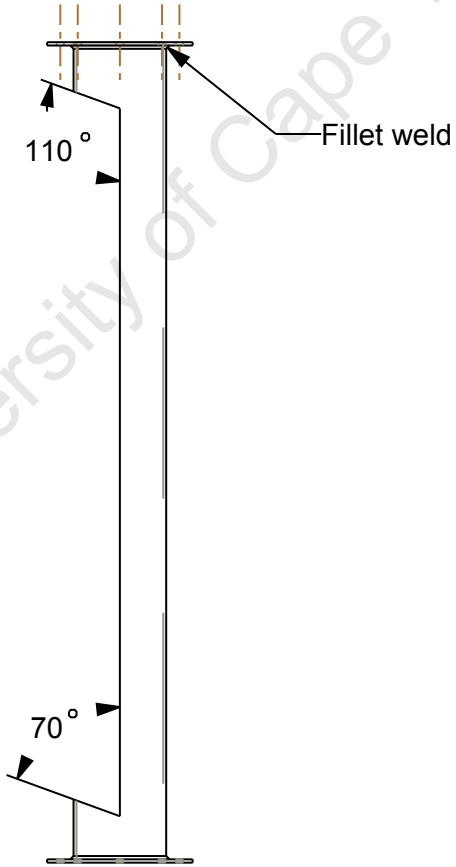




| | Mild Steel | 1 | Welded |
|---|---|---|---|
| Item | Material | Qty | Remarks |

University of Cape Town
Department of Mechanical Engineering

Title
Trough Welded Assembly

| Dimensions in mm Tolerance U.O.S. | Scale | Date | Sheet | of |
|---|---|---|---|---|
| | 0,088 | 17 May 2012 | 5 | 32 |
| | Drawn By | | Drawing Number | |
| 0.1 | WG Randall | | F005 | |

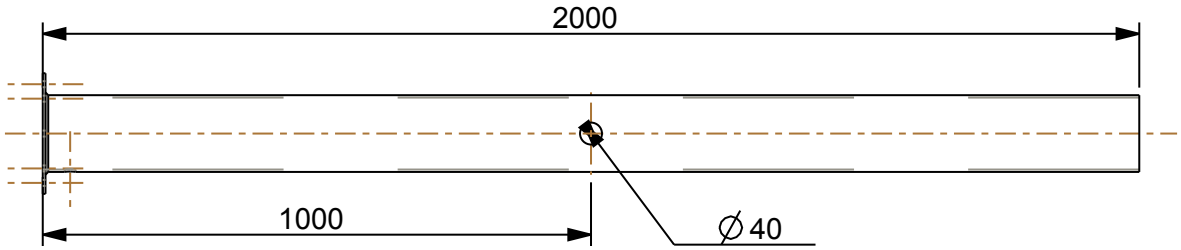


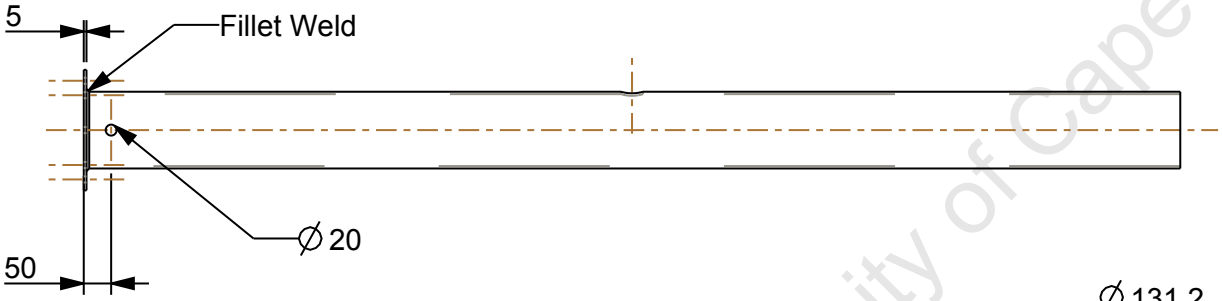


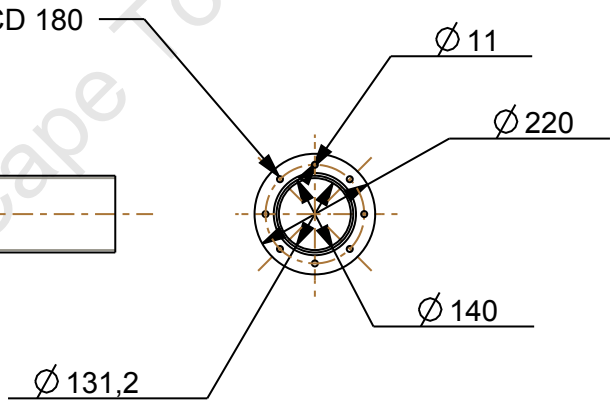


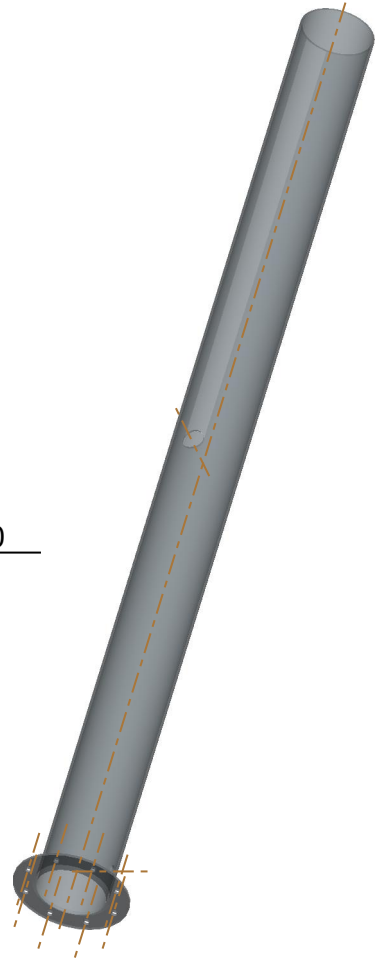



Note: Flange welded at one end of pipe

| | Mild Steel | 1 | Welded |
|---|---|---|---|
| Item | Material | Qty | Remarks |

University of Cape Town
Department of Mechanical Engineering

Title
Pipe Welded Assembly

| Dimensions in mm Tolerance U.O.S. | Scale | Date | Sheet | of |
|---|---|---|---|---|
| | 0,073 | 17 May 2012 | 6 | 32 |
| | Drawn By | | Drawing Number | |
| 0.1 | WG Randall | | F006 | |

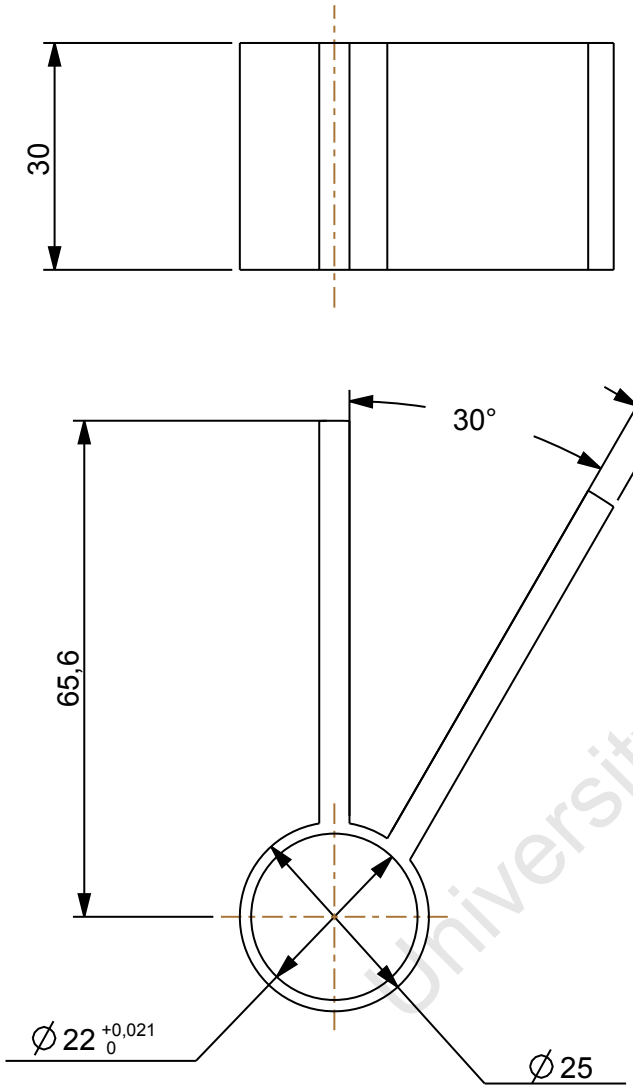




Note: Hanger welded to to outlet of pipe.

| | Mild Steel | 1 | Welded |
|---|---|---|---|
| Item | Material | Qty | Remarks |

University of Cape Town
Department of Mechanical Engineering

Title
Hanger Welded Assembly

| Dimensions in mm Tolerance U.O.S. | Scale | Date | Sheet | of |
|---|---|---|---|---|
| | 1,000 | 17 May 2012 | 7 | 32 |
| | Drawn By | | Drawing Number | |
| 0.1 | WG Randall | | F007 | |

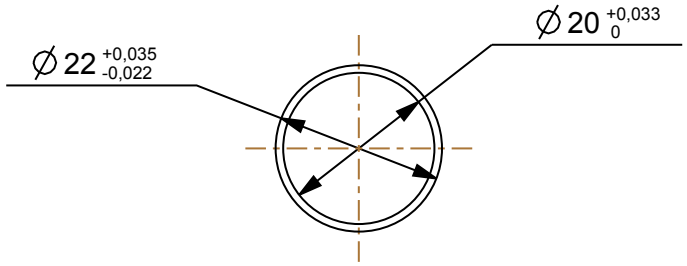


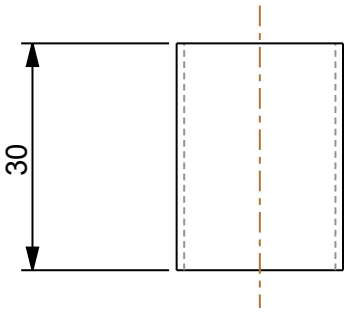


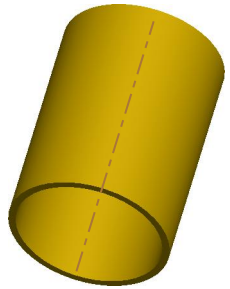



Note: Bush pressed into hanger

| | Bronze | 1 | |
|---|---|---|---|
| Item | Material | Qty | Remarks |

University of Cape Town
Department of Mechanical Engineering

Title: Bush

| Dimensions in mm Tolerance U.O.S. | Scale | Date | Sheet | of |
|---|---|---|---|---|
| | 1,000 | 17 May 2012 | 8 | 32 |
| | Drawn By | | Drawing Number | |
| 0.1 | WG Randall | | F008 | |

Partial view
Length 3m

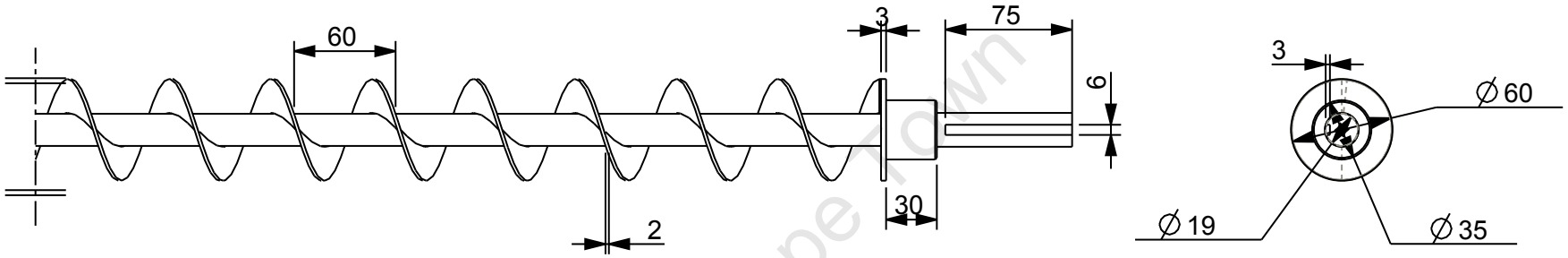


Motor end

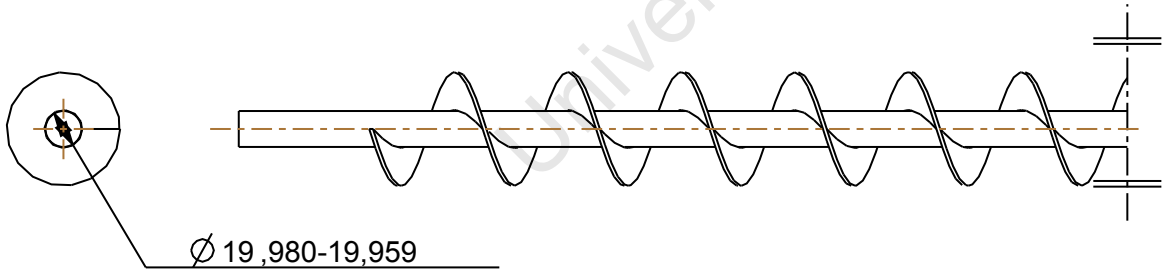


Outlet end



| | Mild Steel | 1 | |
|---|---|---|---|
| Item | Material | Qty | Remarks |

University of Cape Town
Department of Mechanical Engineering

Title: SCREW

| Dimensions in mm Tolerance U.O.S. | Scale | Date | Sheet | of |
|---|---|---|---|---|
| 0.1 | 0,250 | 17 May 2012 | 9 | 32 |

| Drawn By | Drawing Number |
|---|---|
| WG Randall | F009 |

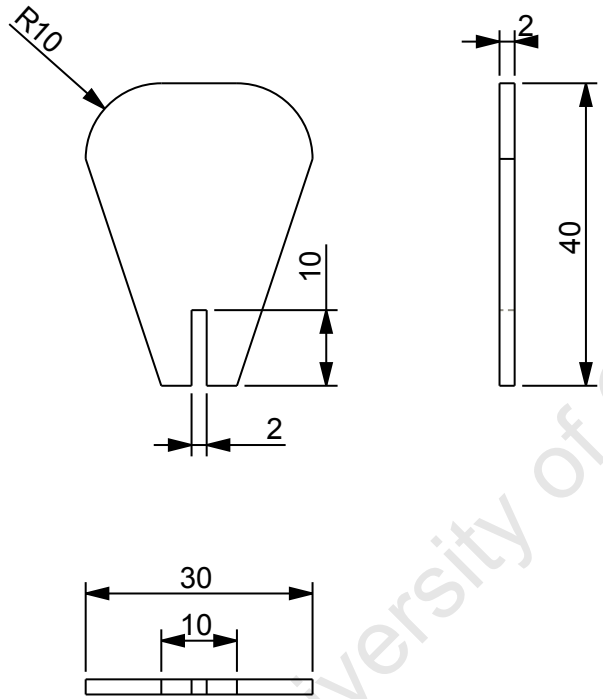




Note: Paddle 1 welded to screw at intervals of 180mm and 120° to each other for first 1m of screw

| | Mild Steel | 10 | Laser Cut |
|---|---|---|---|
| Item | Material | Qty | Remarks |

University of Cape Town
Department of Mechanical Engineering

Title: Paddle

| Dimensions in mm Tolerance U.O.S. | Scale | Date | Sheet | of |
|---|---|---|---|---|
| | 1,000 | 30 July 2012 | 10 | 32 |
| | Drawn By | | Drawing Number | |
| 0.1 | Warren Randall | | F010 | |

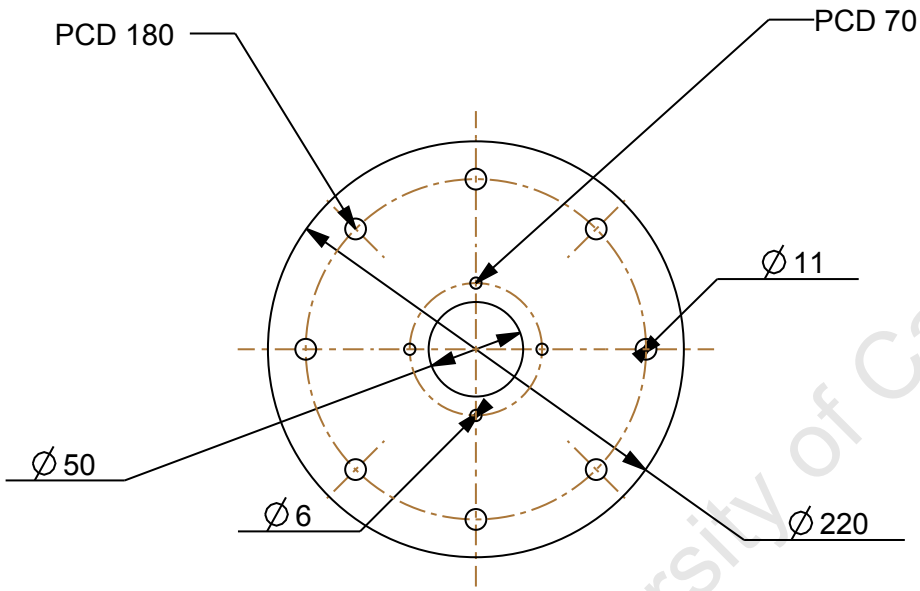


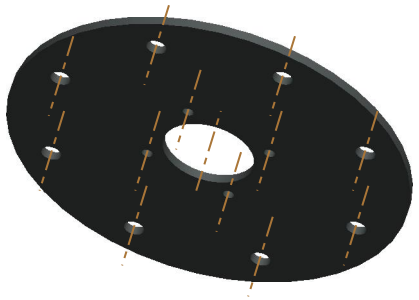




| | Mild Steel | 1 | Laser Cut |
|---|---|---|---|
| Item | Material | Qty | Remarks |

University of Cape Town
Department of Mechanical Engineering

Title
Screw Mount

| Dimensions in mm Tolerance U.O.S. | Scale | Date | Sheet | of |
|---|---|---|---|---|
| | 0,250 | 16 May 2012 | 11 | 32 |
| | Drawn By | | Drawing Number | |
| 0.1 | WG Randall | | F011 | |

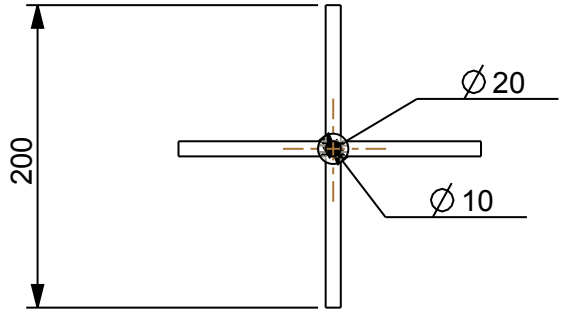


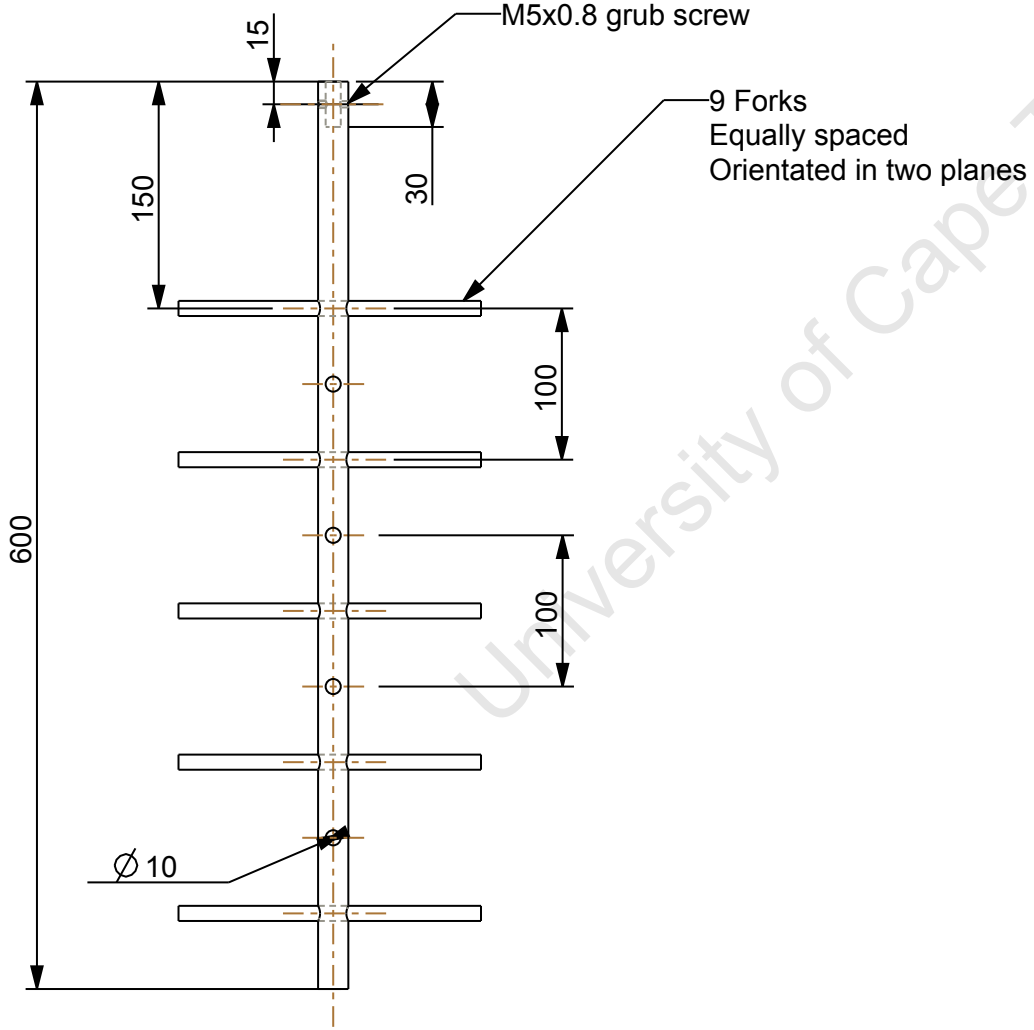


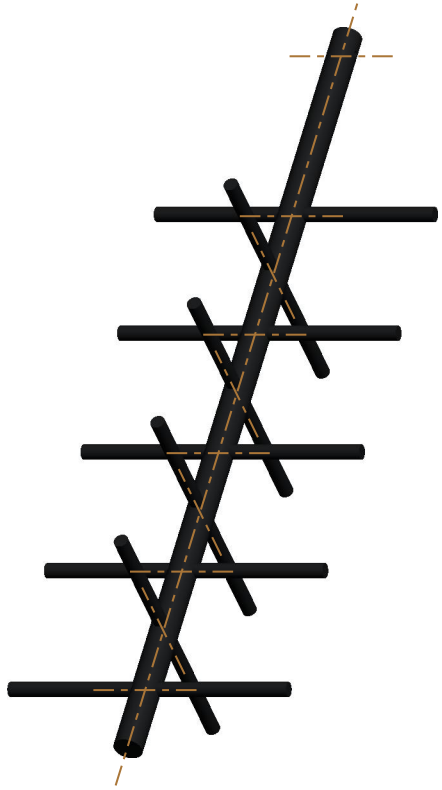



| | Mild Steel | 1 | Welded |
|---|---|---|---|
| Item | Material | Qty | Remarks |

University of Cape Town
Department of Mechanical Engineering

Title
Agitator 1

| Dimensions in mm Tolerance U.O.S. | Scale | Date | Sheet | of |
|---|---|---|---|---|
| | 0,200 | 17 May 2012 | 12 | 32 |
| | Drawn By | | Drawing Number | |
| 0.1 | WG Randall | | F012 | |

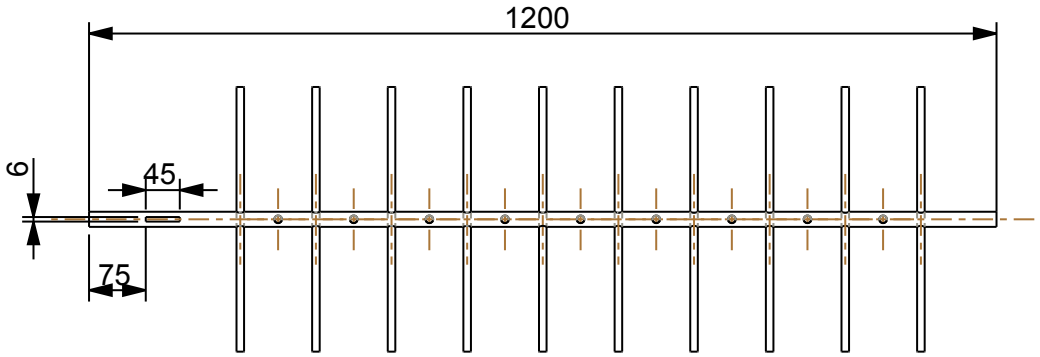


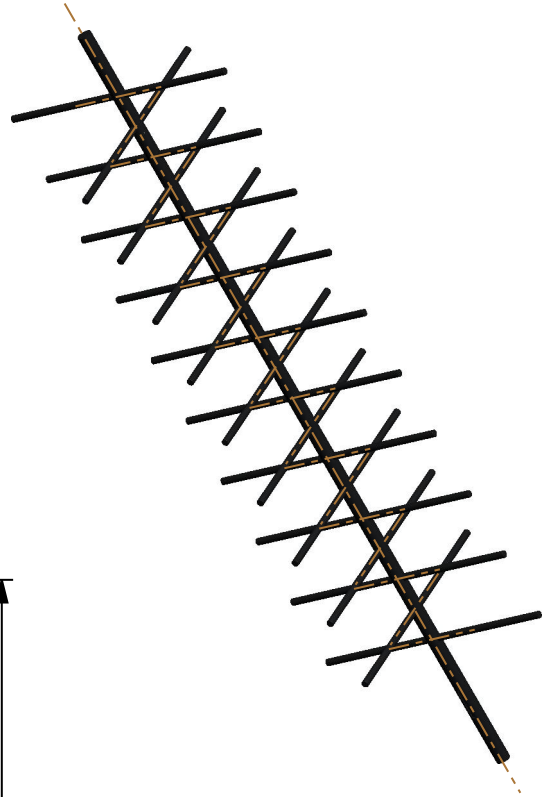

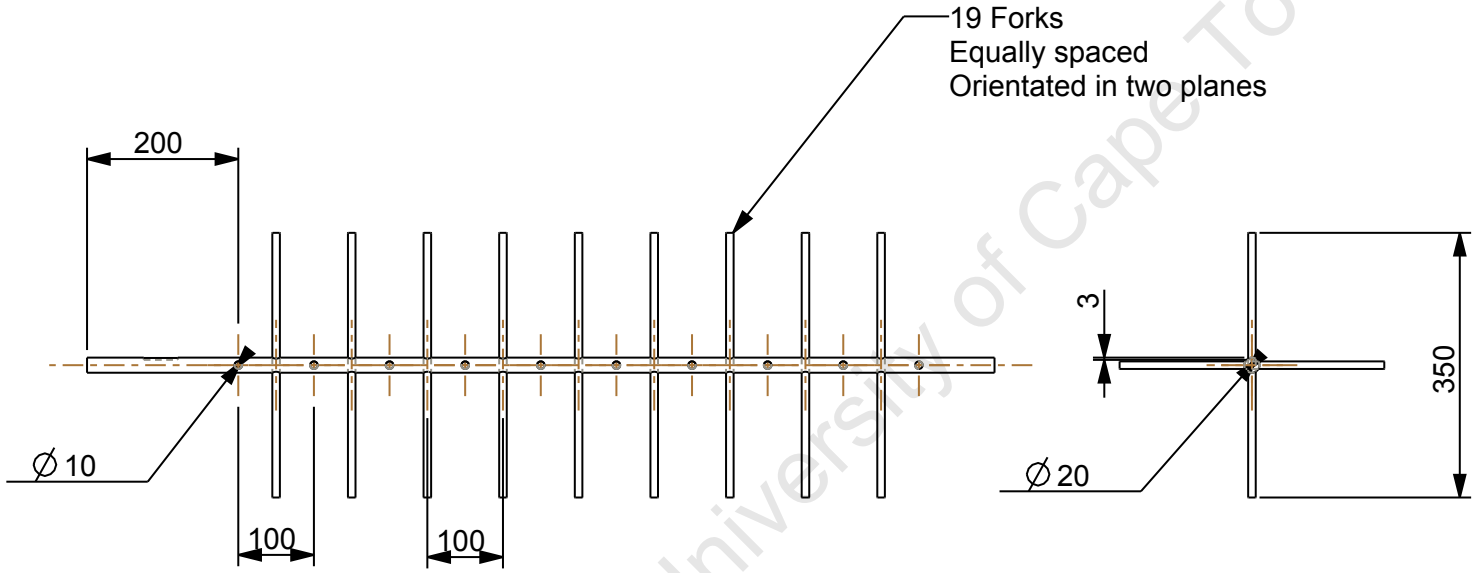




| | Mild Steel | 2 | Welded |
|---|---|---|---|
| Item | Material | Qty | Remarks |

University of Cape Town
Department of Mechanical Engineering

Title: Agitator 2

| Dimensions in mm Tolerance U.O.S. | Scale | Date | Sheet | of |
|---|---|---|---|---|
| 0.1 | 0,100 | 17 May 2012 | 13 | 32 |
| | Drawn By: WG Randall | | Drawing Number: F013 | |

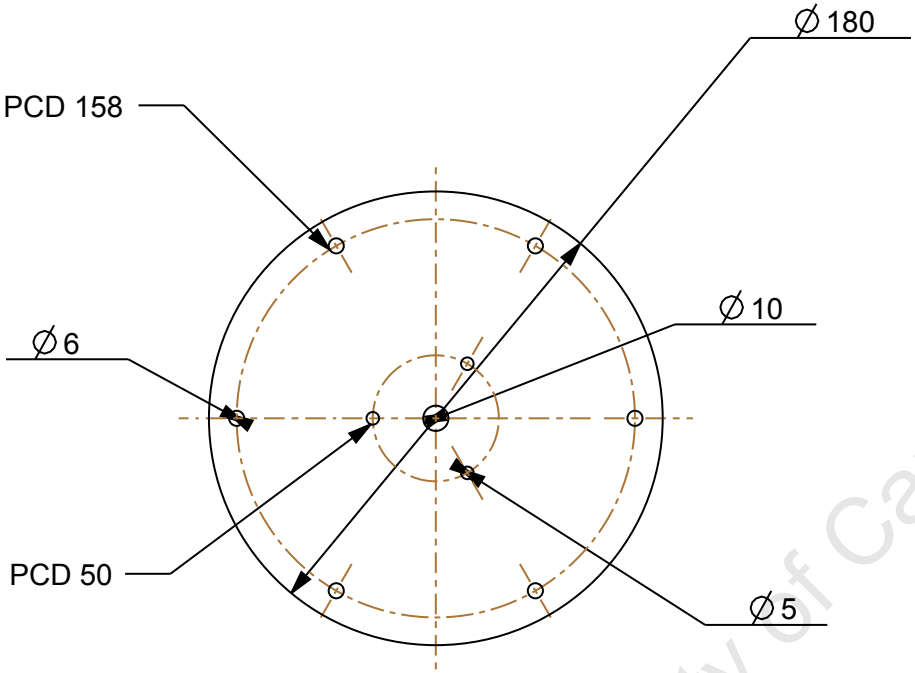


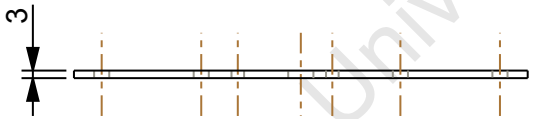


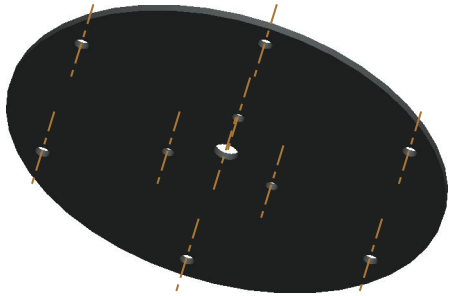



| | Mild Steel | 1 | Laser Cut |
|---|---|---|---|
| Item | Material | Qty | Remarks |

University of Cape Town
Department of Mechanical Engineering

Title: Wiper Flange

| Dimensions in mm Tolerance U.O.S. | Scale | Date | Sheet | of |
|---|---|---|---|---|
| 0.1 | 0,333 | 16 May 2012 | 14 | 32 |

| Drawn By | Drawing Number |
|---|---|
| WG Randall | F014 |

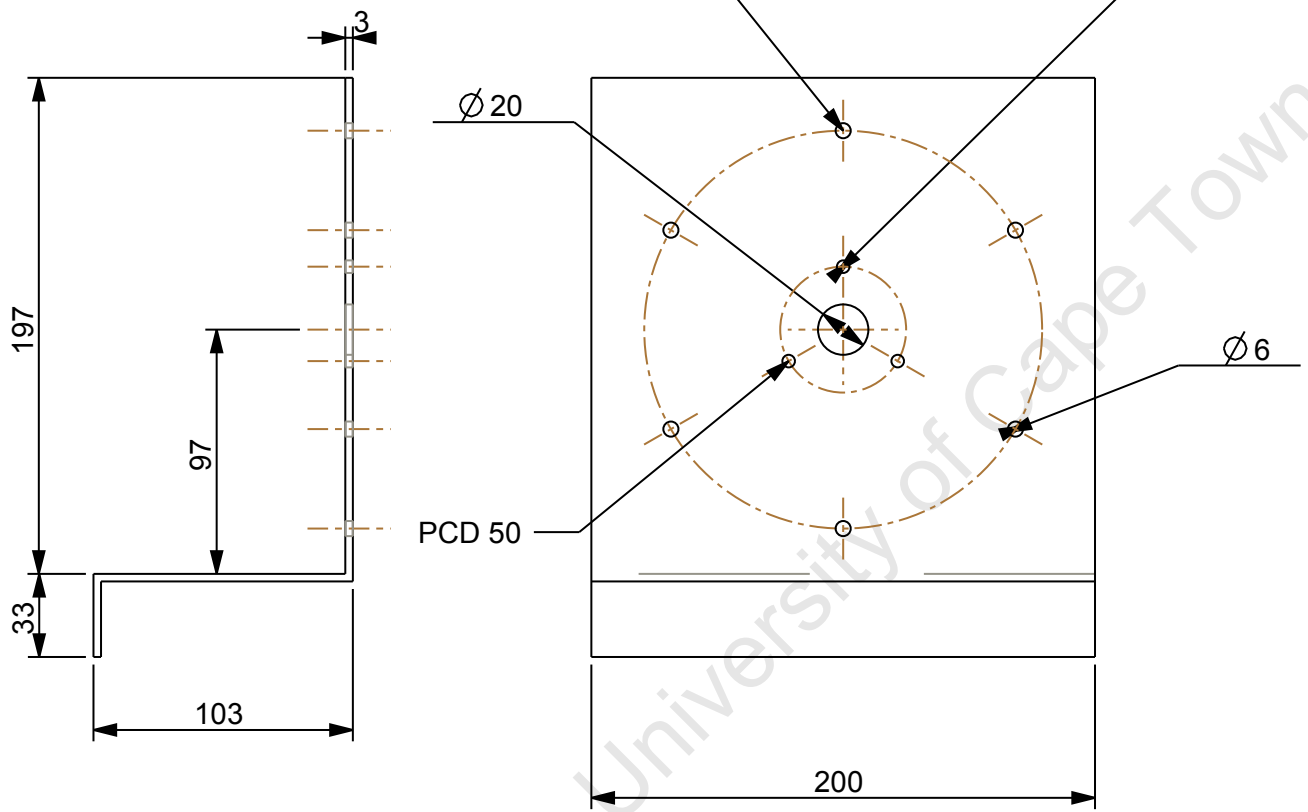


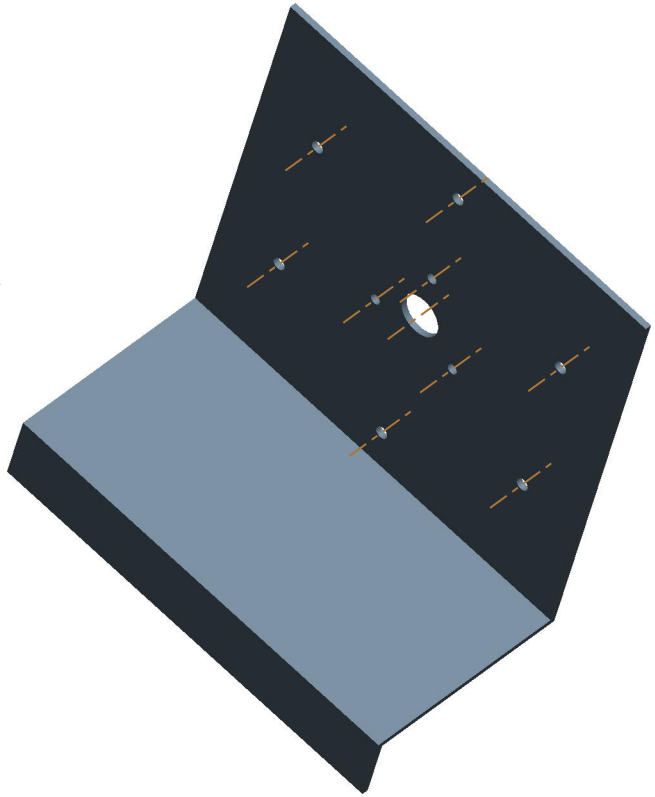

Note: Chain mount welded to Hopper Mount

| | Mild Steel | 1 | Laser Cut & Bent |
|---|---|---|---|
| Item | Material | Qty | Remarks |

University of Cape Town
Department of Mechanical Engineering

Title: Chain Mount

| Dimensions in mm Tolerance U.O.S. | Scale | Date | Sheet | of |
|---|---|---|---|---|
| 0.1 | 0,333 | 22 May 2012 | 15 | 32 |
| | Drawn By: WG Randall | | Drawing Number: F015 | |

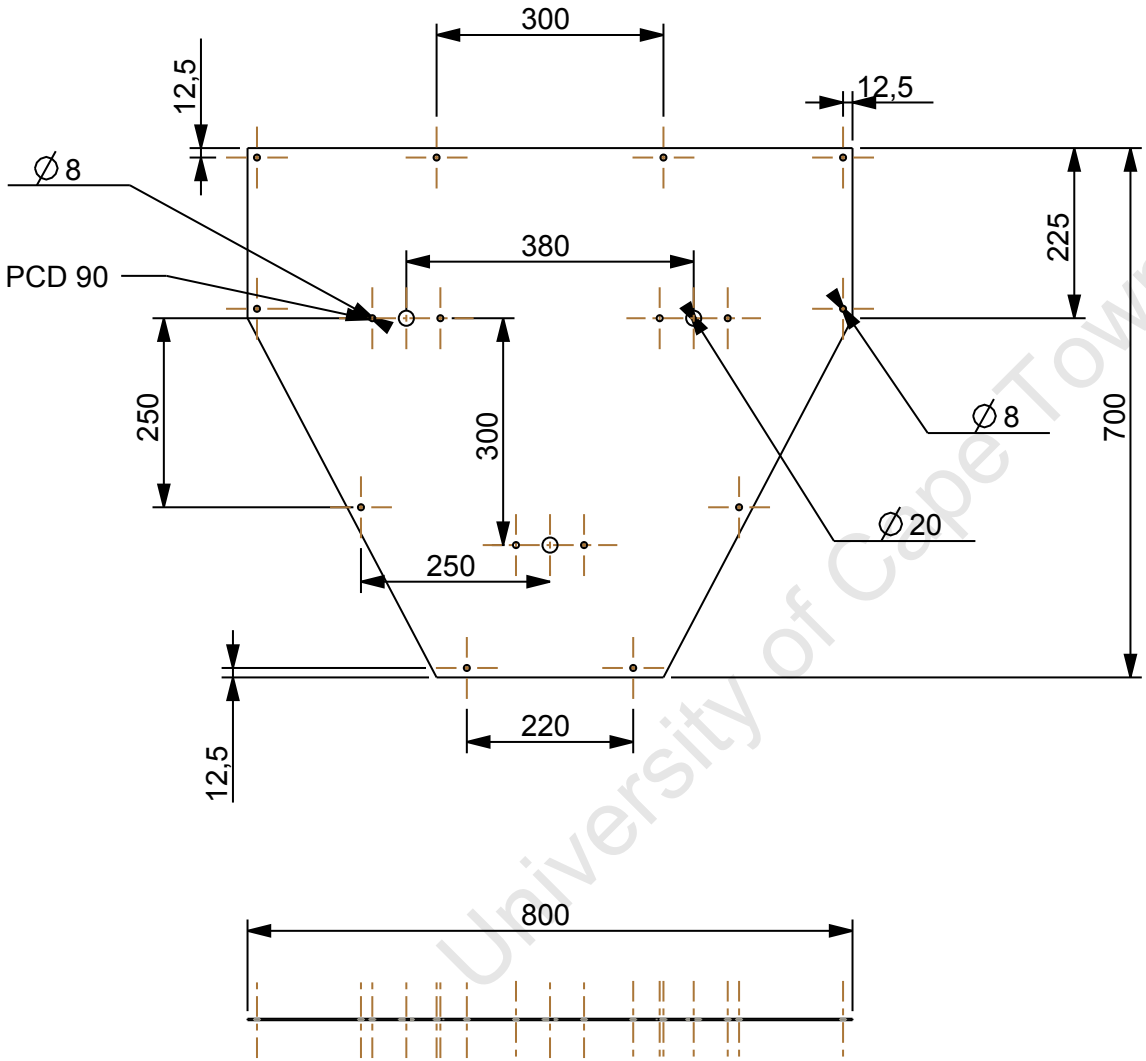




| | Mild Steel | 1 | |
|---|---|---|---|
| Item | Material | Qty | Remarks |

University of Cape Town
Department of Mechanical Engineering

Title
Hopper Mount

| Dimensions in mm Tolerance U.O.S. | Scale | Date | Sheet | of |
|---|---|---|---|---|
| | 0,100 | 22 May 2012 | 16 | xx |
| | Drawn By | | Drawing Number | |
| 0.1 | WG Randall | | F016 | |

# APPENDIX F.2: HEAT EXCHANGER DRAWINGS

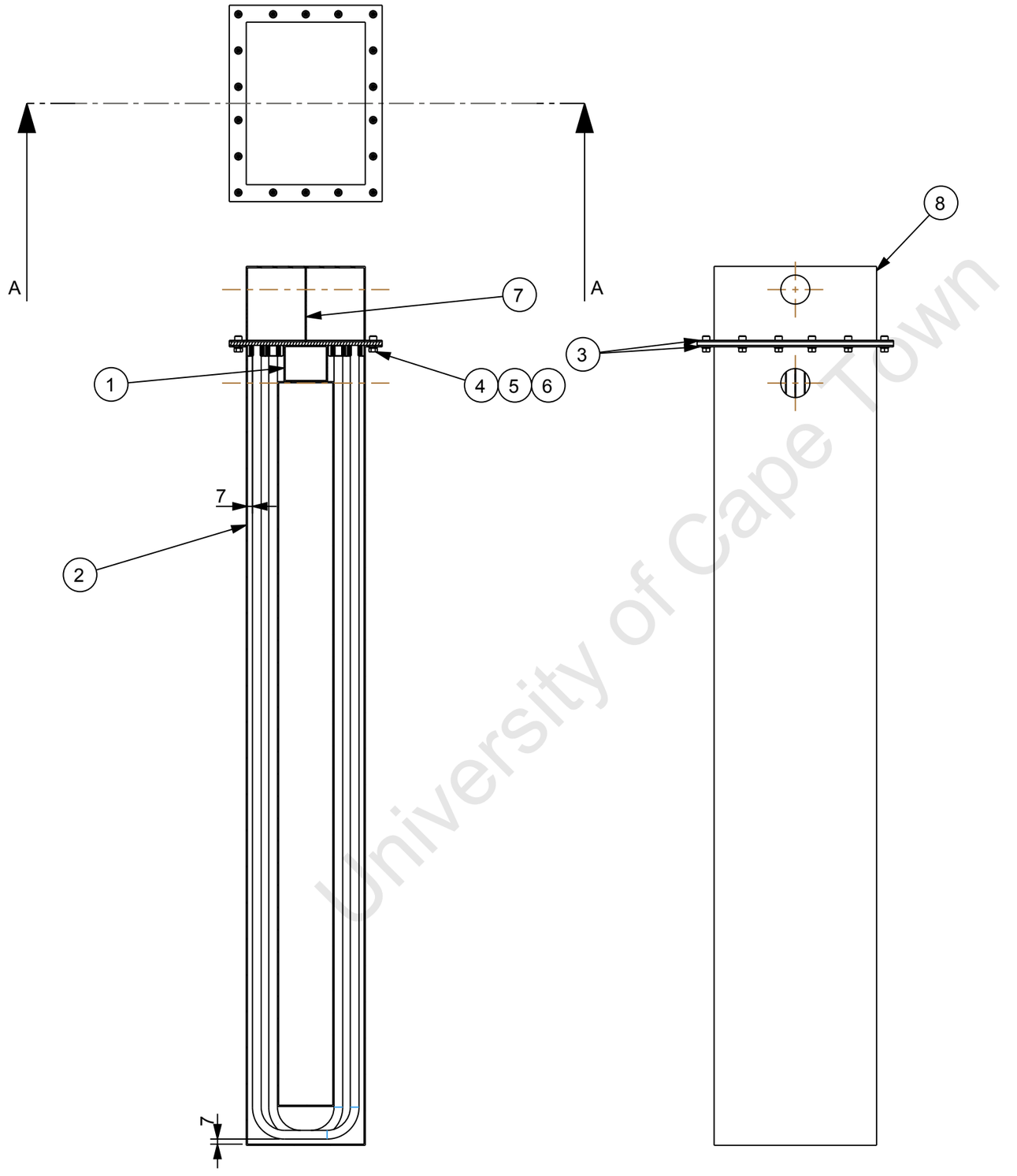


Note: Flanges welded to shell and endcap

| Item | Name | Qty | Material | Remarks |
|---|---|---|---|---|
| 8 | Endcap | 1 | Mild Steel | Welded Assembly |
| 7 | Endcap Pass | 1 | Mild Steel | Laser Cut |
| 6 | M6 Washer | 18 | Mild Steel | Std. Part |
| 5 | M6x1 Hex Nut | 18 | Mild Steel | Std. Part |
| 4 | M6 by 25mm Cap Head | 18 | Mild Steel | Std. Part |
| 3 | HE Flange | 2 | Mild Steel | Laser Cut |
| 2 | Shell | 1 | Mild Steel | Welded Assembly |
| 1 | Tube Bank | 1 | Various | Assembly |

University of Cape Town
Department of Mechanical Engineering

Title
Heat Exchanger Assembly

| Dimensions in mm Tolerance U.O.S. | Scale | Date | Sheet | of |
|---|---|---|---|---|
| | 0,150 | 6 June 2012 | 17 | 32 |
| 0.1 | Drawn By: WG Randall | | Drawing Number: HE001 | |

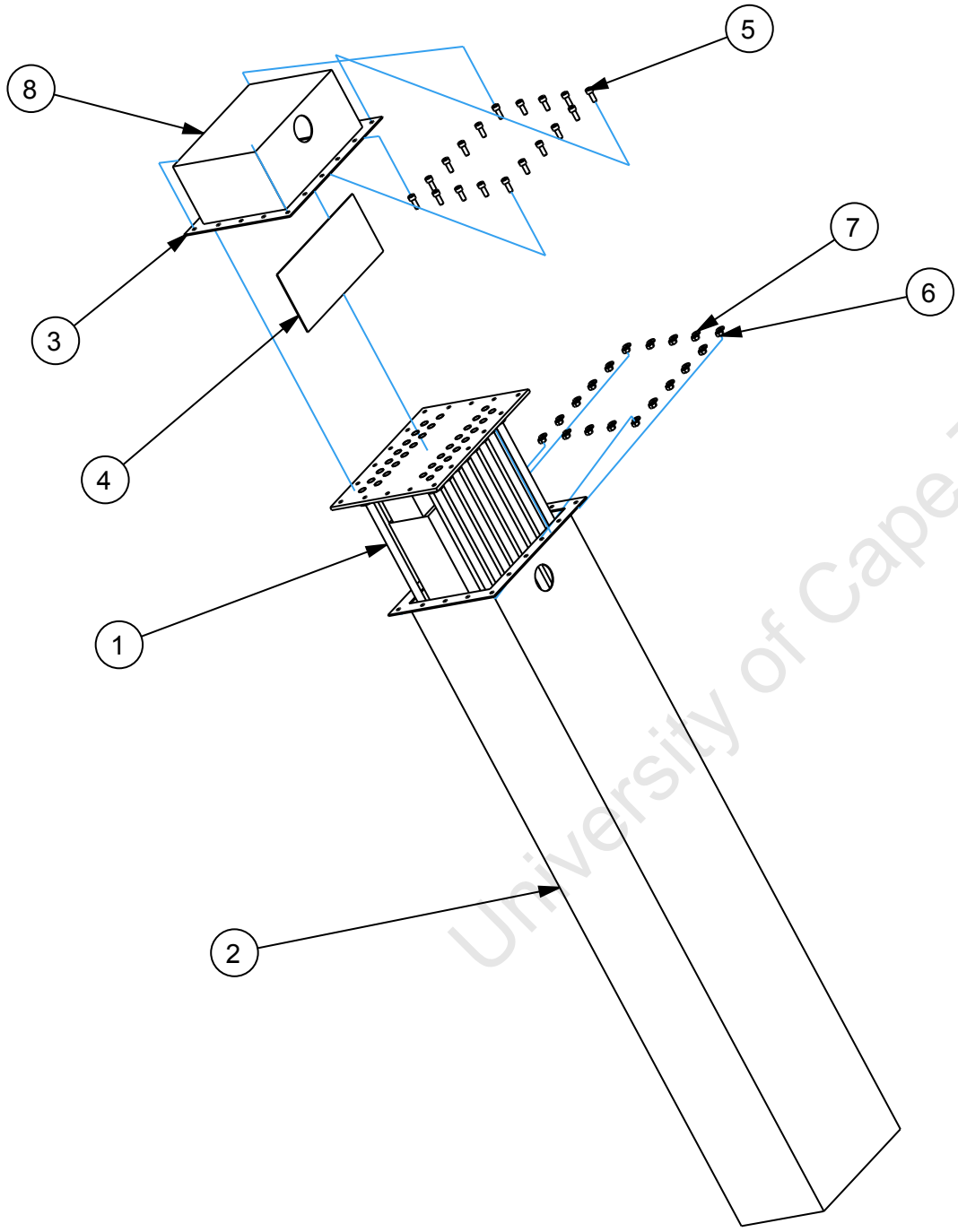




| Item | Name | Qty | Material |
|---|---|---|---|
| 8 | End Cap | 1 | Mild Steel |
| 7 | M6 Washer | 18 | Mild Steel |
| 6 | M6 Hex Nut | 18 | Mild Steel |
| 5 | M6 by 25mm Cap Head | 18 | Mild Steel |
| 4 | Endcap Pass | 1 | Mild Steel |
| 3 | HE Flange | 2 | Mild Steel |
| 2 | Shell | 1 | Mild Steel |
| 1 | Tube Bank | 1 | As Assembled |

University of Cape Town
Department of Mechanical Engineering

Title
Heat Exchanger Exploded

| Dimensions in mm Tolerance U.O.S. | Scale | Date | Sheet | of |
|---|---|---|---|---|
| 0.1 | 0,100 | 6 June 2012 | 18 | 32 |
| | Drawn By: WG Randall | | Drawing Number: HE002 | |

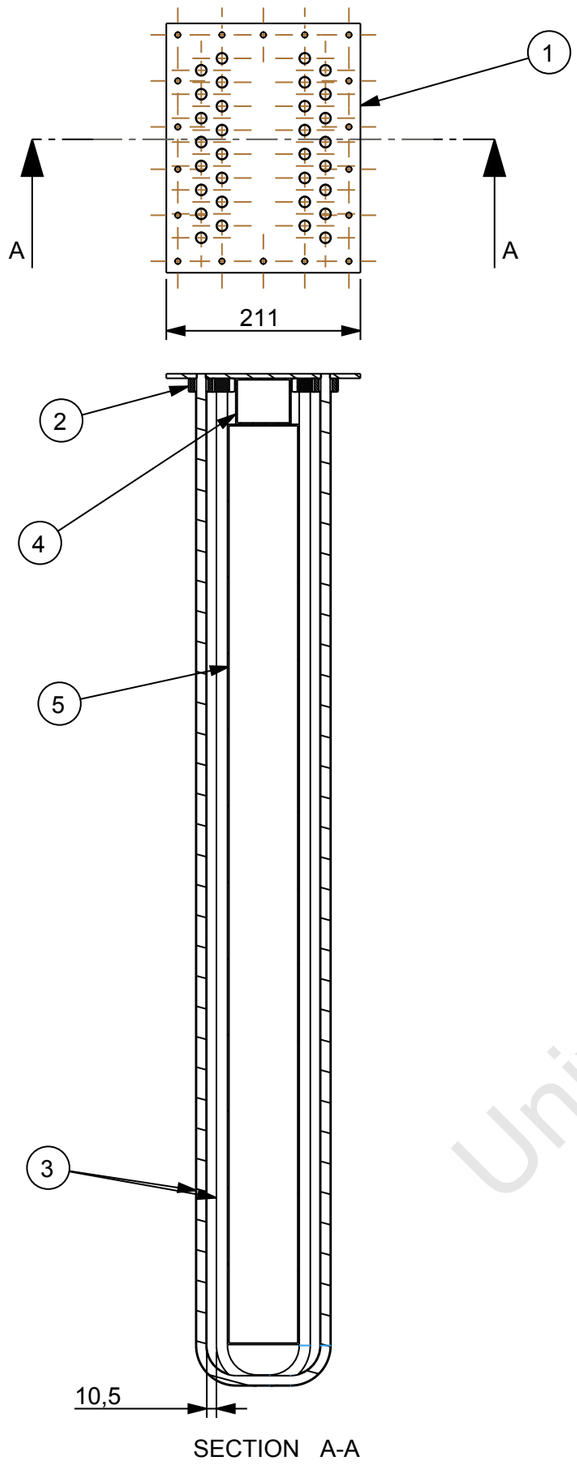


SECTION A-A

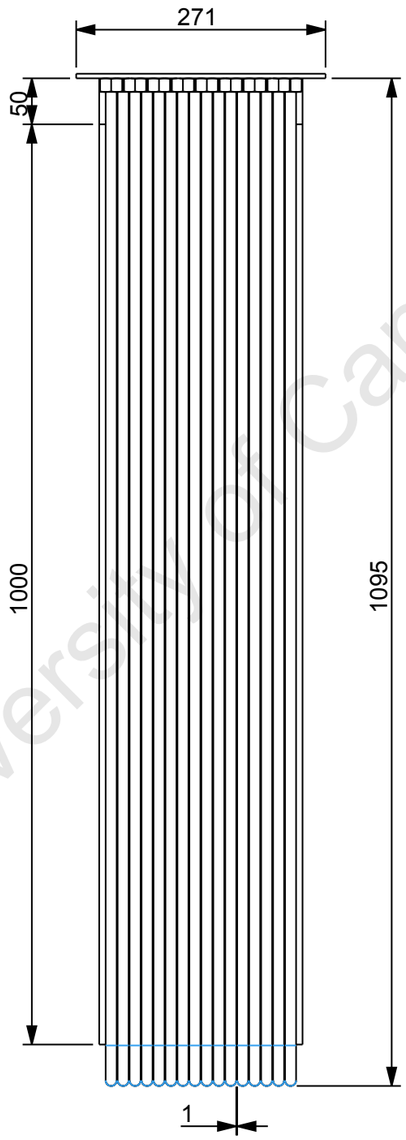


| Item | Name | Qty | Material | Remarks |
|---|---|---|---|---|
| 5 | Large Pass | 1 | Mild Steel | Welded Assembly |
| 4 | Small Pass | 1 | Mild Steel | Welded Assembly |
| 3 | SS-T12M-S-1.0M-6ME | 16 | As Supplied | Bent Tubing |
| 2 | S-12MO-1-4 Fittings | 32 | As Supplied | Tube Fitting |
| 1 | Hole Spacing Plate | 1 | Mild Steel | Laser Cut |

University of Cape Town
Department of Mechanical Engineering

Title
Tube Bank Assembly

| Dimensions in mm Tolerance U.O.S. | Scale | Date | Sheet | of |
|---|---|---|---|---|
| 0.1 | 0,150 | 6 June 2012 | 19 | 32 |
| | Drawn By: WG Randall | | Drawing Number: HE003 | |

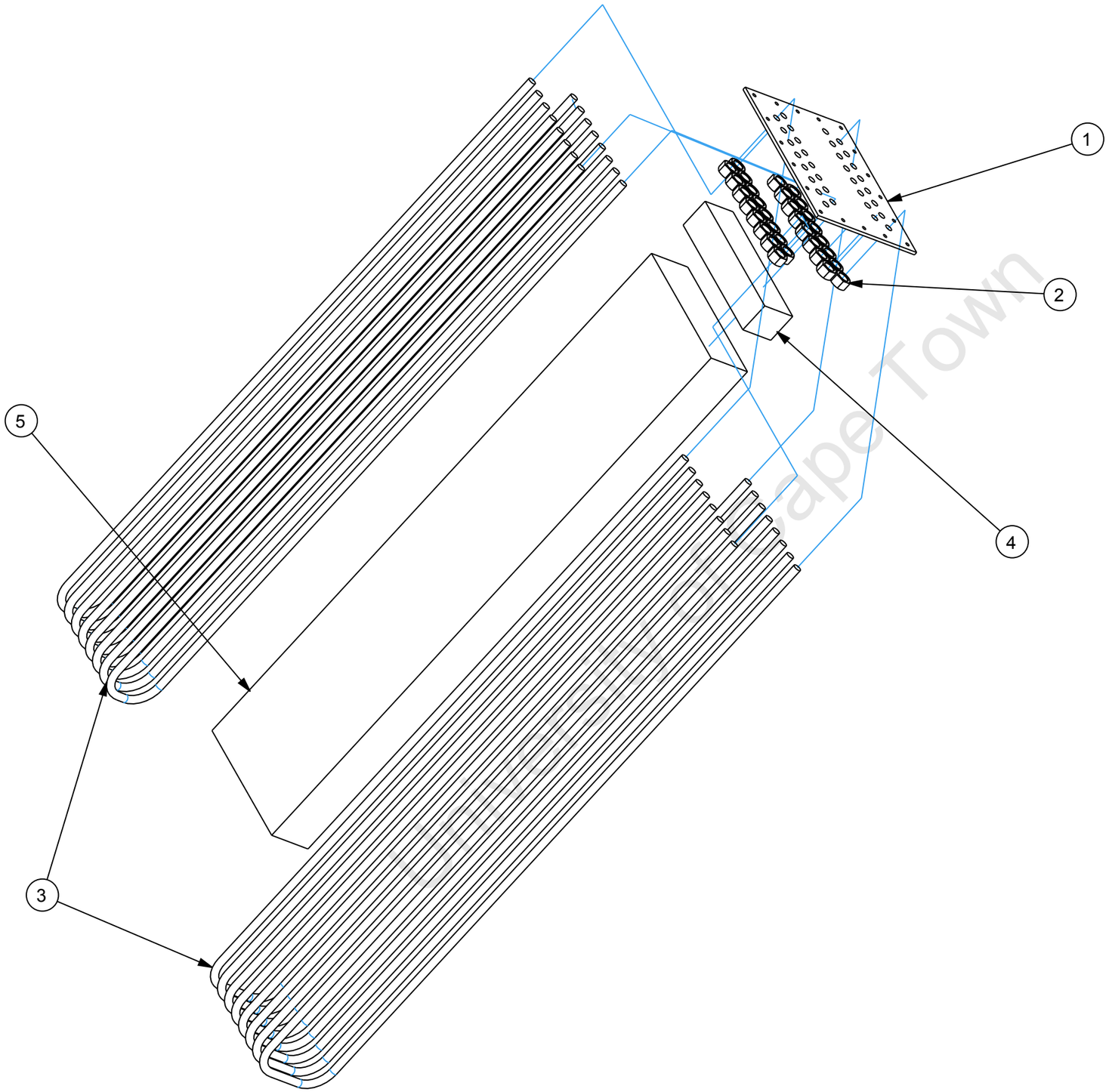




| | | | | |
|---|---|---|---|---|
| 5 | Large Pass | 1 | Mild Steel | Welded Assembly |
| 4 | Small Pass | 1 | Mild Steel | Welded Assembly |
| 3 | SS-T12M-S-1.0M-6ME | 16 | As Supplied | Bent Tubing |
| 2 | S-12MO-1-4 | 32 | As Supplied | Tube Fittings |
| 1 | Hole Spacing Plate | 1 | Mild Steel | Laser Cut |
| Item | Name | Qty | Material | Remarks |

University of Cape Town
Department of Mechanical Engineering

Title
Tube Bank Exploded

| Dimensions in mm Tolerance U.O.S. | Scale | Date | Sheet | of |
|---|---|---|---|---|
| | 0,150 | 6 June 2012 | 20 | 32 |
| 0.1 | Drawn By: WG Randall | | Drawing Number: HE004 | |

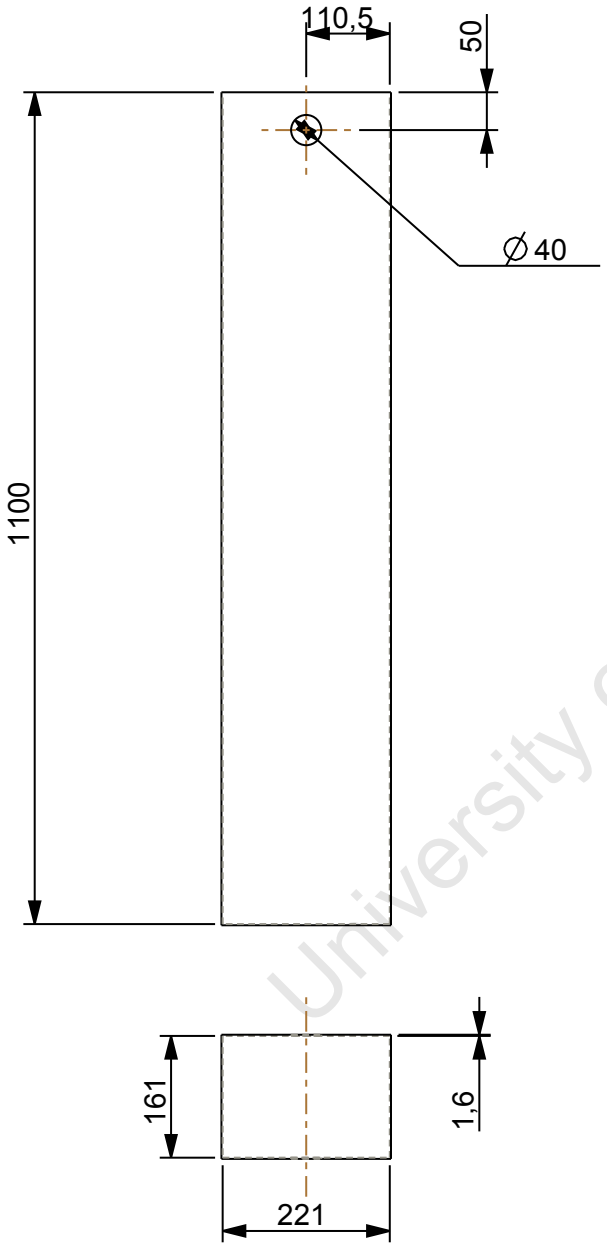


Note: Plates are bent and welded to form the shell

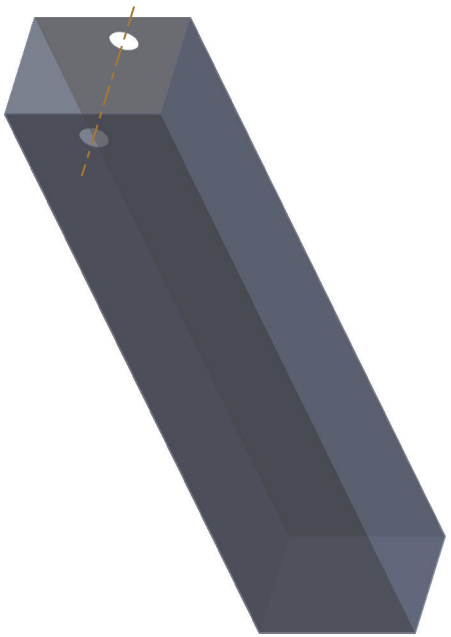



| | Mild Steel | 1 | Bend & Weld |
|---|---|---|---|
| Item | Material | Qty | Remarks |

University of Cape Town
Department of Mechanical Engineering

Title: Shell

| Dimensions in mm Tolerance U.O.S. | Scale | Date | Sheet | of |
|---|---|---|---|---|
| | 0,100 | 14 May 2012 | 21 | 32 |
| | Drawn By | | Drawing Number | |
| 0.1 | WG Randall | | HE005 | |

Note: 16 x1/4" Tapped holes.
11mm thru drill

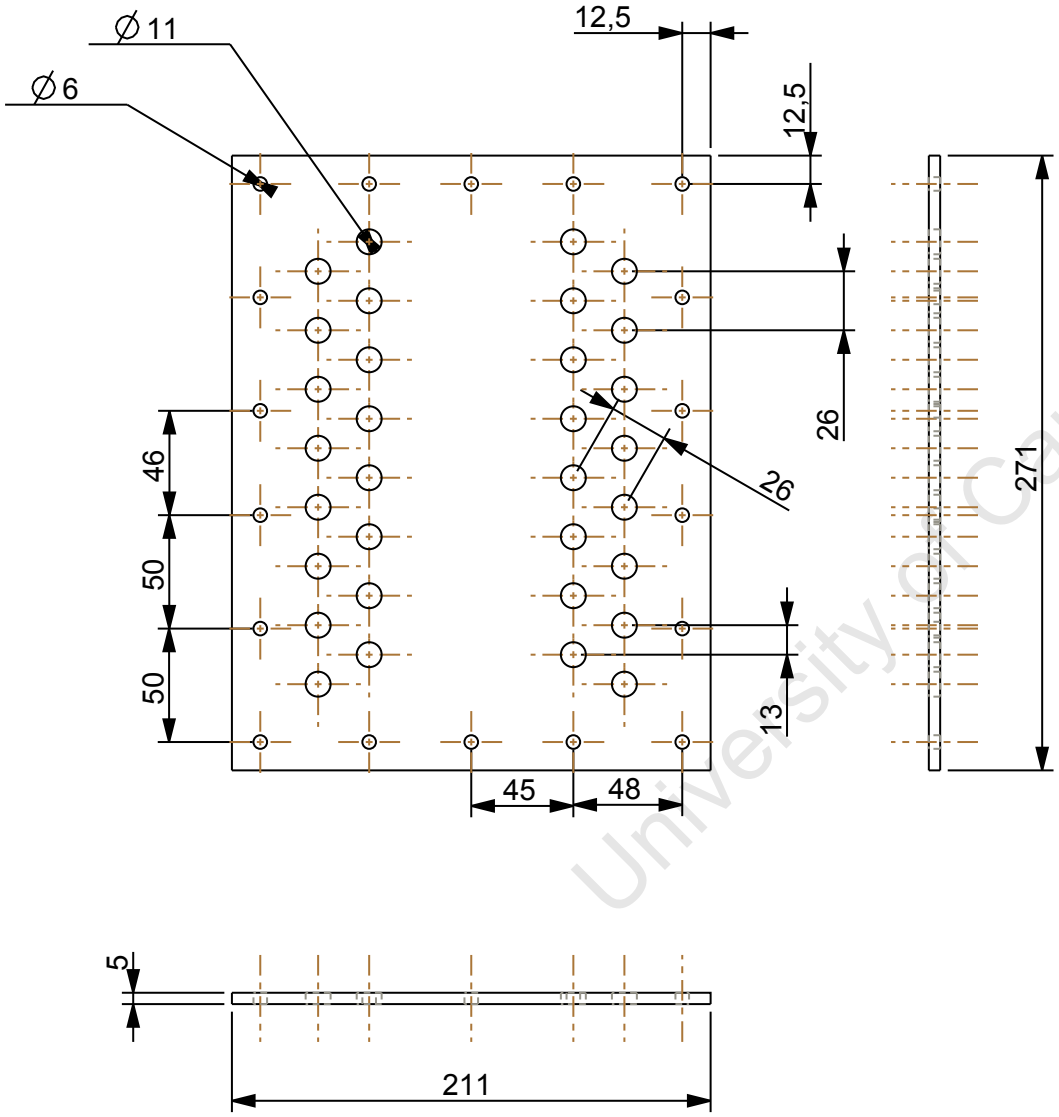


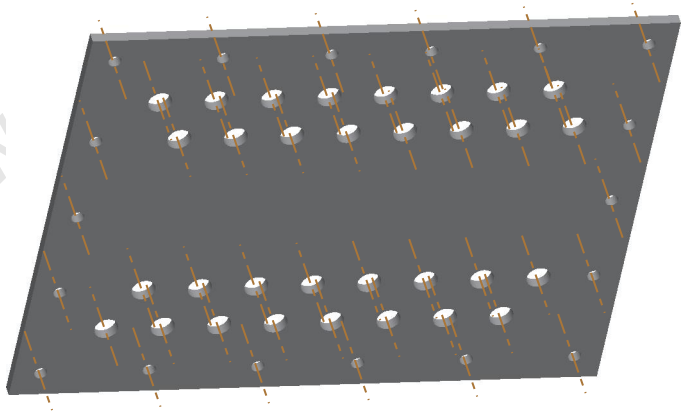



| | Mild Steel | 1 | Laser Cut |
|---|---|---|---|
| Item | Material | Qty | Remarks |

University of Cape Town
Department of Mechanical Engineering

Title
Hole Spacing Plate

| Dimensions in mm Tolerance U.O.S. | Scale | Date | Sheet | of |
|---|---|---|---|---|
| | 0,300 | 28 April 2012 | 22 | 32 |
| | Drawn By | | Drawing Number | |
| 0.1 | WG Randall | | HE006 | |

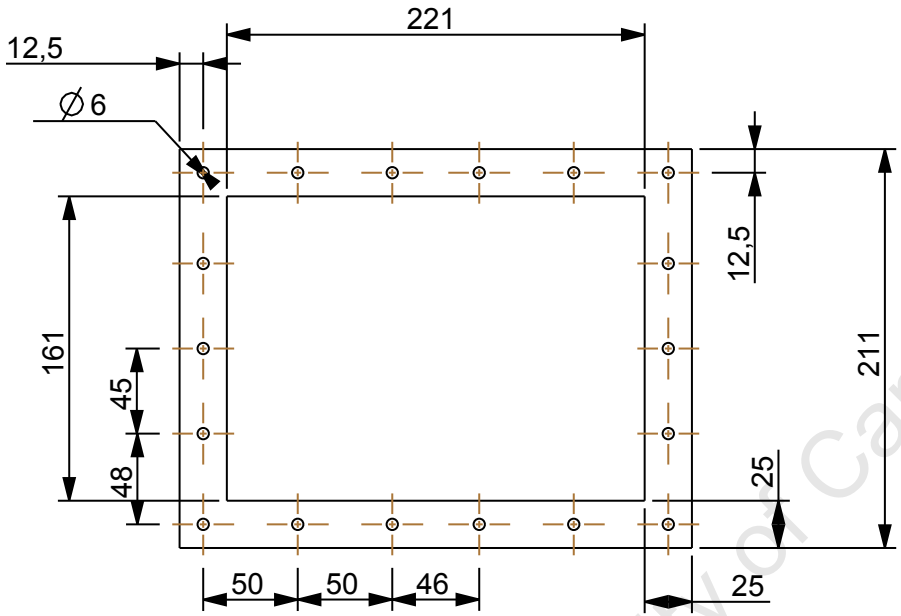


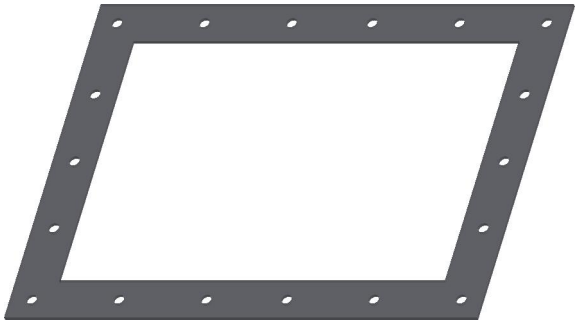

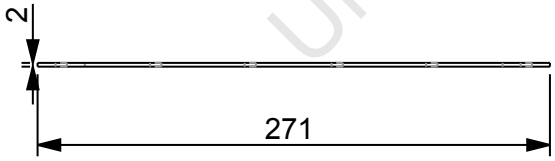




| | Mild Steel | 2 | Laser Cut |
|---|---|---|---|
| Item | Material | Qty | Remarks |

University of Cape Town
Department of Mechanical Engineering

Title
HE Flange

| Dimensions in mm Tolerance U.O.S. | Scale | Date | Sheet | of |
|---|---|---|---|---|
| | 0,250 | 14 May 2012 | 23 | 32 |
| | Drawn By | | Drawing Number | |
| 0.1 | WG Randall | | HE007 | |

Note: Plates are bent and welded to form Endcap

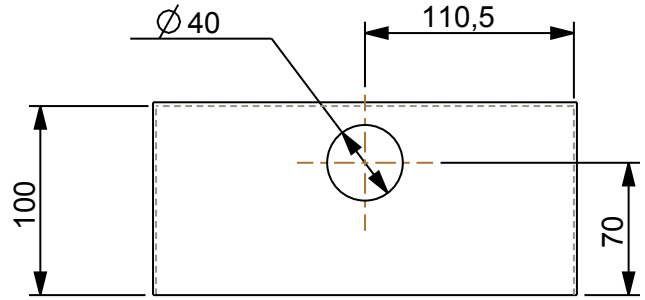


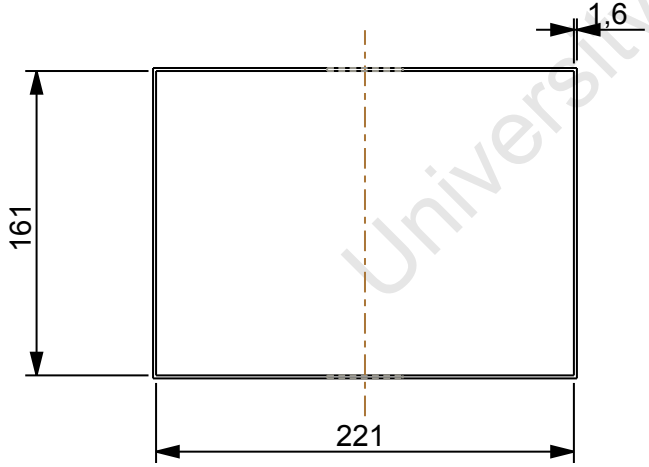


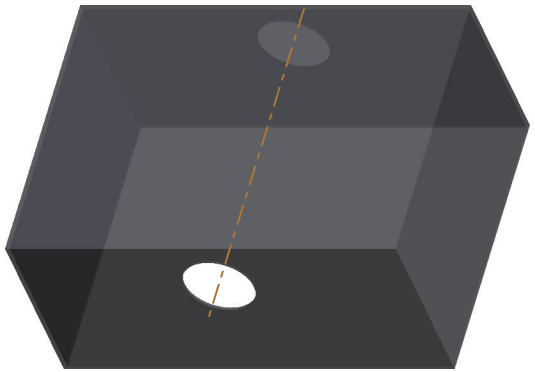



| | Mild Steel | 1 | Bend & Weld |
|---|---|---|---|
| Item | Material | Qty | Remarks |

University of Cape Town
Department of Mechanical Engineering

Title: Endcap

| Dimensions in mm Tolerance U.O.S. | Scale | Date | Sheet | of |
|---|---|---|---|---|
| | 0,250 | 14 May 2012 | 24 | 32 |
| | Drawn By | | Drawing Number | |
| 0.1 | WG Randall | | HE008 | |

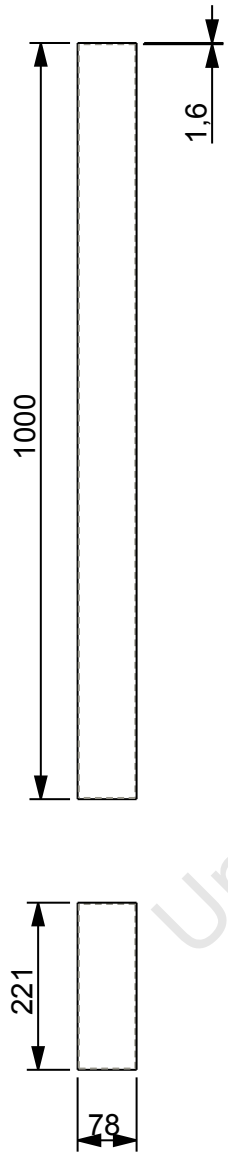


Note: Plates are bent and welded to form the large pass

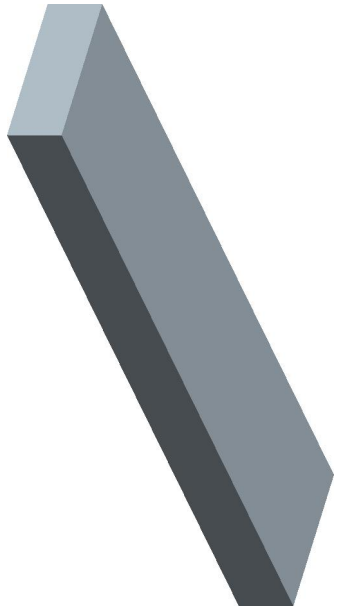



| | Mild Steel | 1 | Bend & Weld |
|---|---|---|---|
| Item | Material | Qty | Remarks |

University of Cape Town
Department of Mechanical Engineering

Title: Large Pass

| Dimensions in mm Tolerance U.O.S. | Scale | Date | Sheet | of |
|---|---|---|---|---|
| 0.1 | 0,100 | 14 May 2012 | 25 | 32 |
| | Drawn By: WG Randall | | Drawing Number: HE009 | |

Note; Plates are bent and welded
to form the small pass

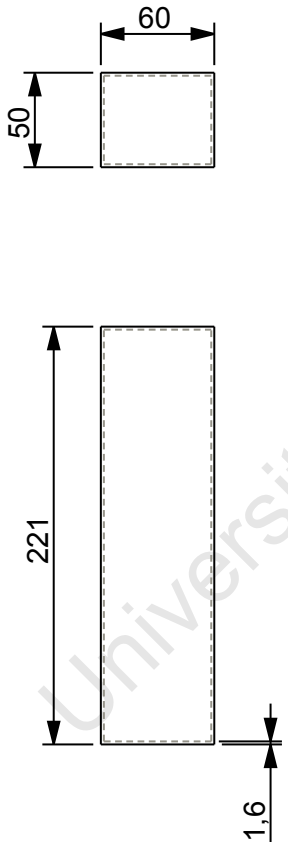


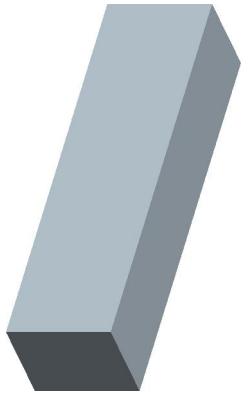



| | | | |
|---|---|---|---|
| | Mild Steel | 1 | Bend & Weld |
| Item | Material | Qty | Remarks |

University of Cape Town
Department of Mechanical Engineering

Title: Small Pass

| Dimensions in mm Tolerance U.O.S. | Scale | Date | Sheet | of |
|---|---|---|---|---|
| | 0,250 | 14 May 2012 | 26 | 32 |
| | Drawn By | | Drawing Number | |
| 0.1 | WG Randall | | HE010 | |

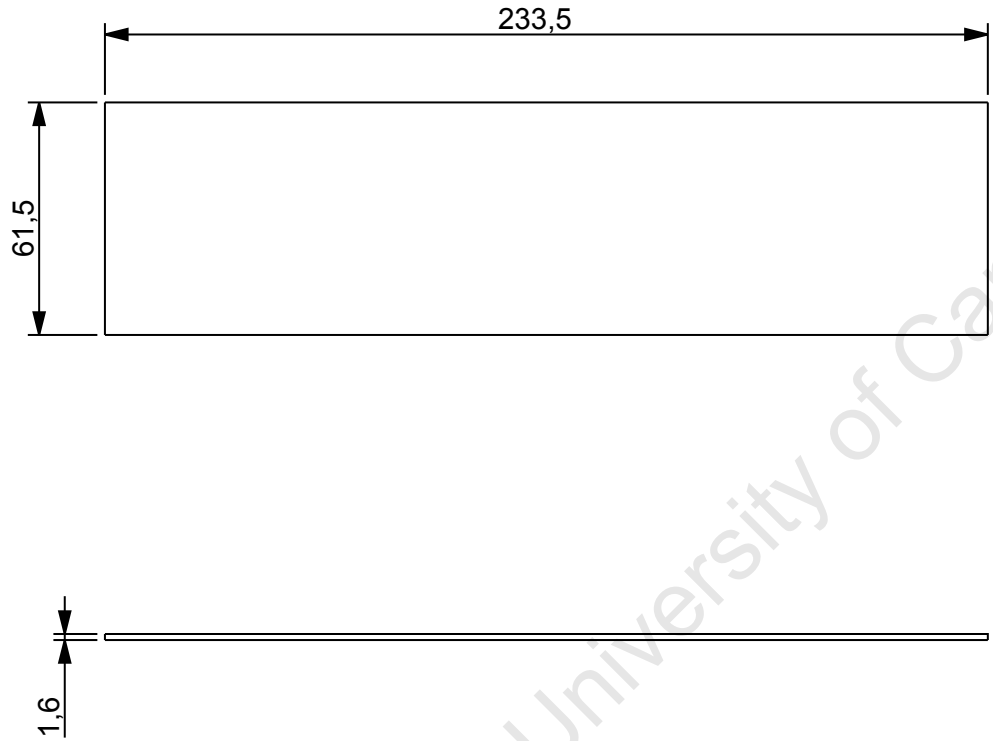




| | | | |
|---|---|---|---|
| | Mild Steel | 1 | |
| Item | Material | Qty | Remarks |

University of Cape Town
Department of Mechanical Engineering

Title: End Cap Pass

| Dimensions in mm Tolerance U.O.S. | Scale | Date | Sheet | of |
|---|---|---|---|---|
| | 0,500 | 16 May 2012 | 27 | 32 |
| | Drawn By | | Drawing Number | |
| 0.1 | WG Randall | | HE011 | |

# APPENDIX F.3: DRIER FAN HOUSING DRAWINGS

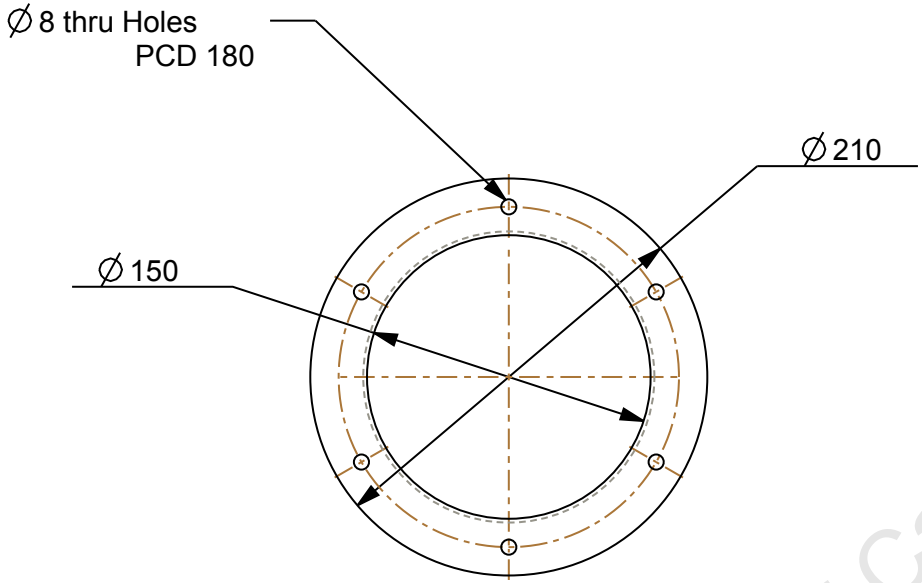


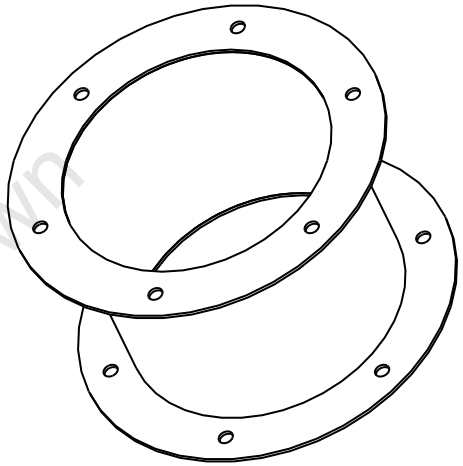

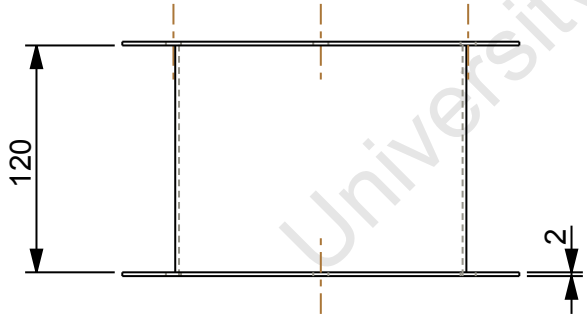




| | | | |
|---|---|---|---|
| | Mild Steel | 1 | Welded Assembly |
| Item | Material | Qty | Remarks |

University of Cape Town
Department of Mechanical Engineering

Title: Fan Housing

| Dimensions in mm Tolerance U.O.S. | Scale | Date | Sheet | of |
|---|---|---|---|---|
| 0.1 | 0,250 | 8 Aug 2012 | 28 | 32 |

| Drawn By | Drawing Number |
|---|---|
| WG Randall | V001 |

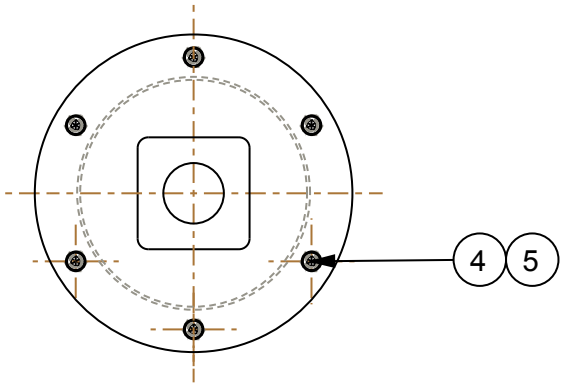


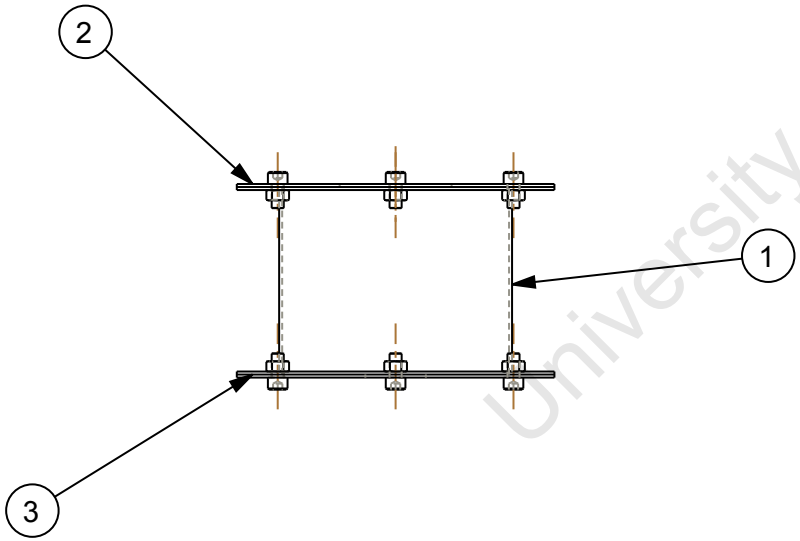




| | | | |
|---|---|---|---|
| 5 | M8 Hex Nut | 12 | Std Part |
| 4 | M8 Cap Head | 12 | Std Part |
| 3 | Vacuum Outlet | 1 | Mild Steel |
| 2 | Vacuum Mount | 1 | Mild Steel |
| 1 | Vacuum Housing | 1 | Welded Assembly |
| Item | Name | Qty | Material |

University of Cape Town
Department of Mechanical Engineering

Title
Fan Housing Assembly

| Dimensions in mm Tolerance U.O.S. | Scale | Date | Sheet | of |
|---|---|---|---|---|
| | 0,200 | 12 Aug 2012 | 29 | 32 |
| | Drawn By | | Drawing Number | |
| 0.1 | WG Randall | | V002 | |

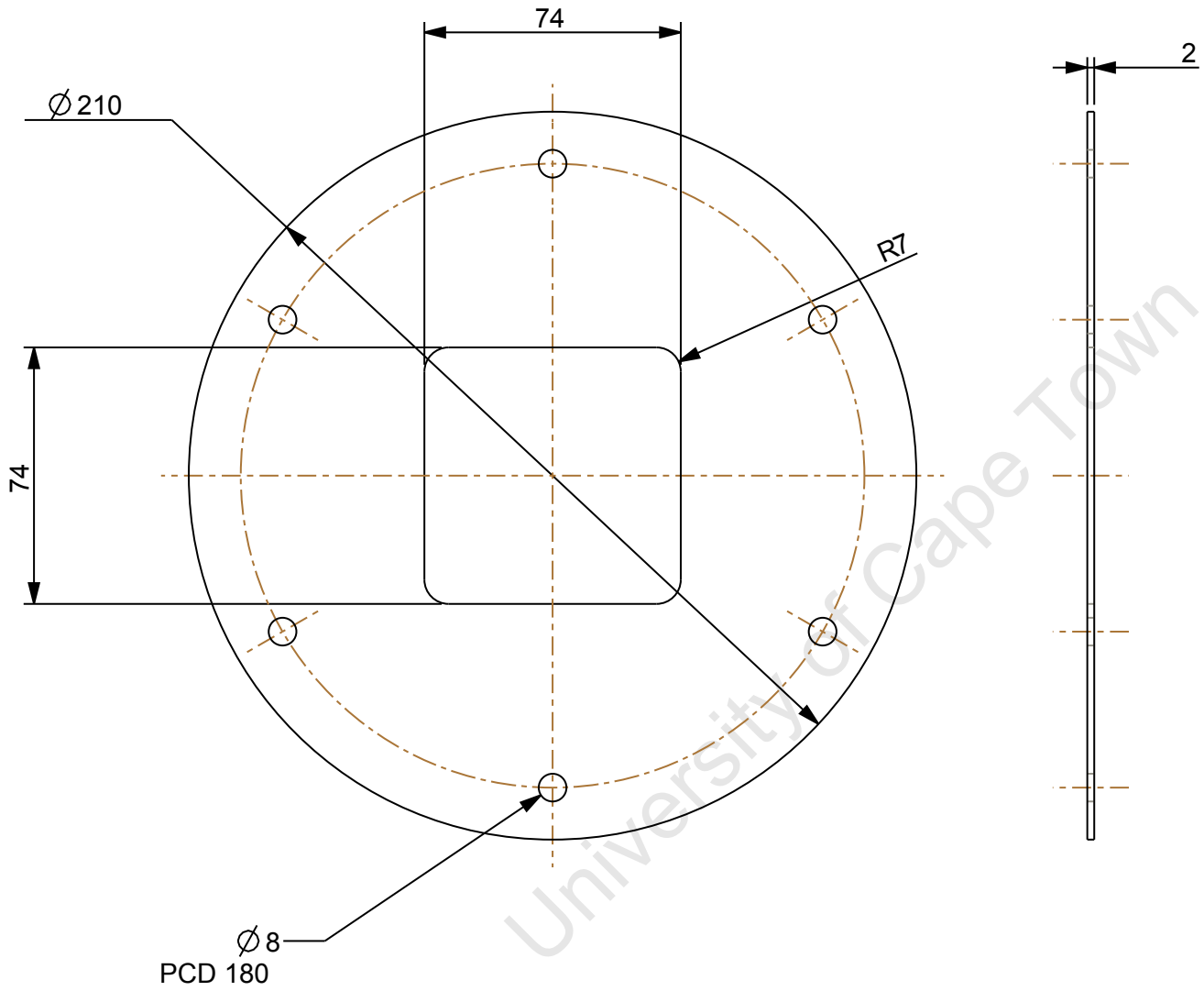




| | Mild Steel | 1 | Lasr Cut |
|---|---|---|---|
| Item | Material | Qty | Remarks |

University of Cape Town
Department of Mechanical Engineering

Title
Fan Mount

| Dimensions in mm Tolerance U.O.S. | Scale | Date | Sheet | of |
|---|---|---|---|---|
| | 0,500 | 13 August 2012 | 30 | 32 |
| | Drawn By | | Drawing Number | |
| 0.1 | WG Randall | | V003 | |

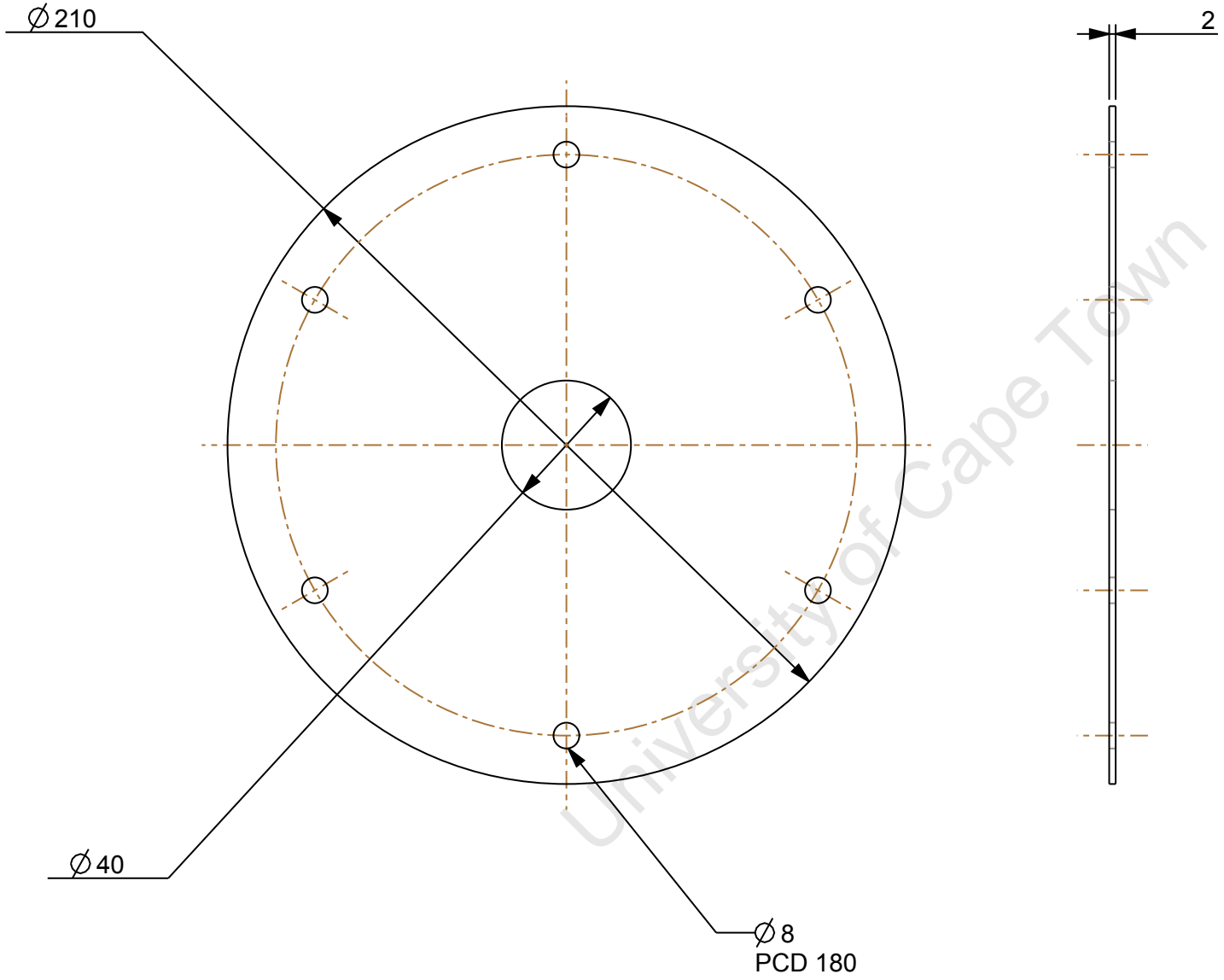




| | Mild Steel | 1 | Laser Cut |
|---|---|---|---|
| Item | Material | Qty | Remarks |

University of Cape Town
Department of Mechanical Engineering

Title
Fan Outlet

| Dimensions in mm Tolerance U.O.S. | Scale | Date | Sheet | of |
|---|---|---|---|---|
| | 0,500 | 13 August 2012 | 31 | 32 |
| | Drawn By | | Drawing Number | |
| 0.1 | WG Randall | | V004 | |

# APPENDIX F.4: FRAME DRAWINGS

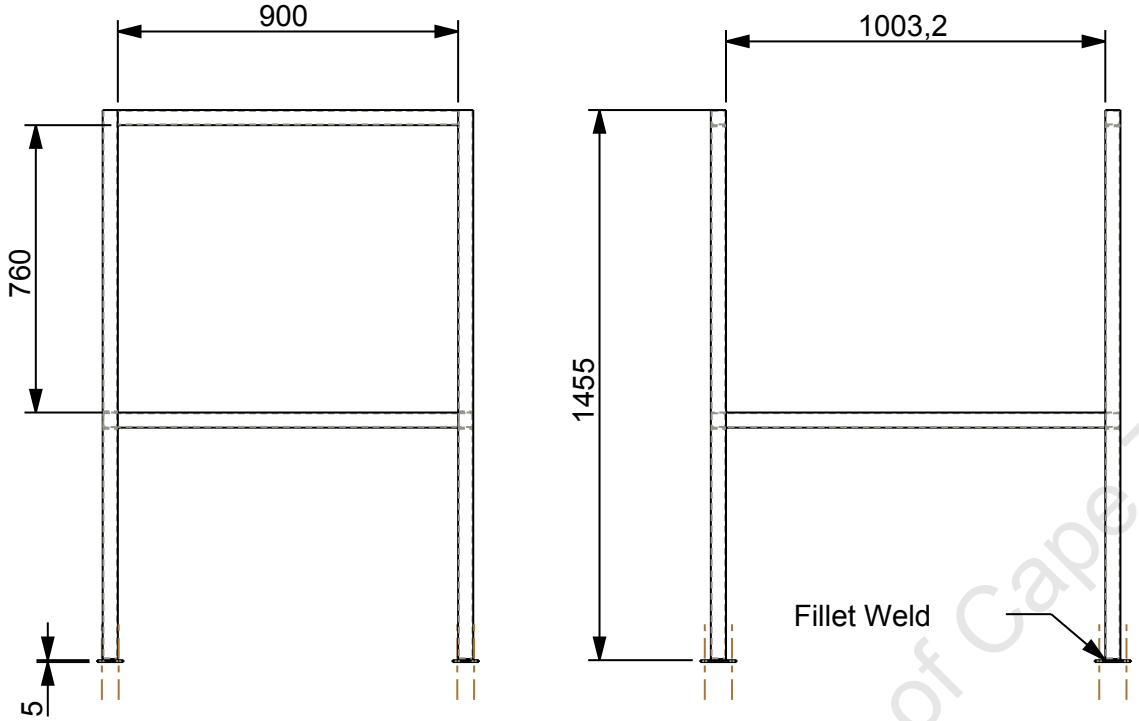


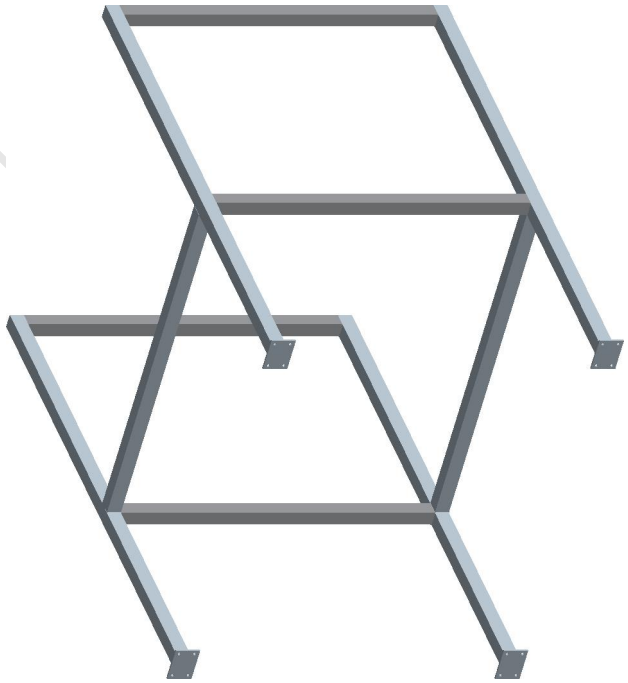

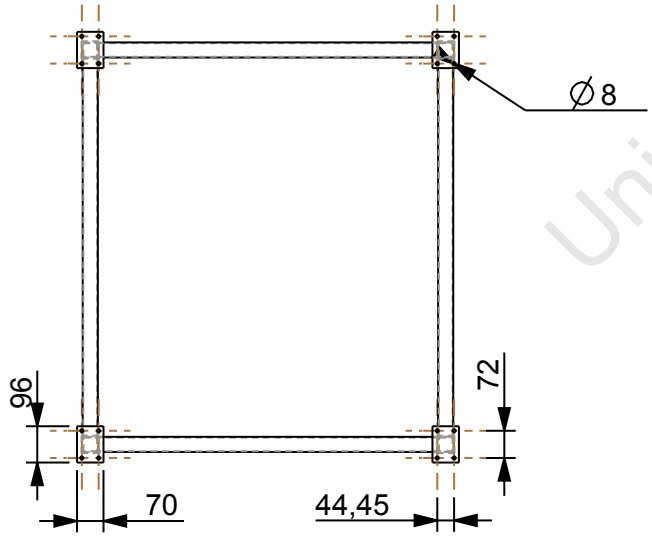


Note: 40x40x2 square tubing
with feet, welded



| | Mild Steel | 1 | Welded |
|---|---|---|---|
| Item | Material | Qty | Remarks |

University of Cape Town
Department of Mechanical Engineering

Title
Support Welded Assembly

| Dimensions in mm Tolerance U.O.S. | Scale | Date | Sheet | of |
|---|---|---|---|---|
| | 0,050 | 22 May 2012 | 32 | 32 |
| | Drawn By | | Drawing Number | |
| 0.1 | WG Randall | | F032 | |